A pH-METRIC SPECIATION AND ANTI-DIABETIC STUDY OF OXOVANADIUM(IV) AMINO ACID DERIVATIVES

A THESIS IN THE CHEMISTRY DEPARTMENT

SUBMITTED IN FULFILMENT OF THE REQUIREMENTS FOR

THE DEGREE OF

MASTER OF SCIENCE IN CHEMISTRY

RHODES UNIVERSITY

BY

ISAAC ZVIKOMBORERO GUNDHLA

JANUARY 2011

SUPERVISOR: DR Z. R. TSHENTU

DECLARATION

I certify that this work was carried out by Mr Isaac Zvikomborero Gundhla in the Department of Chemistry, Rhodes University. This work has not been submitted at any other university for the purpose of obtaining a degree.

I.Z. Gundhla ……..

DEDICATION

TO MY DAUGHTER, RUJEKO;

TO MY WIFE, VIOLET AND LATE TWIN SISTER, GRACE, WHO INSPIRE ME A LOT; AND TO MY LATE MOTHER, JOSEPHINE AND MR P.N. SITHOLE WHO SACRIFICED EVERY PERSONAL COMFORT TO SEE ME THROUGH MY BASIC EDUCATION.

ACKNOWLEDGEMENTS

To the Original Chemist, my creator God, be glory and thanks for His grace and love in my life. Everything that we can discover and investigate was put in place by Him and bears testimony to His glory.

Patience, endurance, tolerance and determination are the traits of the supervisor who made my research successful. The support, guidance and constructive criticism provided by my supervisor, Dr Z. R Tshentu, need to be acknowledged. I owe him my increased passion for chemistry and inorganic chemistry in particular.

I would like to thank Andrew Mellon Scholarship and National Research Foundation for their financial support. I also want to thank the Medical Research Council for funding this research work.

A lot of appreciation goes to Rhodes University for giving me an opportunity to study towards a Master of Science in Chemistry. Prof C.L. Frost of NMMU Biochemistry Department is acknowledged for hosting me in her laboratory. My sincere thanks go to Dr N.O. Mnonopi (NMMU) for her assistance with biological studies. Dr E. Hosten from the NMMU Chemistry Department is also acknowledged for his assistance with solid state UV/Vis studies. Ryan, thank you for your prime advice, you gave me hope to live. Nomapondo and Mr Okewole I thank you for your comradeship and consolation.

I would like to reckon the fraternal love, support and indelible motivation imparted by my twin sister, Grace. Sadly you almost ripped my heart when you were ruthlessly usurped from me by an elephant. I am arming myself to fulfill your wishes. Rest in peace.

My wife, Violet, you were there at all odds. Thank you for your unfailing love, patience and encouragement. I owe you a sterling love. Thank you Rujeko, my daughter, for always reminding me that I should be a responsible, caring and loving father.

Last but not least, I thank my friend, Biggie Samwanda, for giving me a shoulder to lean on whenever I am down. You have been a source of encouragement and inspiration.

LIST OF FIGURES

LIST OF TABLES

LIST OF ABBREVIATIONS

IDDM- insulin dependent diabetes mellitus

NIDDM- non-insulin dependent diabetes mellitus

FDA- Food and Drug Administration

WHO- World Health Organization

TZDs- thiazolidinediones

ATP- adenosine triphosphate

STZ- streptozotocin

BEOV- *bis*(ethylmaltolato)oxovanadium(IV)

BMOV- *bis*(maltolato)oxovanadium(IV)

$VO(pic)_2$- *bis*(picolinato)oxovanadium(IV)

dhp- 1,2-dimethyl-3-hydroxy-4-pyridinone

PTP- protein tyrosine phosphatase

GI- Gastrointestinal

HMM- high molecular mass

LMM- low molecular mass

hTf- human transferrin

HSA- human serum albumin

CD- circular dichroism

EPR- electron paramagnetic resonance

BCM-EPR- blood circulation monitoring – electron paramagnetic resonance

$V^{IV}O$- oxovanadium(IV)

L- ligand

apoTf- apotransferrin

bL- biological ligand

H_{-1}- hydroxo

IR- infrared

FTIR- Fourier transform infrared

ATR- attenuated total reflectance

NMR- nuclear magnetic resonance

ICP- inductively coupled plasma

AES- atomic emission spectroscopy

OES- optical emission spectroscopy

HPLC- high performance liquid chromatography

UV- ultraviolet

Vis- visible

RF- radio frequency

Mp- melting point

^{o}C- degrees Celsius

TMACl- tetramethylammonium chloride

TMAOH- tetramethylammonium hydroxide

DAD- diode array detector

DSC- differential scanning colorimetry

TGA- thermogravimetric analysis

FBS- fetal bovine serum

gly- glycine

ala- alanine

im4COOH- imidazole-4-carboxylic acid

im2COOH- imidazole-2-carboxylic acid

Meim2COOH- 1-methylimidazole-2-carboxylic acid

MTT- thiazolyl blue tetrazolium bromide

Im- imidazole

λ_{max}- maximum wavelength

DMF- dimethylformamide

GSIS- glucose stimulated insulin secretion

ABSTRACT

Novel oxovanadium(IV) complexes of glycine, L-alanine, 1-methylimidazole-2-carboxylic acid, imidazole-2-caboxylic acid and imidazole-4-carboxylic acid were synthesized and isolated in the solid state. The ligands and complexes were characterized by elemental analysis, melting point, NMR, IR and UV-vis spectroscopy. The IR studies showed that glycine and L-alanine coordinate monodentately through the amine nitrogen whilst the imidazole-carboxylic acid derivatives assume a bidentate chelation. The electronic spectroscopic studies indicate distorted octahedral geometry for the oxovanadium complexes of amino acids and a square pyramidal geometry for oxovanadium(IV) complexes of imidazole carboxylic acid derivatives.

The reaction of vanadyl (VO^{2+}) with glycine, L-alanine, imidazole-2-cabrboxylic acid, imidazole-4-carboxylic acid and 1-methylimidazole-2-carboxylic acid was studied in aqueous solution by pH-potentiometry under oxygen and carbon dioxide-free conditions. The data obtained from these titrations were used to calculate the protonation and stability constants. The results showed that all ligands are suitable for bidentate coordination in the formation of monomeric species although the solid state studies of the oxovanadium(IV) complexes of amino acids showed a monodentate coordination. The overall stability constants for the ($V^{IV}O$)-L-alanine system (log β_{120} = 18.27(6)), ($V^{IV}O$)-glycine system (β_{120} = 17.22(6)), ($V^{IV}O$)-imidazole-4-carboxyic acid (β_{120} = 11.38(8)), ($V^{IV}O$)-imidazole-2-carboxylic acid (β_{120} = 11.62(6)) and ($V^{IV}O$)-1-methylimidazole-2-carboxylic acid (β_{120} = 15.49(9)) were obtained. The calculations for the species distribution in the experimental pH range showed that the neutral *bis*-coordinated complexes are dominant over the biological pH range.

The glucose uptake effect of oxovanadium(IV) complex of L-alanine, imidazole-4-carboxylic acid, imidazole-2-carboxylic acid and 1-methylimidazole-2-carboxylic acid was investigated using 3T3-L1 adipocytes, Chang liver and C2C12 muscle cells at various concentrations. The compounds had significant glucose uptake on Chang liver cells only at a concentration of 0.1-10 µM whilst in the C2C12 muscle and 3T3-L1 cells the compounds showed little to no activity probably due to the lower concentrations employed as a result of the cytotoxicity of these compounds on these two cell lines.

Keywords: diabetes mellitus, vanadium, amino acid, imidazole, stability constant, speciation.

CONTENTS

CHAPTER 1

INTRODUCTION

1.1 Diabetes mellitus

Diabetes mellitus is a chronic metabolic disorder that occurs either when the pancreas does not produce enough insulin or when the body cannot effectively use the insulin it produces. Insulin is a hormone that regulates blood sugar. The body of a diabetic patient does not produce or use the insulin necessary to stimulate the uptake of glucose, fatty acids and amino acids from the blood circulation for storage or utilization.[1] For the function and survival of all organs, a continuous supply of the correct amounts of glucose is essential. Undersupply of glucose (hypoglycamia) leads to apoptosis (cell death) and oversupply (hyperglycaemia) leads to various organ damages. It is therefore necessary to maintain the physiological blood concentrations regulated at the optimal level of around 5 mM.[2]

Apart from the intake of food, glucose may also be synthesized from lactate or alanine (gluconeogenesis). In all these processes insulin plays a central role, and its lack, insufficient supply or insufficient recognition by cell receptors causes the chronic disease diabetes mellitus. The lack of insulin causes uncontrolled degradation of fat since lipolysis is not inhibited and thus production of acetyl-coenzyme-A in amounts which can no longer be tackled by the citric acid cycle. As a consequence, ketonic bodies such as acetoacetic acid become the main factor responsible for severe damage of the peripheral blood vessels, creating extensive open wounds and necroses mainly at the limbs.[2] Another typical symptom of diabetes mellitus is diabetic retinopathy, a severe damage of the view (blurred vision and blind spots) caused by destruction of the small blood vessels in the retina, finally leading to blindness. Other complications associated with diabetes are kidney failure, heart disease and neuropathy.[1]

The first symptoms are related to the direct effects of high blood sugar levels. When the blood sugar level rises above 160 to 180 mg/dL, sugar spills into the urine.[2] When the level of sugar in the urine rises even higher, the kidneys excrete additional water to dilute the large amount of sugar. People with diabetes urinate large volumes frequently (polyuria) since the kidneys produce excessive urine. The excessive urination creates abnormal thirst (polydipsia). Diabetic people lose weight because excessive calories are lost in the urine. To compensate for this, diabetic people often feel excessively hungry.

1.1.1 Forms of diabetes

There are many types of diabetes that result from specific conditions such as maturity-onset diabetes of youth, surgery, medications, infections, pancreatic disease, and other illnesses. The most common forms of diabetes mellitus are classified as type 1 or type 2. Gestational diabetes is another form of glucose intolerance which is diagnosed during pregnancy. It is hyperglycemia with onset or first recognition during pregnancy and is common among obese women and women with a family history of diabetes. Immediately after pregnancy, 5% to 10% of women with gestational diabetes are usually found to have type 2 diabetes.[3]

(a) Type 1

This type of diabetes was previously called insulin-dependent diabetes mellitus (IDDM) or juvenile-onset diabetes. It develops when the body's immune system destroys pancreatic beta cells, the only cells in the body that make the hormone insulin to regulate blood glucose. This form of diabetes usually strikes children and young adults, although disease onset can occur at any age. In adults, type 1 diabetes accounts for 5% to 10% of all diagnosed cases of diabetes. Risk factors for type 1 diabetes mellitus may be autoimmune, genetic, or environmental.[1]

The principal treatment of type 1 diabetes mellitus, even in its earliest stages, is the delivery of artificial insulin *via* injection combined with careful monitoring of blood glucose levels using blood testing monitors. Without insulin, diabetic ketoacidosis often develops which may result in coma or death. Treatment emphasis is now also placed on lifestyle adjustments such as diet and exercise although these cannot reverse the progress of the disease. Apart from the common subcutaneous injections, it is also possible to deliver the insulin by a pump, which allows continuous infusion of insulin 24 hours a day at preset levels and the ability to program doses of insulin as needed at meal times. An inhaled form of insulin was approved by FDA in January 2006, although it was discontinued for business reasons in October 2007.[1] Non-insulin treatments, such as monoclonal antibodies and stem-cell based therapies, are effective in animal models but have not yet completed clinical trials in humans.[3]

(b) Type 2

This type of diabetes was formerly called non-insulin-dependent diabetes mellitus (NIDDM) or adult-onset diabetes mellitus. It results from the body's ineffective use of insulin. Type 2 diabetes mellitus is mainly due to insulin resistance or reduced insulin sensitivity, combined with relatively reduced insulin secretion which in some cases becomes absolute. The defective responsiveness of the body tissues to insulin almost certainly involves the insulin receptor in the cell membranes. However, the specific defects are not known but the low receptor density is due to destruction by ketonic bodies. In the early stages of type 2 diabetes, the predominant abnormality is reduced insulin sensitivity, characterized by elevated levels of insulin in the blood. At this stage hyperglycaemia can be reversed by a variety of measures and medication that improve insulin sensitivity or reduce glucose production by the liver. As the disease progresses, the impairment of insulin secretion worsens and therapeutic replacement of insulin often becomes necessary.

Type 2 diabetes mellitus comprises 90% of people with diabetes around the world, and is largely as a result of excess body weight and physical inactivity.[3] Many people destined to develop type 2 diabetes spend many years in a state of pre-diabetes, a condition that occurs when a person's blood glucose levels are higher than normal but not high enough for a diagnosis of type 2 diabetes. As of 2009 there are 57 million Americans who have pre-diabetes.[1]

1.1.2 Statistical epidemiology

Diabetes mellitus is becoming a major health concern for low and middle income countries,[5] as well as developed countries. Currently, more than 6% of the population of developed countries are estimated to have diabetes.[4] In underdeveloped countries, the many undiagnosed diabetic individuals make estimation difficult. World Health Organisation (WHO) estimates that more than 220 million people have got diabetes and the number is set to double by the year 2030.[5] In 2005, an estimated 1.1 million people died from diabetes with a projected rise of 50% in deaths in 10 years time. Almost 80% of diabetes deaths occur in low and middle income countries and half of diabetes deaths occur in people under the age of 70 years, with 55% of diabetes deaths being women.[5] The greatest increase in prevalence is, however, expected to occur in Asia and Africa.[4] The increase in incidence of diabetes in developing countries follows the trend of urbanisation and lifestyle changes, perhaps most importantly a "Western-style" diet. The severity of diabetes is illustrated by figure 1.1.

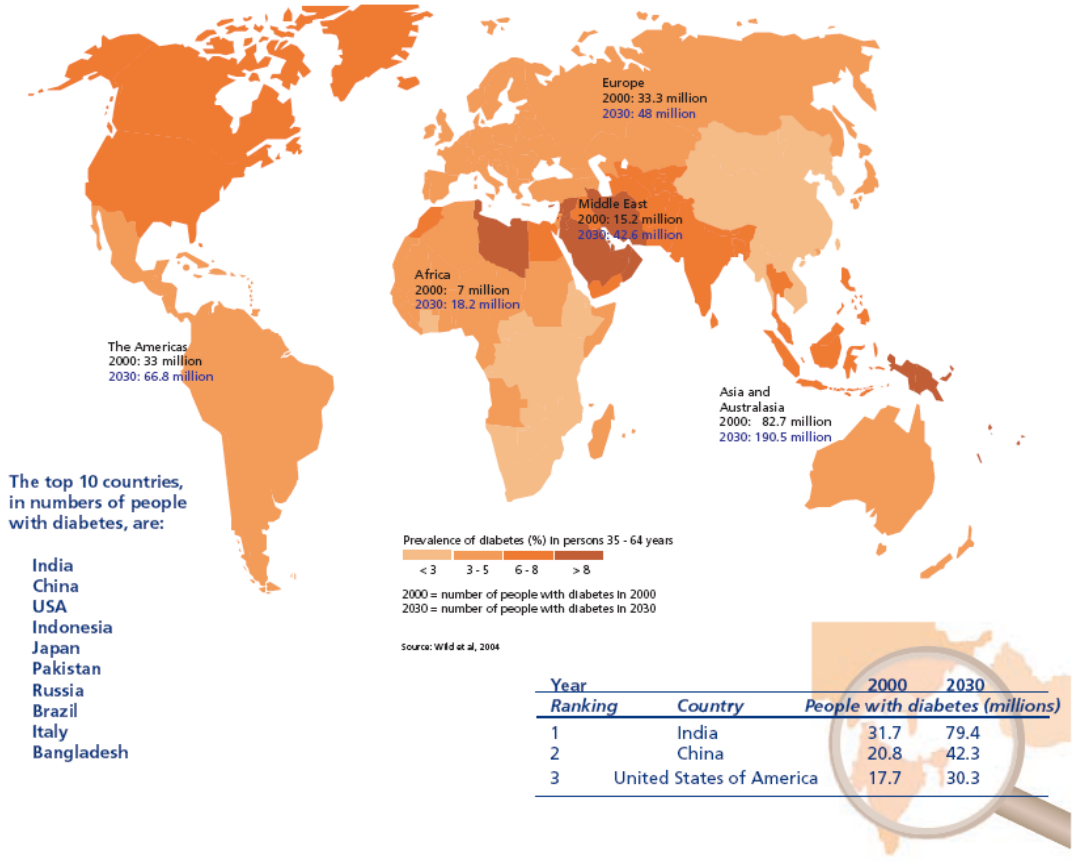

Figure 1.1: Population distribution map of people suffering from diabetes[5]

1.1.3 Current therapy

There is currently no practical cure for diabetes but it can be controlled. The fact that type 1 diabetes is due to failure of the beta cells in the pancreas led to the study of several possible strategies to cure this form of diabetes either by replacing the pancreas or just the beta cells.[4] In 1921 Banting and Best isolated insulin and demonstrated its ability to lower blood glucose levels.[3] However, with obesity frequently being the resulting cause of diabetes, the first approach in treatment should include a healthy diet and exercise plan that will lead to weight reduction.[6] A diet alone is often not always sufficient for glycaemic control until it is coupled with anti-diabetic drugs and occasionally painful insulin injections.[7]

(a) Insulin

Insulin is the principal hormone that regulates uptake of glucose from the blood into most cells, primarily muscle and fat cells but not central nervous systems. Therefore the deficiency

of insulin or insensitivity of its receptors on cell membranes plays a central role in all forms of diabetes mellitus. Insulin is released into the blood by beta cells, found in the Islets of Langerhans in the pancreas, in response to rising levels of blood glucose, typically after eating. Insulin is used by about two-thirds of the body's cells to absorb glucose from the blood for use as fuel, conversion to other needed molecules, or for storage. Insulin is the principal control signal for conversion of glucose to glycogen for internal storage in liver and muscle cells. Lowered glucose levels result both in the reduced release of insulin from the beta cells and in the reverse conversion of glycogen to glucose. This is mainly controlled by the hormone glucagon which acts in an opposite manner to insulin.[3] Insulin is utterly necessary for controlling type 1 diabetes and the artificial form is usually derived from pork or beef. Insulin is often administered as a complex with protamine and zinc. This slows down its action, providing longer glucose control.[3]

(b) Sulfonylureas

Sulfonylureas are a class of drugs that treat type 2 diabetes.[1] The discovery of sulfonylureas was by chance. It was observed that certain sulphonamide antibacterials often resulted in hypoglycaemia and hence non-antibacterial sulfonylureas which reduced blood glucose levels were developed.[9] These drugs only function by stimulating the release of endogenous reserves of insulin from the pancreas and are therefore only effective in patients who are still able to synthesize and secrete insulin.[3] Examples of such drugs are glybenclamide and tolbutamide (see figure 1.2). Unfortunately, sulfonylureas do not always succeed in controlling diabetes. With sulfonylurea therapy, some 10% to 20% of type 2 diabetic patients immediately fail to control their blood glucose levels adequately on the highest recommended dose, a situation called "primary failure".[1]

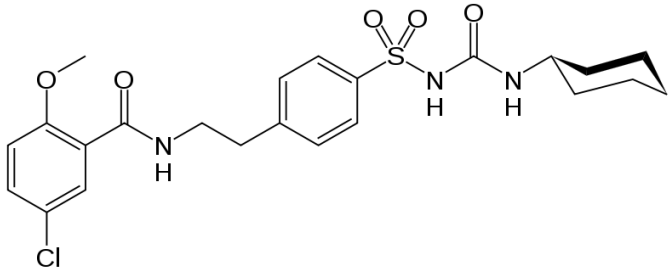

Glybenclamide

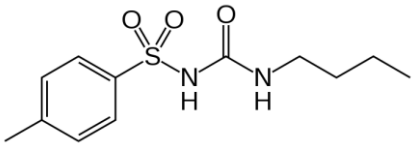

Tolbutamide

Figure 1.2: Chemical structures of sulfonylureas

Sulfonylureas themselves tend to overwork the pancreas until it eventually "burns out" and is unable to secrete an adequate amount of insulin. Some 5% to 10% of patients who initially respond to sulfonylurea therapy subsequently fail to sustain the response each year, a situation called "secondary failure". About 80% to 90% of people with diabetes are obese and sulfonylureas tend to make them gain weight. Sulfonylureas can also cause hypoglycemia, abnormally low blood glucose level, which posses its own dangers.[1] The other side effects of sulfonylureas are the gastrointestinal distress, drowsiness, dizziness and skin reactions.

(c) Biguanides

It was found that a guanidine derivative lowered blood glucose levels in rabbits.[1] This led to the development of phenformin and metformin that make muscle and fat cells more sensitive to insulin in the bloodstream, resulting in better glucose uptake. Unlike sulfonylureas, biguanides lower blood glucose levels without stimulating the release of insulin from the pancreas. The three proposed modes of action are[3]:

1. inhibition of intestinal transport and absorption of sugars
2. inhibition of gluconeogenisis at the liver
3. effect metabolism in peripheral tissues by enhancing the uptake of glucose.

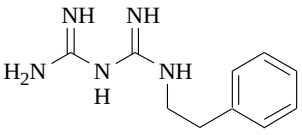

phenformin

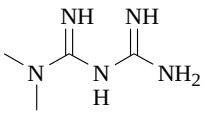

metformin

Figure 1.3: Chemical structures of biguanides

The side effects of biguinides are weight loss, decrease in absorption of folic acid and vitamin B12, stomach pain and gastrointestinal effects such as anorexia, flatulence and metallic taste.

(d) Thiazolidinediones

Thiazolidinediones (TZDs), also known as glitazones, act on target tissues to decrease resistance of insulin. They bind to PRAY, a type of nuclear regulatory protein involved in transcription of genes regulating glucose and fat metabolism.[9] Examples of glitazones are rosiglitazone (Avandia) and pioglitazone (Actos) (see figure 1.4).

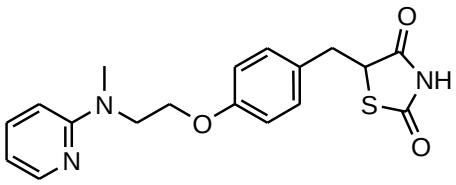

rosiglitazone

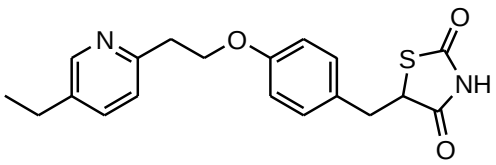

pioglitazone

Figure 1.4: Chemical structures of glitazones

As a result of multiple retrospective studies, there is concern about rosiglitazone's safety. Although it is established that this class of drugs has a beneficial effects on diabetes, there is concern about the increase in the number of severe cardiac events in patients taking it.[11] The safety of rosiglitazone arose when a retrospective meta-analysis was published in the New England Journal of Medicine.[10] There have been a significant number of publications since then, and a Food and Drug Administration panel[14] voted (20:3) with some controversy that available studies supported a signal of harm and yet voted (22:1) to keep the drug on the market. The meta-analysis was not supported by an interim analysis of the trial designed to evaluate the issue, and several other reports have failed to conclude the controversy. This weak evidence for adverse effects has reduced the use of rosiglitazone, despite its important and sustained effects on glycaemic control.[12] Safety studies are continuing. In contrast, at least one large prospective study has shown that pioglitazone may decrease the overall incidence of cardiac events in people with type 2 diabetes who have already had a heart attack.[13] Some other adverse reactions of the glitazones are edema, anemia and weight gain.

(e) Meglitinides

Meglitinides lower blood glucose by stimulating the release of insulin from the pancreas. It achieves this by closing adenosine triphosphate (ATP)-dependent potassium channels in the membrane of the beta cells. This depolarizes the beta cells, opening the cells' calcium channels, and the resulting calcium influx induces insulin secretion.[1] Examples of meglitinides are repaglinide (prandin) and nateglinide (starlix).

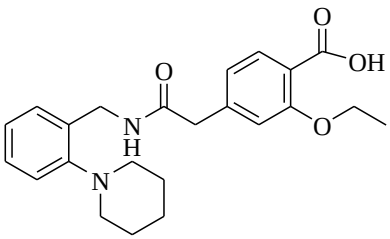

Repaglinide

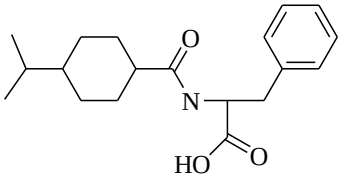

nateglinide

Figure 1.5: Chemical structures of meglitinides

Meglitinides are taken with or shortly before meals to boost the insulin response to each meal. If a meal is skipped, the medication is also skipped. The adverse reactions of meglitinides are weight gain and hypoglycemia.

Several shortcomings are associated with all these type 2 drugs, therefore it is necessary to design new drugs with improved side-effect profiles.

1.2 Vanadium in treatment of diabetes mellitus

The investigation of the biochemistry of vanadium has only recently begun to catch up to that of its transition metal neighbours in the first row. Vanadium compounds are being considered for mitigating insufficient insulin response in diabetes mellitus. They cannot, however, entirely substitute for lack of insulin (as in type 1 diabetes) but can reduce reliance on exogenous insulin or perhaps substitute for other oral hypoglycaemic agents used in treatment of type 2 diabetes.[14-16] Inorganic salts of vanadium have shown promising insulin-enhancing effects but the potential toxicity of vanadate and low absorption rate of vanadyl sulfate have pushed the focus towards designing new organovanadium compounds.[17,18] In the development of oral anti-diabetic drugs, tailoring of the properties of these vanadium complexes can be achieved by simple modification of the organic carrier ligand.

Vanadium is by no means the only metal that has therapeutic effects for the treatment of diabetes mellitus. Metals or minerals which have anti-oxidant status such as copper, manganese, zinc and selenium exhibit increased sensitivity to insulin.[19] However, the American Diabetes Association does not recommend supplementation of metals by patients with diabetes due to a possibility of them becoming pro-oxidant at higher doses and only recommends supplementation in the form of dietary habits to include food richer in metals.

The role of chromium in glucose metabolism has also resulted in the marketing of chromium as a nutritional supplement with chromium picolinate being available over the counter in a form of pills, sports drinks and nutrition bars.[19]

The interest in vanadium chemistry was initiated by the discovery that the vanadate ion was a potent inhibitor of protein tyrosine phosphatases.[20] Vanadium has been implicated in performing many functions of insulin such as inhibition of lipolysis and gluconeogenesis as well stimulating lipogenesis and cellular glucose uptake, hence its compounds are referred to as insulin-mimetics.[2,21,22] Several vanadium compounds seem to have insulin-enhancing effects due to their ability to mediate signal transduction downstream of the insulin signalling pathway through post-insulin receptor kinase mechanism (by inhibiting phosphatases).[23] The following section will briefly describe a selected few of such compounds.

1.2.1 Anti-diabetic vanadium compounds

In 1897-98, aqueous solutions of sodium vanadate were tested with respect to vanadium's possible benefits in the treatment of 44 test subjects with various health problems including anemia, tuberculosis, rheumatism, arnyotrophia, hysteria, neurasthenia and diabetes.[24] The test subjects were treated orally over 24 hours, and three times per week, with 4-5 mg of $Na[VO_3]$ dissolved in water prior to meals. All the patients showed an increase in appetite, a gain in weight, and an improvement in their physical status. For the diabetic patients, a slight decrease in blood sugar was observed for two out of three patients. This was the first report on the possible benefits of vanadate in the treatment of diabetes mellitus.[25] The medication of humans with vanadate has been resumed only sporadically, probably due to the toxicity of vanadate in non-physiological doses.[2] The *in vivo* effects of vanadate in streptozotocin (STZ)-induced diabetic rats was first reported by Heyliger *et al*[26] and Meyerovitch *et al.* [27] Vanadyl sulfate was shown to have comparable effects in STZ rats.[28] Vanadyl sulfate is advantageous over vanadate because it is sufficiently less toxic but its disadvantage is its low rate of absorption in the gut, estimated to be less than 1% of the dose. The unsatisfactory absorption is due to the formation of insoluble vanadyl hydroxides under the slightly alkaline conditions (see section 1.3.3) in the small intestine.

The potential toxicity of vanadate and the very low absorption rate of the less toxic vanadyl sulfate also exclude these inorganic salts from potential use as anti-diabetic drugs. As an alternative, vanadium coordination compounds containing organic ligands have been developed and tested. It is important that these ligands should not pose a threat to the body

once cleaved from the vanadium ion in the bloodstream since these are prodrugs and the necessary metabolite is vanadium in a form of vanadate. The successful vanadium complexes contain organic ligands that are reasonably soluble in both organic and aqueous environments and which are compatible with human metabolism. The recent successes achieved with organo-vanadium complexes suggest that modification of the metal ion chemistries by the organic ligands not only increased absorption and therefore efficacy but also decreased toxicity.[29] As oral anti-diabetic drug candidates all the vanadium complexes should have the desirable properties of an oral drug namely low molecular weight, water solubility, balanced lipophilicity and/or hydrophility, neutral charge and thermodynamic stability. Among others, the following organo-vanadium compounds have been studied extensively.

(a) *Bis*(maltolato)oxovanadium(IV) and *bis*(ethylmaltolato)oxovanadium(IV) complexes

Bis(ethylmaltolato)oxovanadium(IV) (BEOV) was first synthesized in the late 1990s, as one in a series of compounds containing maltolato ligand variants. BEOV and BMOV (figure 1.6) consist of a vanadyl ion bound to the anion of ethylmaltol (3-hydroxy-2-ethyl-4-pyrone) and maltol (3-hydroxy-2-methl-4-pyrone) respectively. An interest in maltol, a flavoring agent to baked foods and some beverages, is partly due to its ability to deprotonate readily for the ease of coordination to the vanadyl ion and for its non-toxicity.

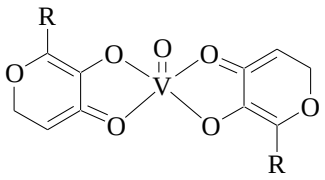

$R = CH_3$ BMOV
$R = C_2H_5$ BEOV

Figure 1.6: Chemical structures of BMOV and BEOV

BMOV is the most widely and intensively tested of the many proposed insulin mimetic vanadium complexes.[30] In addition to lowering glucose and lipid levels *in vivo* BMOV delays or prevents long term diabetes-induced pathology (including cardiomyopathy) and attenuates hyperinsulinemia and hyperlipidemia in genetically diabetic rats.[30] BEOV passed Phase I clinical trials where safety and tolerability of single escalating doses of orally administered 10 mg, 25 mg, 35 mg, 60 mg and 90 mg single doses were confirmed in non-diabetic volunteers.[15] BEOV is the only vanadium compound that has passed Phase II clinical trial where safety and efficacy was assessed in type 2 diabetic volunteers.[15] The overall bioavailability of vanadium from BMOV and BEOV was 2-3 times that from vanadyl sulfate.[15]

(b) *Bis*(picolinato)oxovanadium(IV) complex

Several oxovanadium(IV) complexes with a $VO(N_2O_2)$ chromophore have been proposed as insulin-enhancers. One example is *bis*(picolinato)oxovanadium(IV), $VO(pic)_2$, the synthesis of which was reported in 1964[31] but which was only recently characterized structurally and tested biologically.[32]

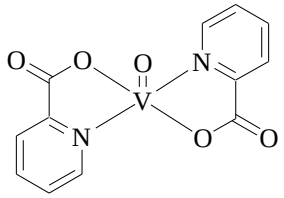

Figure 1.7: Chemical structure of *bis*(picolinato)oxovanadium(IV) ($[VO(pic)_2]$)

The insulin-enhancing effects of picolinato chelates of oxovanadium(IV) have been clearly shown to be dependent on dose as well as delivery method. When $[VO(pic)_2]$ was admitted orally to STZ-induced diabetic rats (0.2 $mmol.kg^{-1}$ for 2 days followed by 0.1 $mmol.kg^{-1}$ for 11 days), plasma glucose levels normalised while plasma insulin levels increased.[31] However, when administered as a solution (2.4 mM), as a substitute for drinking water, only glucose-lowering tendencies and not insulin-elevation was observed. The latter method was also accompanied with signs of gastrointestinal irritation.[31] On the other hand, comparing $[VO(pic)_2]$ with BMOV,[32] the picolinate complex had lower solubility and more gastrointestinal irritation for an equivalent dose, suggesting that there is room for further structural improvement in order to increase bioavailability and lessen side effects.

(c) *Bis*(pyridinonato)oxovadium(IV) complex

1,2-dimethyl-3-hydroxy-4-pyridinone (dhp) is an acetogenin which occurs as a fungal carbohydrate metabolite and can be produced as a byproduct of fermentation. Like maltol, hdp can selectively alter the water-solubility, hydrolytic stability and lipophilicity of its metal complex.[31]

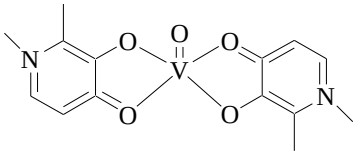

Figure 1.8: Chemical structure of $VO(dhp)_2$ complex

$VO(dhp)_2$ demonstrated its insulin-mimetic action in glucose uptake by primary isolated rat adipocytes and its capacity to inhibit free fatty acids release from these cells.[33] In fact, it presents a relevant inhibitory effect on lipolysis. Moreover it was found that it promotes total protein tyrosine phosphorylation, an evidence that this protein of the insulin signalling cascade is a target for its action. Thus $VO(dhp)_2$ appears as a promising candidate for the treatment of diabetes.

1.2.2 Mechanism of action of vanadium

The true form of the necessary vanadium species under physiological conditions is a subject of much debate but a focal mechanism of action which seems to enjoy a broad consensus is its involvement in the inhibition of phosphate-metabolizing enzymes.[2,21,22] The action of vanadium at an intracellular level is due to the structural similarity between phosphate and vanadate. Once the vanadium compounds are in the blood they may dissociate and vanadium is shuttled by proteins such as transferrin in the vanadate form ($H_2VO_4^-$) which is the species involved in the mechanism explained in figure 1.9.

Scenario **I:** Describes the situation prior to docking of insulin (In) to its receptor (IR).

Scenario **II**: Docking of insulin to the outside (α subunit) of its receptor leads to phosphorylation of tyrosine at the inside β subunit of the receptor, which initiates the phosphorylation of IRS. Phosphorylation of IRS in turn induces a signal transduction (zigzag arrow) by which Glut 4 is translocated to the membrane thereby internalising glucose (curved arrow). Glucose is either oxidized, metabolized to triglycerides or used up in glycogen synthesis.

Scenario **III**: In the absence of insulin, or in the case of a lack of insulin response (type 2 diabetes), autophosphorylation of the β subunit is counteracted by a protein tyrosine phosphatase (PTP), annulling the phosphorylation of IRS and thus the signal transduction (broken lines).

Scenario **IV:** Vanadium enters the cell by diffusion, endocytosis or via ion channels, such as phosphate channels (P/VCh) in the case of the vanadate, inhibiting the phosphatase and thus re-establishing signal transduction. Vanadate binds tightly in the active site of phosphatases forming hydrogen bonds with OH-, SH-, or N- functional amino acid side chains, and thus prevent phosphatases from hydrolyzing IRS and there is a crystal structure evidence of this interaction.[44] It has also been shown that wortmannin, a classical suppressor of insulin-

signaling activities, does not suppress IR and IRS phosphorylation stimulated by vanadium (or vanadium and insulin), providing evidence that vanadium compounds exert their activity at an early stage.

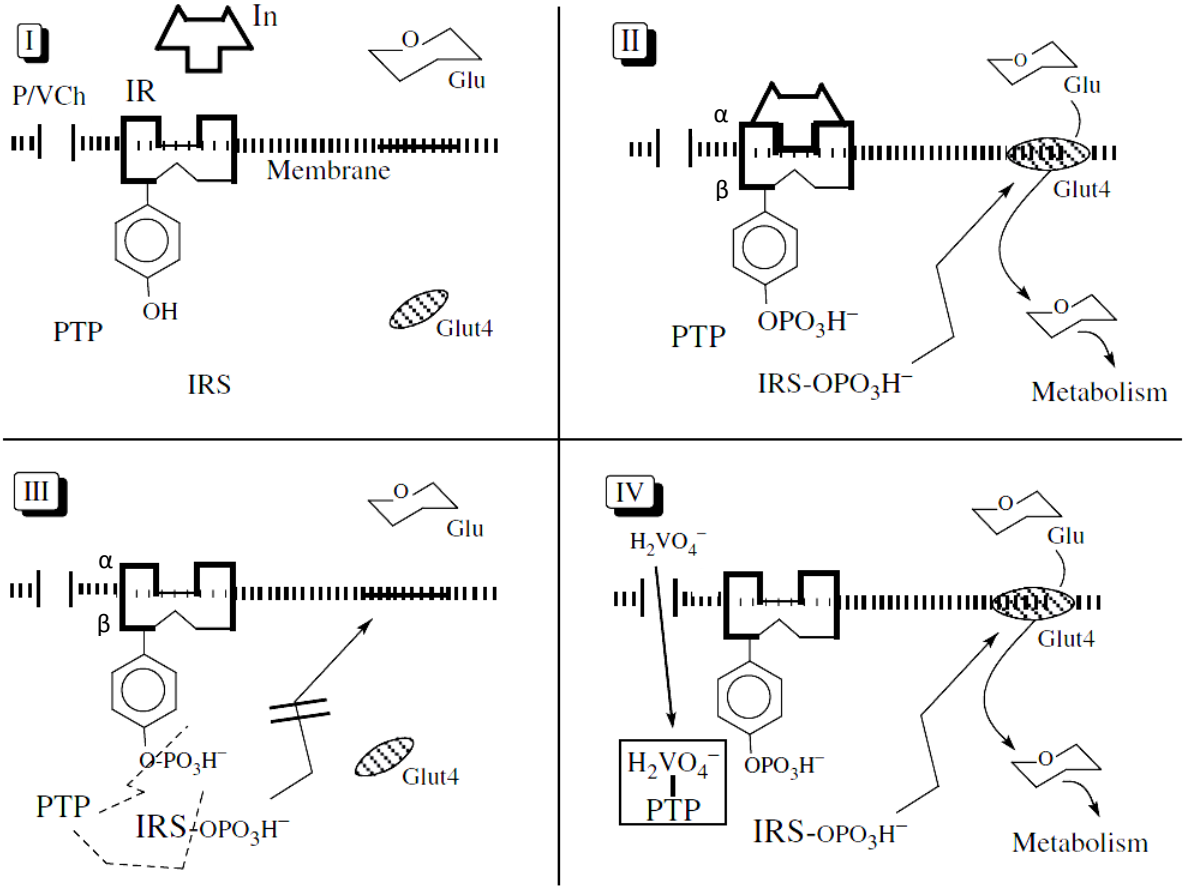

Figure 1.9: Mechanism of the stimulation of glucose uptake by insulin or vanadate.[2] In=insulin; IR=insulin receptor; P/VCh=anion channel for phosphate and vanadate; Glu= glucose; Glut 4 = glucose transporter 4; PTP = protein tyrosine phosphatase; IRS = insulin receptor substrates

1.3 Vanadium chemistry

Vanadium was named after Vanadis, the Scandinavian goddess of beauty, due to its display of colours in the different oxidation states, for example, +5 is yellow, +4 is blue, +3 is green and +2 is lavender.[2] Vanadium has an electronic configuration of $[Ar]d^3 4s^2$ in the ground state and can exist in eight oxidation states ranging from -3 to +5 but with the exception of -2.[34] Only the three highest oxidation states, +3, +4 and +5, are important in biological

systems.[36-38] The element was initially thought to have been discovered in 1801 by A.M del Rio in a sample of Mexican lead ore. He later withdrew his claim when it was incorrectly suggested by his peers that the sample he found was in fact lead chromate. In 1830, N.G Sefström rediscovered it in Swedish iron ore.[8]

Vanadium, element number 23 of atomic weight 50.94, is present at very low concentrations in plant and animal cells.[39] This transition metal is relatively abundant (~0.02%) in nature. Under physiological conditions it exists predominantly in the anionic form ($[H_2VO_4]^-$) with the oxidation state +5, or in the +4 oxidation state as the vanadyl cation (VO^{2+}). As with the other metal ions in biological systems vanadium is primarily complexed *in vivo*. In mammals, approximately 90-95% of the circulating vanadium in the bloodstream (32-95 pg/ml) is associated with plasma components such as transferrin, albumin and hemoglobin, as well as low molecular weight compounds such as glutathione.[40] It is believed to be nutritionally essential in mammals, but its specific biological use in humans is still to be elucidated. However, the total body pool of vanadium in humans is approximately 100-200 μg,[39] suggesting some importance.

1.3.1 Redox chemistry

The one-electron redox reactions for the three oxidation states of relevance are represented by the equations below.[2]

$$V^{V}O_2^{+} + 2H^{+} + e^{-} \rightleftharpoons V^{IV}O^{2+} + H_2O$$

$$[H_2V^{V}O_4]^{-} + 4H^{+} + e^{-} \rightleftharpoons V^{IV}O^{2+} + 3H_2O$$

$$V^{IV}O^{2+} + 2H^{+} + e^{-} \rightleftharpoons V^{3+} + H_2O$$

Table 1.1: Redox potentials for inorganic vanadium species and selected physiological systems versus the normal hydrogen electrode (NHE).[2]

Species	$\mathbf{E^{o}}$	$\mathbf{E^{pH=7}}$
VO^{2+}/V^{3+}	+0.359	-0.462
$H_2VO_4^{-}/VO^{2+}$	+1.31	-0.34
VO_2^{+}/VO^{2+}	+1.016	+0.19
O_2/H_2O_2	+0.695	+0.295
$\frac{1}{2}O_2/H_2O$	+1.23	+1.23

Table 1.1 reveals that, under aerobic conditions V^{V} is stable whereas in anoxic environments, which normally prevail in the cytoplasm reducing agents such as ascorbate and glutathione readily reduce $V^{V}O_2^{+}$ to $V^{IV}O^{2+}$, provided that the inorganic species are available as such, i.e. not complexed to ligands present in the intra- and extracellular fluids. Vanadate ($[H_2VO_4]^{-}$) is less readily reduced, and the reduction of $V^{IV}O^{2+}$ to V^{3+} does not take place under common conditions. V^{III} is therefore of minor importance when it comes to physiological actions of vanadium, with the exception of ascidians and Polychaeta fan worm systems where this oxidation state is the predominant one.[2]

1.3.2 Coordination chemistry

The coordination numbers of 5 and 6 are the most common in oxovanadium(IV) complexes, based on the VO^{2+} moiety.[41] Independent of the oxidation state, the coordination geometry for the five coordinate compounds is commonly square pyramidal, usually slightly distorted. The trigonal bipyramidal arrangement is less frequent. Typical bi- to tetradentate ligands used for the stabilization of the oxo- and dioxovanadium centers contain the O-donors (phenolate and carboxylate) and the N-donors (aromatic and aliphatic amines, and imine nitrogens).

The chemistry of the square pyramidal geometry has been well established with the oxygen of the oxovanadium(IV) unit in the apical position and the vanadium atom lying above the plane defined by the donor atoms of the four equatorial ligands. These square pyramidal complexes generally exhibit a strong tendency to remain five coordinate.[42] However, orange polynuclear linear chain structures (···V=O···V=O···) have been observed with 2-(2'-hydroxylphenyl)benzoxazole and 2(2-hydroxyphenyl)bezothiozole, as ligand.[42-45] The absorption band due to V=O stretching vibration of oxovanadium(IV) is usually observed at higher wavenumber compared to those of vanadate complexes. The V=O stretching vibration, however, is susceptible to a number of influences including electron donation from basal plane ligand atoms, solid state effects, and coordination of additional solvent molecules.

1.3.3 Solution chemistry

A vanadium complex that is to be used as an orally-administered drug for lowering glucose levels, must be thermodynamically stable in both acidic and neutral environments.[47] This stability is required because the vanadium complex must survive the digestion process in the stomach where the pH can be as low as 2.0, and must also remain intact under pH condition

of the intestines and be delivered into the bloodstream where the pH is 7.4. The determination of the thermodynamic stability of the vanadium complexes as a function of pH is a prerequisite for evaluating the usefulness of such complexes to serve as glucose-lowering drugs. It is therefore important to understand the aqueous chemistry of vanadium in order to design the correct ligands for the stabilization of vanadyl ions.

Acidification of vanadate(V) solutions yields yellow solutions of decavanadate, $[H_nV_{10}O_{28}]^{6-n}$ (n=0-3, depending on the pH) or for pH<2, the colourless hydrated dioxovanadium monocation, $[VO_2(H_2O)_4]^+$. If these V^V-containing solutions are reduced, gradual formation of vanadyl $V^{IV}O^{2+}$ (blue), V^{3+} (green) and V^{2+} (violet) occurs, again existing in the form of the aqua cations. V^{2+} is not stable in aqueous media, it is rapidly reoxidised to V^{3+} by protons. In aqueous solutions containing the V^{3+} the following octahedral species, depending on pH and concentration, can be present; $[V(H_2O)_6]^{3+}$, $[V(OH)(H_2O)_5]^{2+}$, $[V(OH)_2(H_2O)_4]^+$ and $[\{V(H_2O)_5\}_2(\mu\text{-}O)]^{4+}$. The only vanadium oxidation states relevant to the biological systems are +3, +4 and +5. At concentrations less than 1 nM, the oxo-bridged dinuclear complex can be neglected.[2] The equations below[47] show the acid-base equilibria of the mononuclear V(III) species.

$$[V(H_2O)_6]^{3+} + H_2O \rightleftharpoons [V(OH)(H_2O)_5]^{2+} + H_3O^+ \qquad (pK_{a1}=2.7)$$

$$[V(OH)(H_2O)_5]^{2+} + H_2O \rightleftharpoons [V(OH)_2(H_2O)_6]^+ + H_3O^+ \qquad (pK_{a2}=4.0)$$

The presence of sulfate in acidic solutions of V^{3+} leads to the formation of aqua-sulfato complexes which is of interest in the light of the conditions in the vanadium containing blood cells of ascidians.[48]

$$[V(SO_4)(H_2O)_5]^+ + H_2O \rightleftharpoons [V(SO_4)(OH)(H_2O)_4] + H_3O^+ \qquad (pK_a=3.35)$$

In contrast to V^{III}, V^{IV} forms monooxo complexes in aqueous media, based on the stable vanadyl ion, VO^{2+}. The vanadyl ion remains in solution only under sufficiently acidic conditions as shown below.[2]

$$[VO(H_2O)_5]^{2+} + H_2O \rightleftharpoons [VO(OH)(H_2O)_4]^+ + H_3O^+ \qquad (pK_a=6.0)$$

$$2[VO(H_2O)_5]^{2+} + 2H_2O \rightleftharpoons [\{VO(H_2O)_4(\mu\text{-}OH)\}_2]^{2+} + 2H_3O^+ \qquad (pK_a=6.9)$$

Precipitation of insoluble hydroxide, $VO(OH)_2$, (see equations below) and formation of oligonuclear hydroxo species such as $\{[(VO)_2(OH)_5]^-\}_n$ begins above pH 5. Concomitantly, $[VO(OH)_3]^-$ starts to be present at nanomolar concentrations, gaining importance at pH 10 and above.

$$[VO(OH)(H_2O)_4]^+ + H_2O \rightleftharpoons H_3O^+ + [VO(OH)_2(H_2O)_3]=VO(OH)_2$$

$$VO(OH)_2 + OH^- \rightleftharpoons [VO(OH)_3]^-$$

All vanadium(V) species present in water at ambient pH are anionic. The cationic VO^{3+} and VO_2^+ exist only when they are stabilised by ligands. At pH 7, the diprotonated forms $[H_2VO_4]^-$ (pK_a=8.17) and $[H_2V_2O_7]^{2-}$ (pK_a=8.50) for physiological ionic strength predominate. As far as monovanadate is concerned, this is of interest in the context of its similarity with phosphate which, at pH 7, is present mainly in its monoprotonated form, i.e. $[HPO_4]^{2-}$ (pK_a of $[H_2PO_4]^-$ = 6.7). In the medium to strong alkaline range, only mono- and divanadate exist. On acidification, decavanadate forms starting at pH 6. Below pH 3, decavanadate becomes unstable and $[VO_2(H_2O)_4]^+$ begins to form and below pH 2 this is the only cationic species that can exist.[48] Although thermodynamically unstable above pH 6, decavanadate breaks down slowly in the mildly alkaline region to form lower nuclearity vanadates.

Ligands such as maltol, ethylmaltol, picolinic acid and 1,2-dimethyl-3-hydroxy-4-pyridinone have been used to stabilize vanadium under aqueous conditions. The stability of these complexes in aqueous medium and under physiological conditions enables the vanadium to be shuttled from the stomach *via* the intestines into the bloodstream. The pH-metric chemical speciation of the vanadium compounds can be appropriately designed through the correct combination of donor atoms involved in the bidentate coordination of the ligands in order to achieve the requisite stabilization under the physiological pH range. The imidazole-carboxylic acids and amino acids are simple ligands which have been used in this work for testing the ability of (N,COO^-) donor set for stabilizing $V^{IV}O$.

1.4 Biospeciation of vanadium

Long-term supplementation with vanadium revealed that vanadium is stored in several organs including the liver, kidney, spleen, bone, heart and muscles.[49] The main source of vanadium

is from food (e.g mushrooms, fish, black pepper, fresh fruits and parsley), even though most foods contain low quantities (< 1 $ng.g^{-1}$).[50] Vanadium is poorly absorbed in living systems, with only less than 1% of an oral dose being absorbed in the gastrointestinal tract.[31] The absorption, distribution, metabolism and excretion of vanadium compounds has been summarised schematically in Figure 1.10. Both anionic and cationic forms of vanadium have been detected in the bloodstream and both can penetrate the intracellular space by means of passive diffusion. Vanadium speciation in the blood is a vital process that determines what form of vanadium will enter the cells. Therefore determining what form the vanadium enters the bloodstream in and what form it takes upon interacting with blood serum proteins is vital in understanding the insulin-enhancing action of vanadium drugs.

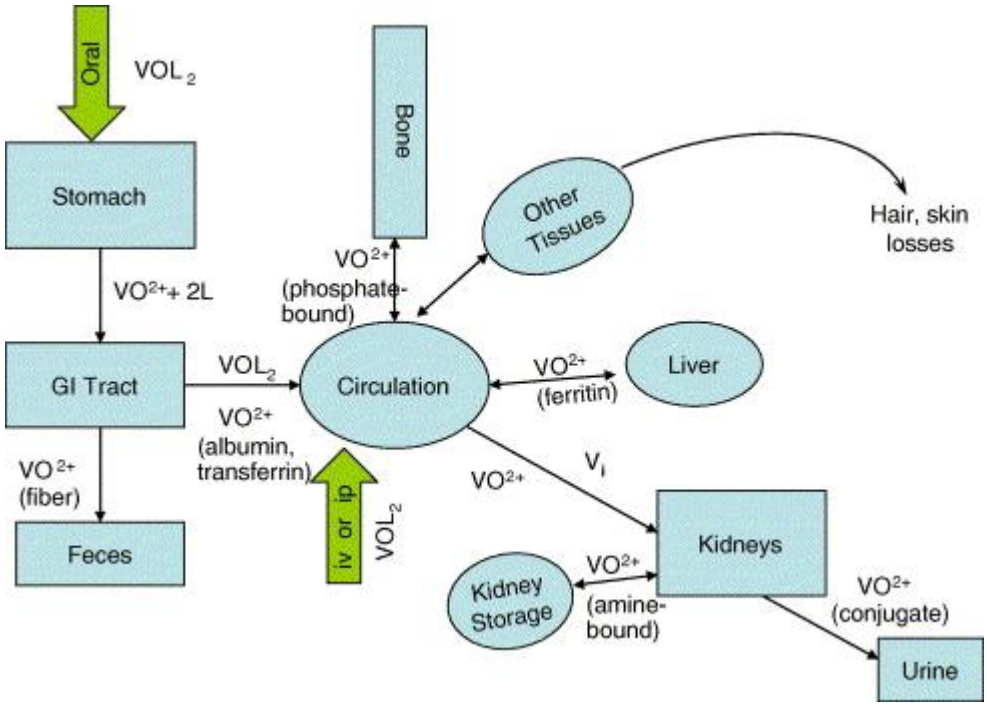

Figure 1.10: A schematic diagram showing the metabolic fate of oxovanadium compounds[15]

In the bloodstream vanadium comes into contact with high molecular mass (HMM) and low molecular mass (LMM) proteins. Complexation occurs with the blood proteins which facilitates cellular uptake. The two main HMM proteins are known as human transferrin (hTf) and human serum albumin (HSA). When hTf is loaded with an ion and it comes into contact with a receptor specific for hTf on a cell wall, hTf binds to that receptor. The hTf is taken into the cell by means of a vesicle where the internal pH of the vesicle is reduced by means of a hydrogen ion pump.[51] Human serum albumin (HSA) is the most abundant protein in the

blood and has a variety of functions including the transport of various hormones and the transport of drugs.[52] HSA also interacts with vanadium species in the blood.

Studies[53,54] using blood circulation monitoring-electron paramagnetic resonance (BCM-EPR) have shown that the majority of vanadium in the blood binds to hTf (approx 77%), therefore it is safe to designate hTf as the primary transport protein for vanadium. It has also been shown that hTf can bind the metal ion far more strongly than HSA despite the fact that HSA is the most abundant HMM serum protein. Results from both CD and EPR spectroscopic data show that complexation occur between hTf and $V^{IV}O$ and that the reactions result in ternary complexes.[53] The ternary complexes are in the form; $(V^{IV}O)hTf(L)$, $(V^{IV}O)_2hTf(L)_2$ and $(V^{IV}O)_2hTf(L)$, where L is a bidentate carrier ligand. Figure 1.11 shows some proposed equilibria and ternary complexes of $V^{IV}O$ formed with serum proteins and carrier ligands in the blood serum.[53] The strength of the bond between VO^{2+} and the carrier ligand play a role in the speciation within the blood.

(1) $(V^{IV}O)apoTf(L) + L \rightleftharpoons apoTf + V^{IV}OL_2$

(2) $(V^{IV}O)_2apoTf(L)_2 + A \rightleftharpoons (V^{IV}O)apoTf(L) + V^{IV}OL_2$

(3) $(V^{IV}O)_2apoTf(L) + L \rightleftharpoons (V^{IV}O)apoTf + V^{IV}OL_2$

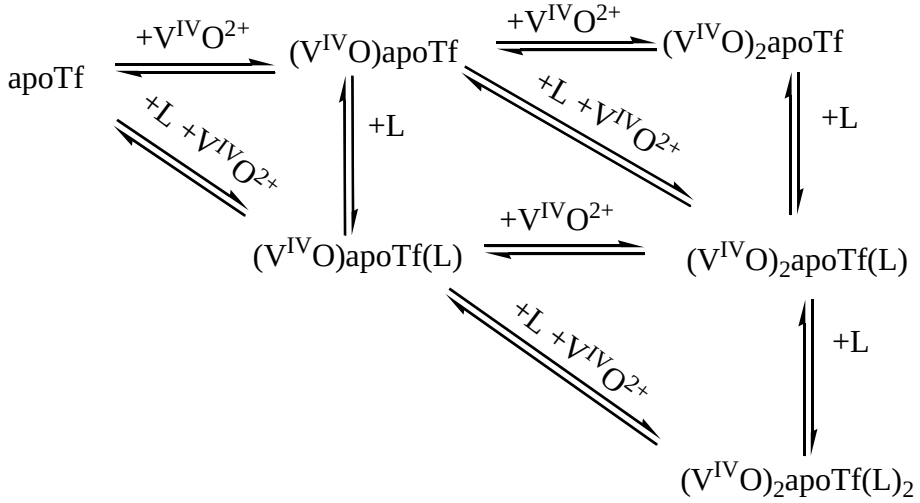

Figure 1.11: Various equilibra proposed for the formation of ternary complexes of $V^{IV}O$ with serum bioligands and carrier ligands (L)

The design of the organovanadium complexes should meet optimum conditions. The thermodynamic stability should not be weak because the complexes decompose before transportation into the blood circulation and it should not also be too strong because the

complexes should be able to dissociate to accommodate ligand substitution by bioligands (bL) and redox reactions. Figure 1.12 shows a simplified flow diagram of interactions between the absorbed vanadium prodrug, whether its carrier ligands are weak (for example picolinic acid), intermediate (for example maltol) or strong (for example dph), and the HMM and LMM serum proteins. The formed adducts are listed as well as their concentrations in comparison to each other.[54,55]

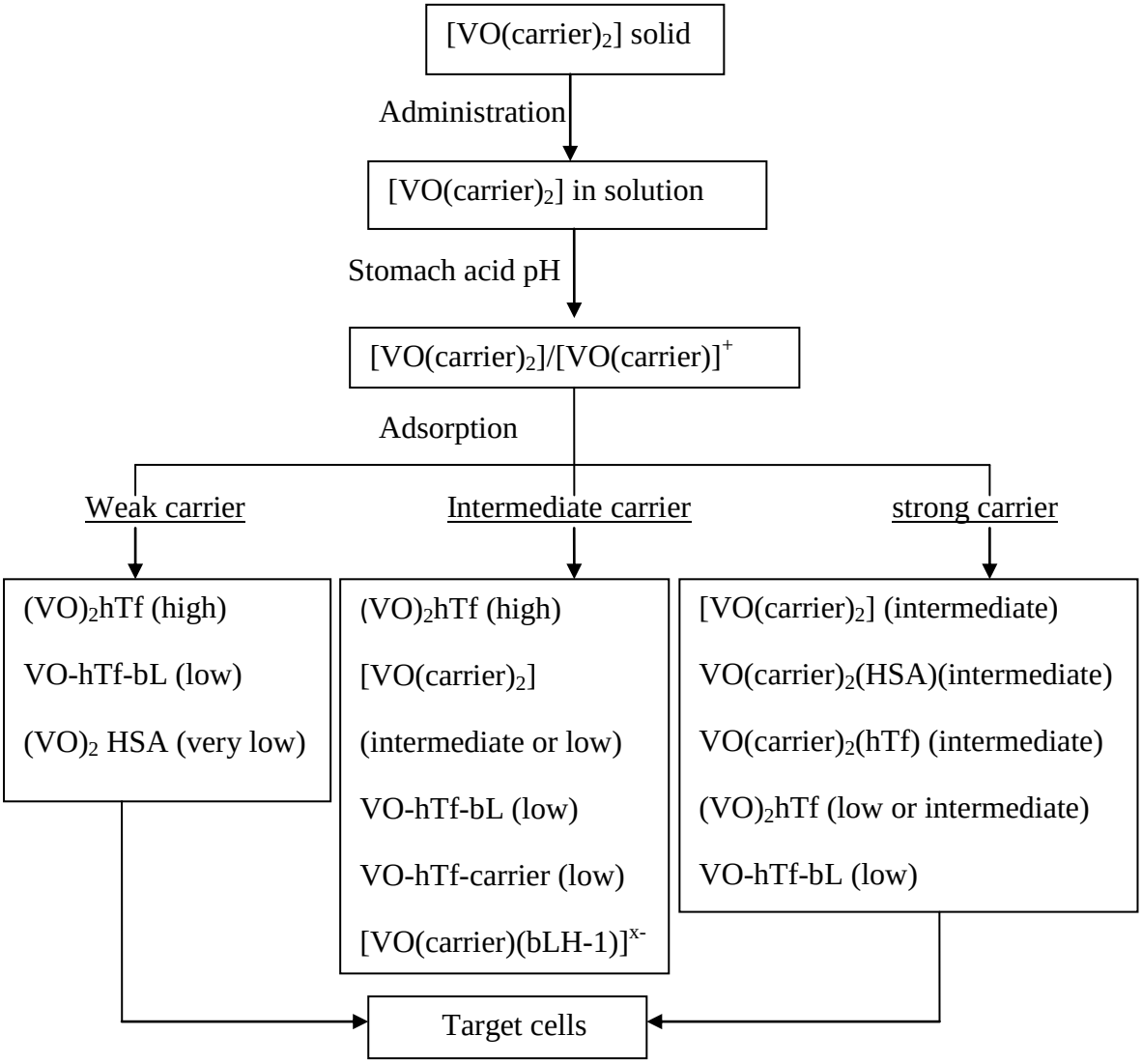

Figure 1.12: Speciation model of insulin-enhancing compounds of the type $VO(carrier)_2$, in the blood

The various studies mentioned have all had specific results in terms of the drugs that were tested, however similarities are indeed present, for example, all studies that dealt with the

binding of vanadium to hTf concluded that this HMM protein is the primary binder of vanadate in serum. This conclusion was apparent each time despite the more abundant HMM protein HSA. Different conclusions have been reached about whether or not (VO)-HSA adducts should be considered negligible. The key question is whether or not albumins' high concentration in the serum compensates for its weaker affinity for binding VO^{2+}.

There has, however, not been a study which relates the binding affinity of the carrier ligand to vanadium to the activity of these vanadium metallopharmaceuticals nor has there been a study that investigates the necessary therapeutic amounts of vanadium also in relation to the stability of the complexes. But these two abovementioned gaps as well as the biospeciation are deemed outside the scope of this investigation.

1.5 Objectives of the study

1. The synthesis of V(IV) complexes using amino acid derivatives as possible anti-diabetic pharmaceuticals will be carried out. The current prescription drugs (based on organic compounds) that are being used have toxic side effects including nausea, diarrhea, skin rash, weight gain, respiratory infections, liver damage and headache. Hence there is need for an alternative class of drugs that devoid these side effects. Inorganic salts of vanadium have shown promising insulin-enhancing effects but the potential toxicity of vanadate and low absorption rate of vanadyl sulfate have pushed the focus towards designing new organovanadium compounds.[17,18] The amino acids have been chosen as ligands because they are non-toxic biological molecules and the imidazoles are also found in many biological systems.

2. The thermodynamic stability of the vanadium(IV)-amino acid derivatives will be determined over a pH range of 2 to 11 using potentiometric acid/base titrations and HYPERQUAD to calculate the stability constants. Vanadium complexes that are to be used as orally-administered drugs for lowering glucose levels must be thermodynamically stable in both acidic and neutral environments.[47] This stability is required because the vanadium complex must survive the digestion process where the pH can be as low as 2.0 and must be delivered into the bloodstream where the pH is 7.4.

3. The species distribution diagrams will be generated in order to evaluate the species existing over the biological pH range. The species distribution plots of % vanadium as a

function of pH are important for evaluating the usefulness of such complexes to save as glucose lowering drugs.

4. The biological studies will be performed to determine the cytotoxicity and the glucose lowering effect of the synthesized vanadium complexes. The cytotoxicity and glucose uptake of the synthesized vanadium complexes will be studied using three primary cell culture lines, i.e muscle (C2C12), fat (3T3-L1) and liver (Chang) cells.

1.6 References

1. http://www.diabetesselfmanagement.com/articles/Diabetes_Definitions/Hypoglycemia (last accessed 15/09/2010).
2. Rehder D, (2008), *Bioinorganic Vanadium Chemistry, Wiley*, 157.
3. Burger A, (1981), In *Burger's Medicinal Chemistry, Part II, Wiley-Interscience*, **4**, 1302.
4. Saatchi K, Thompson K.H, Patrick B.O, Pink M , Yuen V.G , O'Neill J.H, Orvig C, (2005), *Inorg. Chem*., **44,** 2689.
5. Zimmet P, Alberti K. G. M. M, Shaw J, (2001), *Nature*, **414**, 782.
6. Panunti B, Jawa A. A, Fonseca V. A, (2004), *Drug Discovery Today*, **1**, 151.
7. Goc A, (2006), *Central European J. of Biol.*, **1**, 314.
8. Greenwood N. N, Earnshaw A, (2005), *In Chemistry of the Elements; Elsevier*, **2**, 23.
9. Rendell R, (2004), *Medscape Gen. Med.*, **6(3**), 9.
10. Nissen, Wolski K, (2007), *The New England J. Med.,* **353**, 2643.
11. Wood, Shelley (2007). *FDA Advisory Panels Acknowledge Signal of Risk With Rosiglitazone, but Stop Short of Recommending Its Withdrawal. Heartwire*.
12. Ajjan, Grant P. J, (2008), *Expert Opin. Drug Safety*, **7(4)**, 367.
13. Erdmann, Dormandy J. A, Charbonnel B, Massi-Benedetti M, Moules I. K, Skene A. M, (2007), *J. Am. Coll. Cardiol*., **49(17)**, 1772.
14. Thompson K. H, McNeill J. H, Orvig C, (1999), *Chem. Rev*., **99(9)**, 2561.
15. Thompson K. H, Lichter J, LeBel C, Scaife M. C, McNeill J. H, Orvig C, (2009), *J. Inorg. Biochem.*, **103(4)**, 554.
16. Bordbar A, Creagh A. L, Mohammadi F, Haynes C. A, Orvig C, (2009), *J. Inorg. Biochem*., **103(4)**, 643.
17. Cohen M. D, (1996), *Toxicol. & Ecotoxicol.*, **3(5)**, 132.
18. Setyawati I. A, Thompson K. H, Yuen V. G, Sun Y, Battell M, Lyster D. M, Vo C, Ruth T. J, Zeisler S, McNeill J. H, Orvig C, (1998), *J. Appl. Pysiol.*, **84(2)**, 569.
19. Meyer J. A, Spence D.M, (2009), *Metallomics*, **1**, 32.
20. Butler A. J, Carrano C. J, (1991), *Coord. Chem. Rev.*, ***109***, 61.
21. Shukla R, Blonde R. R, (2008), *Biometals*, **21**, 205.
22. Hiromura M, Adachi Y, Machida M, Hattori M, Sakurai H, (2009), *Metallomics*, **1**, 92.
23. Rehder D, (1995), *Met. Ions Biol. Syst*., 311.
24. Lyonnet B, Martz X, Martin E, (1899), *Presse Med*.,**1**, 191.
25. Hoppe G, Siemroth J, Damaschun F, (1990), *Chem Erde*, **50**, 81.

26. Heyliger E. C, Tahiliani A. A, McNeil J. M, (1985), *Science*, **227**, 1474.
27. Meyerovitch J, Farfel Z, Sack J, Shechter Y, (1987), *J. Biol. Chem*., **262**, 6658.
28. Ramadham S, Mongold J. J, Brownsey R. W, Cros G. H, McNeill J. H, (1989), *Am. J. Phsiol. Heart Circ. Physiol*., **257**,904.
29. Zhang S, Zhong X, Lu W, Zheng L, Sun F, Fu G, Zhang Q, (2005), *J. Inorg. Biochem*., **99**, 1064.
30. Burgess J, De Castro B, Oliveira C, Rangal M, Schlindwein W, (1997), *Polyhedron*, **16**, 789.
31. Thomson H. K, Orvig C, (2001), *Coord. Chem. Rev*., **1033**, 219.
32. H. Sakurai K, Fujii H, Watanabe H, Tamura, (1995), *Biochem. and Biophys. Res. Commun*., **214**, 1095.
33. Passadouro M, Metelo A. M, Melao A. S, Pedro J. R, Faneca H, Carvalho E, Margarida M, Castro C. A, (2010), *J. Inorg. Biochem*., **8**, 642.
34. Sanna D, Buglyo P, Micera G, Garribba E, (2010), *J. Biol. Inorg. Chem*., **15**, 825.
35. Wilkinson G, (1987), *Comprehensive coordination chemistry, Pergamon Pres., Oxford*, 1.
36. Butler A, Carrano C, (1991), *J. Coord. Chem. Rev.*, **109**, 61.
37. Chasteen N. D, (1990), *Vanadium in biological systems: Physiology and Biochemistry, Kluwer Accademy. Dordrecht*, 203.
38. Crans D. C, Amin S. S, Keramidas A. D, (1998), *Vanadium in the environment, Part One: Chemistry and Biochemistry, John Wiley& Sons, New York*, 11.
39. Shechter Y, Goldwaser I, Mironchik M, Fridkin M, Gefel D, (2003*), Coord. Chem. Rev*., **3,** 237.
40. Haratake M, Fukunaga M, Ono M, Nakayama M, (2005), *J. Biol. Inorg. Chem.*, **10**, 250.
41. Gätjens, J, Meir B, Adachi Y, Sakurai H, Rehder D, (2006), *Inorg. Chem*., 3573.
42. Page E. M, Wass S. A, (1997), *Coord. Chem. Rev*., **164**, 172.
43. Matthew M, Carty A. J, Palenik G. J, (1970*), J. Am. Chem. Soc*., **92**, 3197.
44. Peters K. G, Davis G. M, Howard B. W, Pokross M, Rastogi V, Diven C, Greis K. K, Eby-Wilkens E, Maier M, Evdokimov A, Soper S, Genbauffe F, (2003), *Biochem*., **96**, 321.
45. Guptalk S. K, Mishra K, (1978*), J. Inorg. Nucl. Chem*., **41**, 890.
46. Serrette P. J, Carrol T, Swager M, (1992), *J. Am. Chem. Soc*., **114**, 1887.

47. Fites R. F, Yeager A. T, Sarvela T. L, Howard W. A, Zhu G, Pang K, (2006), *Inorg. Chim. Acta,* **359**, 248.
48. Meier R, Boddin M, Mitzenheim S, Kanamori K, (1995), *Met. Ions Biol. Syst*., 74.
49. Mukherjee B, Patra B, Mahapatra S, Banerjee P, Tiwari A, Chatterjee M, (2004), *Toxicol. Lett*., **150**, 135.
50. Barceloux D. G, (1999), *J. Toxicol., Clin.,* **37**, 265.
51. Yang R, Arem R, Chan L, (1984), *Arch Intern Med.,***144(6)**, 1251.
52. Rajbar S, (1968), *Clin. Chim. Acta,* **22 (2)**, 296.
53. Kiss T, Jakusch T, Hollenders D, Dornyei A, Enyedy E. A, Pessoa J. C, Sakurai H, Sanz-Medel A, (2008), *Coord. Chem. Rev.*, **252**, 1153.
54. Sanna D, Buglyo P, Micera G, Garribba E, (2010) , *Inorg. Chem*., **49**, 174.
55. Jakusch T, Dean A, Oncsik T, Benyel A. C, Di Marco V, Kiss T, (2009), *Dalton Trans.*, **39**, 212.
56. Sanna D, Micera G, Buglyo P, Kiss T, Gajda T, Surdy P, (1998), *Inorg. Chim. Acta*., **268**, 297.

CHAPTER 2

EXPERIMENTAL TECHNIQUES AND METHODS

2.1 Instrumentation

The infrared spectra were recorded on a Perkin Elmer 400 FTIR spectrophotometer in the mid range (4000-400 cm^{-1}) as KBr pellets or as neat solids using a Perkin Elmer 100 ATR-FTIR. ^{1}H and ^{13}C NMR spectra were recorded on a Bruker AMX 400 NMR MHz spectrophotometer and results reported relative to tetramethylsilane (δ 0.00). Melting points were done using Gallenkamp Melting point apparatus equipped with a thermometer (0-400 ^{o}C). The vanadium content was determined using a Thermo Electron (iCAP 6000 Series) inductively Coupled Plasma (ICP) spectrophotometer equipped with an OES detector. Chromatographic separations were done on an Agilent 1100 High Performance Liquid Chromatograph (HPLC) fitted with a DAD detector and a Gemini C18 (100 mm x 4.6 mm x 5 µm) column. Solid reflectance spectra were recorded on the Shimadzu UV-3100 UV-vis-NIR spectrophotometer (1000-250 nm) fitted with a MPCF-3100 sample compartment. The samples were mounted between two quartz discs which fitted into sample holder coated with $BaSO_4$. Microanalysis was carried out using a Vario Elementar Microcube ELIII. Potentiometric studies were performed using a Metrohm 794 Basic Titrino equipped with tiamo version 1.2 and Metrohm LL electrode. The pH measurements were done using a Metrohm 827 pH lab meter. Analytical weights were measured on a Sartorius Micro electronic microbalance. A Bio-Tek KC4 powerwave XS microtiter plate reader was used to measure absorbance for 3-(4,5-dimethylthiazol-2-yl)-2,5-diphenyl tetrazolium bromide (MTT) and for the glucose assay.

2.2 Characterization techniques

The oxovanadium(IV) complexes were characterized by using a wide variety of techniques including, but not limited to UV/Vis spectroscopy, infrared spectroscopy, microanalysis and ICP-OES analysis for the vanadium content.

2.2.1 ICP-OES analysis

Inductively coupled plasma optical emission spectrometry (ICP-OES), also referred to as inductively coupled plasma atomic emission spectroscopy (ICP-AES), is an analytical technique used for the detection of trace metals. It is a type of emission spectroscopy that uses the inductively coupled plasma to produce excited atoms and ions that emit electromagnetic radiation at wavelengths characteristic of a particular element.[1,2] The intensity of this emission is indicative of the concentration of the element within the sample. The intensities of all wavelengths (within the system's range) can be measured simultaneously, allowing the instrument to analyze for every element to which the unit is sensitive all at once. Thus, samples can be analyzed very quickly. The intensity of each line is then compared to previously measured intensities of known concentrations (standards) of the elements, and their concentrations are then computed by interpolation along the calibration lines. The strength of the ICP-OES technique is that many elements (up to 70) can be determined simultaneously in a single sample analysis but its limitation is that the emission spectra are complex and inter-element interferences are possible if the wavelength of the element of interest is very close to that of another element.[2] In our case, only single-element analysis was carried out to determine the vanadium content in the vanadium complexes.

Table 2.1: ICP-OES method and operating parameters

Parameter	**Setting**
Plasma Ar gas Flow rate	5.0 L/min
Auxiliary Ar gas flow rate	1.00 L/min
Nebulizer Ar gas flow rate	0.90 L/min
Sampling depth	8.5 mm
Pump rate	100 rpm
N_2 addition flow rate	0.5 L/min
Cooled spraying chamber temperature	4 ^{o}C
Selected wavelength	292.4 nm
Sample flush time	30 s
Points per peak	3
Time scan acquisition	50 ms/point
RF power	1150 W

2.2.2 UV-vis spectrometric studies

The UV-vis spectrophotometric technique was used to characterize the geometric structure of oxovanadium(IV) complexes. Vanadium compounds exhibit a multitude of stereochemical arrangements (figure 2.1), with V(V) complexes being found in tetrahedral, octahedral, trigonal and pentagonal bipyramidal geometries. V(IV) exhibits fewer geometries due to its rigidity, and mainly square pyramidal, trigonal bipyramidal and distorted octahedral (if a sixth position is occupied) complexes are found.[3]

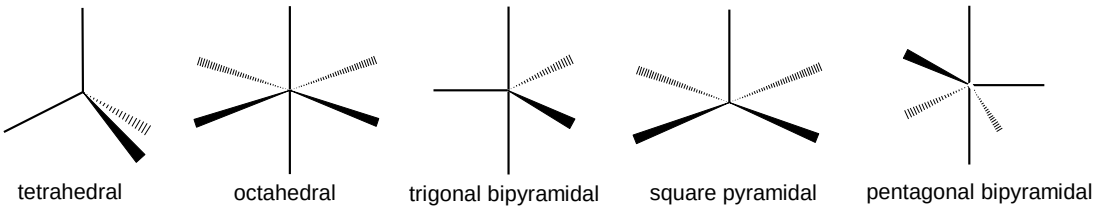

Figure 2.1: Some typical geometry of vanadium compounds

Ballhausen and Gray,[4] considered VO^{2+} in an aqueous solution as the $[VO(H_2O)_5]^{2+}$ molecular ion to elucidate the molecular orbital description of the vanadyl ion. They proposed that the vanadium 3d, 4s, and 4p orbitals, along with the 2s, $2p_\sigma$ ($2p_z$) and $2p_\pi$ ($2p_x$, $2p_y$) oxide oxygen orbitals, and the sp_σ hybrid oxygen (from water) orbitals were involved in bonding. The possibility of π-bonding of water oxygens was regarded as unlikely. The bonding strengths were arranged in the order (oxide oxygen) > (four square planar waters) > (axial water). With this in consideration, one can predict the following (symmetry in parenthesis):

- A strong σ bond between the sp_σ oxygen hybrid orbital and the ($4s + 3d_{z^2}$) vanadium hybrid orbitals (a_1)
- Two π-bonds between the oxygen $2p_x$ and $2p_y$ orbitals and the vanadium $3d_{xz}$ and $3d_{yz}$ (e)
- Four σ bonds between sp_σ orbitals of the water oxygens and the vanadium ($4s\text{-}3d_{z^2}$) (a_1), $4p_x$ and $4p_y$ (e), and $3d_{x^2-y^2}$ (b_1) orbitals
- The axial water oxygen is bonded to the remaining $4p_z$ (a_1) orbital
- The vanadium $3d_{xy}$ (b_2) is non-bonding

From this information, the energy level scheme was predicted for this d^1 system and is shown in figure 2.2. McGlynn proposed, using a ligand field approach, that the π-bonding of the

equatorial ligands should not be neglected.[5] This consideration only affects the order of the b_1* and e_π*, however these energy levels are so close together that the inversion might occur between different complexes.[6] This model predicts the following three transitions for the C_{4v} symmetrical VO^{2+} molecular ion:

$b_2 \rightarrow e_\pi^* (^2B_2 \rightarrow {}^2E)$

$b_2 \rightarrow b_1^* (^2B_2 \rightarrow {}^2B_1)$

$b_2 \rightarrow I\,a_1^* (^2B_2 \rightarrow {}^2A_1)$

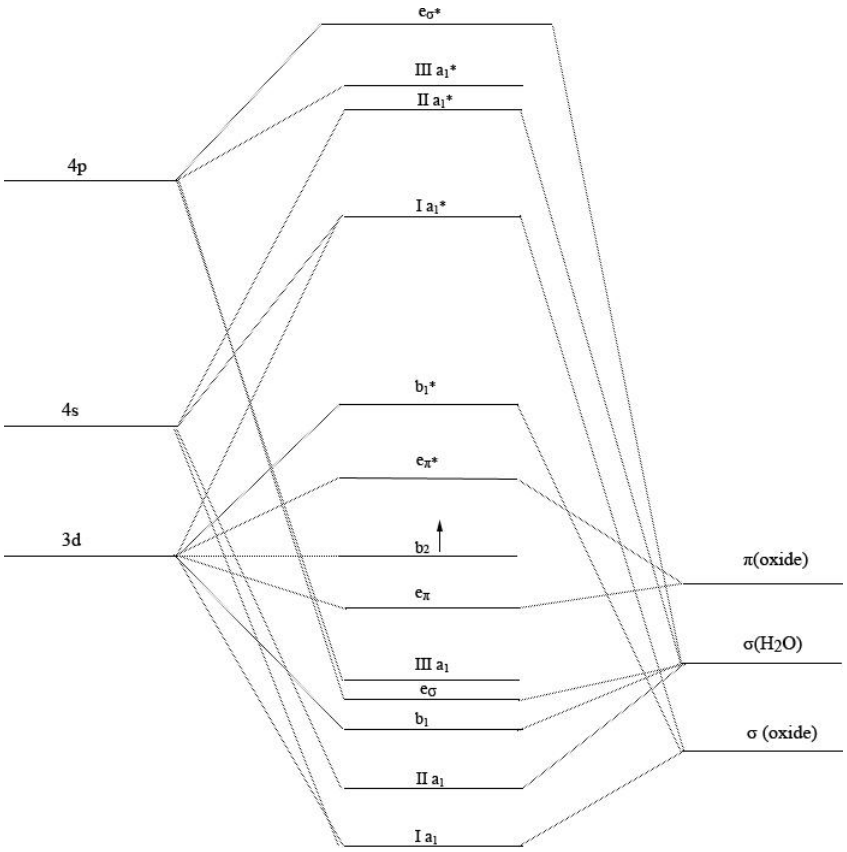

Figure 2.2: Molecular orbital scheme for the VO^{2+} species as outlined by Ballhausen and Gray[4]

Bands appearing at a lower wavelength than 200 nm are assumed to be charge transfer. The lowering of symmetry from C_{4v} to C_{2v} usually has little or no effect on the observed spectra, since the splitting of the e_π* level is too small to be observed experimentally most of the time.[4]

The Ortolano, Selbin and McGlynn (OSM) scheme also predicts three visible transitions from the ground state, b_2 (d_{xy}). These include; $d_{xy} \rightarrow (d_{xz}, d_{yz})$; $d_{xz} \rightarrow (d_{x^2-y^2})$ and $d_{xz} \rightarrow (d_{z^2})$ as shown in figure 2.3. The first two transitions may invert depending on the σ-donor strength of the ligands. The third transition may overlap or be completely occluded by charge transfer bands. The difference in the field strength of the equatorial ligands may also cause the doubly degenerate e_π to split, resulting in four electronic transitions observed. The insertion of a sixth ligand on the axial position would not be expected to lead to any noticeable effects from the square pyramidal (C_{4v}) geometry.[7]

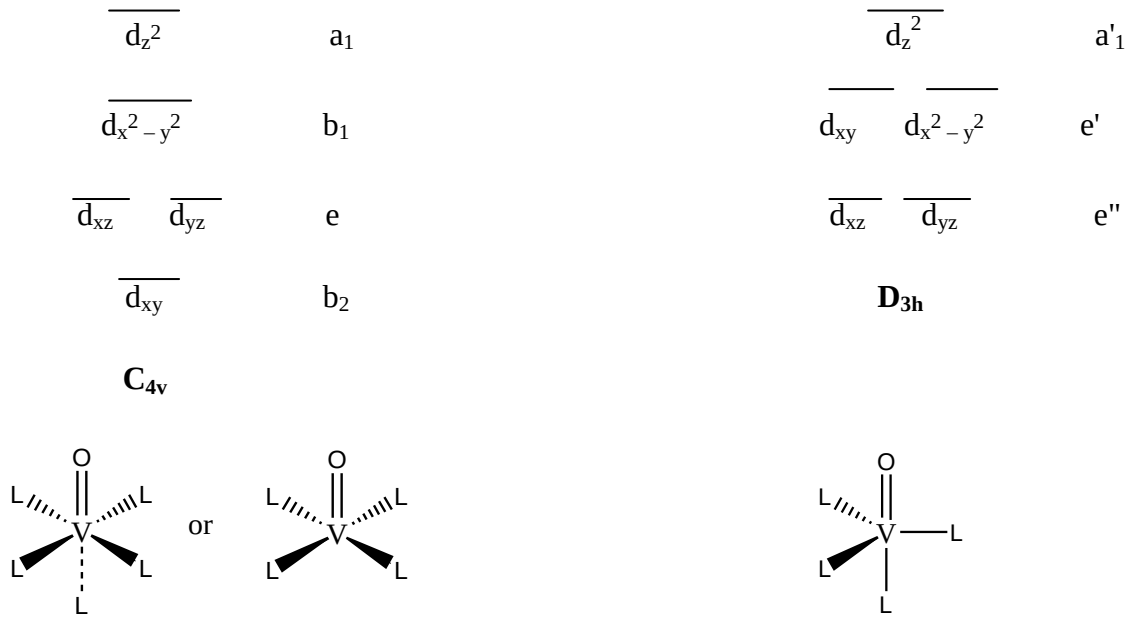

Figure 2.3: Clustered energy level schemes for C_{4v} and D_{3h} symmetries in oxovanadium(IV) complexes[7]

2.3 Chemical speciation modeling

Chemical speciation describes the composition (i.e. types and concentration of chemical compounds) of a solution.[8] Speciation analysis is the analytical activity of identifying and measuring the quantities of one or more individual chemical species in a sample. The concern in this work is molecular speciation and not the oxidation state of vanadium species since the solution studies are carried out in the +4 oxidation state. Chemical speciation depends, amongst other factors, on the composition of the system, pH, temperature, ionic strength and

time.[9] The pH-metric speciation was done on the biological pH range of 2 to 7.4. The species distribution diagrams were generated using the program HySS.[10] In this study the speciation modeling was done through the stability constants approach. The stability constants of oxovanadium(IV)-amino acid derivatives in aqueous solution were studied potentiometrically and results were computed using the program HYPERQUAD. The glass electrode was calibrated for a strong acid-base reaction by the Gran method[11] using the software GLEE to obtain E^o.[12] The data obtained from these titrations were used to calculate the protonation and stability constants.

2.3.1 Potentiometry and HYPERQUAD

The concentration stability constants (β_{pqr}) were calculated using the computer program HYPERQUAD[13] (extension of SUPERQUAD). This program makes use of the following assumptions to calculate the formation constants:

(i) For each chemical species $M_pL_qH_r$ in the solution equilibra there is a chemical constant which is expressed as: $\beta_{pqr} = \frac{[M_pL_qH_r]}{[M]^p[L]^q[H]^r}$; where M, L and H represent a metal, ligand and proton respectively.

(ii) The electrodes used, have a pseudo-Nernstian behaviour.

(iii) Careful calibration of the electrode, accurate standardization of reagents, elimination of weighing and dilution errors, elimination of carbonate impurities, elimination of temperature variance and purity of water minimise the systematic errors. All statistical tests are based on the assumption that systematic errors are absent.

(iv) The program assumes that the independent variables (such as titre volume) are not subject to errors and that the dependent variables (such as measured potential) have a normal distribution. If this is the case then the calculated residuals should not show systematic trends.

(v) For any equilibrium system, a model exists that will fit the experimental data. All least-square refinements are performed in terms of the assumed model. The model that is found may not be the true model, but it will be the one that fits the observed data. It will have no ill-defined constant and the standard deviation. A constant is considered ill-defined if its standard deviation is more than 33% (such standard deviations are labelled "Excessive") or if its value is negative.

The program calculates the stability constants using a non-linear least-square refinement algorithm based on following the acid concentration in complex acid-base equilibra using the proton sensitive glass electrode. The concentration of the hydrogen ion in solution is related to the potential measured with the electrode by the modified Nernst equation, $E = E^o + RT/F \ln[H^+]$. The standard potential, E^o, must be determined for the specific conditions of operation *via* the calibration of an electrode for a strong acid-base titration using the Gran method.[11]

The concentrations of the chemical species are determined by solving the non-linear simultaneous equations of mass-balance using the Newton-Raphson method. The program allows for up to four reactants and up to 18 species. The equilibra for the specific interactions of the reagents, M (metal) and L (ligand), with H (proton) are $M + iH = H_iM$; $L + jH = H_jL$; and the total concentrations (T_M, T_L, T_H) of the species is given by:

$$T_M = [M] + \sum_{pqr} p\beta_{pqr}[M]^p[L]^q[H]^r + \sum_i \beta_{10i}[M][H]^i$$

$$T_L = [L] + \sum_{pqr} q\,\beta_{pqr}[M]^p[L]^q[H]^r + \sum_j \beta_{10j}[L][H]^j$$

$$T_H = [H] + \sum_{pqr} r\,\beta_{pqr}[M]^p[L]^q[H]^r + \sum_i \beta_{10i}\, i[M][H]^i + \sum_j \beta_{10j}\, j[L][H]^j - [OH^-]$$

Mass-balance equations must be satisfied and hence the total concentrations of a reagent is the sum of its concentrations in all the chemical species in the mixture. Once the free reactant concentrations ([M], [L], [H]) have been calculated, the concentrations of the complexes are derived from them and the equilibrium constants (during model fitting, the constants must be estimated). The best fit to the experimental data is determined by minimizing the error square sum of the residuals, $U = \sum w_i (E_I^{Obs} - E_I^{cal})^2$, where w_i is the weighting factor. The model can be proposed for the equilibrium system, which adequately accounts for the experimental observations. The model is specified by a set of coefficients (p,q,r), one for each species in terms of the assumed model. Choice of the "best" model is based on two statistical values, sigma (σ) and chi^2 (χ^2). Ideally σ should be equal to one but it has been proposed that any fit with $\sigma < 3$ is satisfactory. χ^2 is also useful for model selection, with $\chi^2 < 12.6$ corresponding to a 95% confidence level. If σ and χ^2 are large, then the experimental data points with larger residuals must be removed during the refinement if the specified model is a promising fit.

2.3.2 HPLC speciation studies

The recognition of the fact that the chemical, biological, toxicological properties of an element are critically dependent on the form in which the element occurs in the sample has spurred a rapid development of an area of analytical chemistry referred to as speciation analysis.[8] A fundamental tool used for the speciation studies is the chromatographic separation techniques, that ensure that the species leave the column unaccompanied by other species of the analyte element.[14] Particular attention is given to the limitations related to the chromatographic signals identification due to unavailability of standards for many species since a large number of compounds have not yet been identified and characterized.[14-16] Recently, several reports on the determination of trace amounts of heavy metals by high performance liquid chromatography (HPLC) have appeared.[17-20] For example, Hidekazu Yamada *et al*[21] determined trace amounts of vanadium in plant materials by reverse–phase liquid chromatography.

This technique was used to identify and separate oxovadium(IV)-amino acid species. This study was carried out to complement the pH-metric speciation modeling study done on the VO-amino acid system by potentiometry and HYPERQUAD. Our model fitting results contradicted with those obtained by other researchers but this will be discussed in detail in chapter 3. The method and operating conditions are shown in table 2.2.

Table 2.2: HPLC isocratic method and operating parameters.

Parameter	**Setting**
Mobile phase	0.01 M phosphate buffer, pH 7.4
Wavelength	250 nm
Detector	DAD
Column	Gemini C18, 100mm x 4.6 mm x 5 µm
Column temperature	ambient
Flow rate	0.5 ml/min
Sample injection volume	20 µL
Run time	15 minutes

2.4 Biological studies

The *in vitro* testing for the biological anti-diabetic activity of the synthesized oxovanadium(IV) complexes was done. Three primary cell culture lines C2C12 (muscle), 3T3-L1 (fat) and Chang liver cells were used to investigate the potential of the synthesized oxovanadium(IV) complexes on glucose uptake. Cell viability tests were done before the glucose uptake studies to establish non-toxic concentrations of the compounds.

2.4.1 Maintenance of cells lines

3T3-L1 preadipocytes, were maintained in Dulbecco's modified eagle medium (DMEM) supplemented with 10% fetal bovine serum (FBS), while C2C12 mouse skeletal myoblasts and Chang liver cells were maintained in RPMI-1640 medium (Sigma) supplemented with 10% FBS. These were incubated at 37 ^{o}C in a humidified incubator with 5% CO_2. Cells were subcultured at 70% confluence and seeded at a density of 35 000 cells/ml (for 3T3-L1) and 25 000 cells/ml (for Chang and C2C12) in 24-well culture plates.

2.4.2 MTT Assay

Methods for cell viability determination *in vitro* are required for many different biological assays. The MTT-cell proliferation assay is a quantitative colorimetric assay for measurements of cellular proliferation, viability, and cytotoxity.[22-24] The assay is based on cleavage of the yellow tetrazolium salt, MTT, which forms water-insoluble, dark blue formazan crystals. This cleavage only takes place in living cells by the mitochondrial enzyme succinate-dehydrogenase.[24] The water-insoluble formazan can be solubilised using isopropanol or another organic solvent. The optical density of the dissolved material is measured spectrophotometrically, yielding absorbance as a function of concentration of converted dye, which directly correlates to the number of metabolically active cells in the culture.[22,26,27]

Cells were seeded in 24-well plates (Nunc) at densities of 25 000 for C2C12 and Chang liver cells, and 35 000 cells/mL for 3T3-L1. After overnight attachment, the culture medium was replaced with medium containing the test compounds at a range of concentrations (0.01–10 µM). Cells were incubated for 48 h at 37 ^{o}C, after which the MTT assay was performed.[22]

2.4.3 Glucose assay

The glucose uptake studies was performed using the GLUCOSE (Glu-cinet) kit (BAUER)[28] which contains glucose oxidase and peroxidase. Glucose oxidase catalyses the conversion of glucose to gluconic acid and hydrogen peroxide. The hydrogen peroxide reacts with a reduced dye, 4-aminoantipyrine, to produce oxidized dye and water. The reduced form of the dye is colourless while the oxidized form is reddish in colour. The coloured compound is then measured spectrophotometrically at a wavelength of 492 nm (A_{492}).[28]

Control cells were represented by untreated differentiated fat (3T3-L1), liver (Chang) and muscle (C2C12) cells incubated in culture media. Positive control cells (Met) were represented by untreated differentiated fat, liver and muscle cells exposed to metformin. Cells were then exposed for 48 h to the test compounds. Thereafter glucose uptake was determined and the cell number was normalized using the MTT assay, as laid out by Mossman.[22]

2.4.4 Statistical analysis

Error bars indicate the standard error of the mean (SEM) unless specified otherwise (n = 3). The two-tail paired test was used to determine significance of results ($p < 0.05$) and ($p < 0.01$).

2.5 References

1. Stefánsson A, Gunnarsson I, Giroud N, (2007), *Anal. Chim. Acta*, **582 (1)**, 69.
2. Mermet, J. M, (2005), *J. Anal. At. Spectrom.*, **20**, 11.
3. Page E, **(**1998), *Coord. Chem. Rev*., **172,** 111.
4. Ballhausen C. J, Gray H, (1962), *Inorg. Chem*., **1,** 111.
5. Selbin J, Holmes L. H, McGlynn S. P, (1963**),** *J. Inorg. Nucl. Chem.*, **25**, 1359.
6. Selbin J, (1965), *Chem. Rev*., **65**, 153.
7. Selbin J, (1966**),** *Coord. Chem. Rev*., **1**, 293.
8. Rai D, Eary L, Zachara, (1989), *J. Sci. Tot. Environ*., **86**, 15.
9. Templeton D. M, Ariese F, Cornelis R, Danielsson L. G, Muntau H, Van Leeuwen H. P, Lobinski R, (2000), *Pure Appl. Chem*., **72**, 1453.
10. Alderighi L, Gans P, Lenco A, Peters D, Sabatini A, Vacca A, (1999), *Coord. Chem. Rev*., **184**, 311.
11. Gran G, (1952), *Analyst*, **77**, 661.
12. Gans P, O'Sullivan B, (2000), *Talanta*, **51**, 33.
13. Gans P, Sabatini A, Vacca A, (1996), *Talanta*, **43(10)**, 1739.
14. Wang J. S, Tomlinson M. J, Caruso J. A, (1995), *J. Anal. Atomic Spectrom*., **10**, 601.
15. Lobinski R, (1997), *Appl. Spectrosc*., **51**, A260.
16. Zoorob G. K, McKiernan J. W, Caruso J. A, (1998), *Mickro Chim. Acta*, **128**, 145.
17. Hoshino H, Yotsuyanagi T, Aomura K, (1978), *Bunseki Kagaku (Jap. Anal.)*, **27**, 315.
18. Hoshino H, Yotsuyanagi T, (1982), *Bunseki Kagaku (Jap. Anal.)*, **31**, E435.
19. Sawatani I, Oshima M, Motomizu S, Toei K, (1984), *Bunseki Kagaku (Jap. Anal.)*, **33,** 119.
20. Yamada H, Hattori T, (1985), *J. Chromatogr*., **320**, 403.
21. Yamada H, Hattori T, (1986), *J. Chromatogr*., **361**, 331.
22. Mosmann T, (1983). *J. Immunol*., **65**, 55.
23. Denizot F, Lang R, (1986), *J. Immunol*., **89**, 271.
24. Twentyman P. R, Luscombe M, (1987), *J. Cancer*, **56**, 279.
25. Slater T. F, Sawyer B, Strauli U, (1963), *Biochim. Biophys. Acta*, **77**, 383.
26. Heeg K, Reinmann J, Kabelitz D, Hardt C, Wagner H, (1985). *J. Immunol*., **77**, 237.
27. Carmichael J, DeGraff W. G, Gazda A. F, Minna J. D, Mitchell J. B, (1987). *Cancer Res*., **47**, 936.
28. Keston A. S, (1956), *129th Meeting American Chemistry Society*, 31c.

CHAPTER 3

AMINO ACID COMPLEXES OF OXOVANADIUM(IV)

3.1 Introduction

The equilibria in aqueous solutions of vanadium have been studied thoroughly by different experimental methods.[1] The data in the literature, however, are rather contradictory. The soft character of the VO^{2+} ion was stated by Ramakrishna *et al*[2] by comparing the stability constants of the complexes formed with thiosalycilic and salycilic acids, although Chatt and Ahrland[3] as well as Pearson[4] classfied the vanadyl ion as a typical hard acid. Reeder and Rieger[5] interpreted the stability of the VO^{2+} α-OH-carboxylic and α-SH-carboxylic acids as due to the formation of coordinative δ and π bonds. They concluded that the VO^{2+} ion cannot form stable complexes with ligands containing no electron pair for π-bonding (e.g. amines), yet several authors have reported the formation of stable complexes with ligands containing an amine donor group.[6-7] Solution studies have been carried out on the interaction of VO^{2+} with amino acids; L-alanine, glycine, L-serine, L-threonine, L-cysteine, D-penicillamine, L-aspartic acid, L-glutamic acid and L-histidine using potentiometric, spectroscopic and NMR relaxation techniques.[8-11] The results show different solution chemistry models but there is evidence of bidentate coordination in the complexation.

In pH-potentiometric investigations of solutions containing VO^{2+} and N-donor ligands, a relatively high pH is necessary to achieve an appropriate free ligand concentration for complex formation.[8] At pH>4, however, hydrolysis of VO^{2+} ion takes place and oxidation to V(V) may also be significant unless deoxygenation is carried.[9] Another difficulty is that the nature (and formation constants) of the hydrolysis products of VO^{2+} in the pH range 5-12 is not very well understood.[8] Studies done on glycine-VO^{2+} system in the pH range 2-7 mainly by spectrophotometric measurements used models that included hydrolysis species, $[VO(OH)]^{+}$ and $[(VO)_2(OH)_2]^{2+}$.[9] The equilibria in aqueous solution in the VO^{2+}-amino acid systems show results with models that include species; MLH, ML, $ML(OH)_2$, ML_2H_2, ML_2H, ML_2, ML_2OH, $M_2L_2(OH)_2$ and $M_2L_2(OH)_3$ (where M denotes vanadyl ion and L denotes a deprotonated amino acid ligand).[9] A potentiometric and spectroscopic study of the complexation of oxovanadium(IV) by the sulphur-containing amino acids L-cysteine and D-penicillamine differ from those for the L-alanine, L-Serine, L-threonine, L-aspartic acid and L-

glutamic acid systems for much of the pH range studied (1.8-13.5).[10] This difference stems from coordination of the thiol group at quite low pH (~ 4). The nature of species present in neutral or basic solutions is still controversial but it is clear that for pH>5 other hydrolysis products predominate which should be included in any equilibrium model, especially for systems like L-alanine-VO^{2+} and glycine-VO^{2+} where, even using high ligand-to- metal ratios for pH>7-8, solutions have a brown colour, in contrast to serine-$VO^{2+,}$ cysteine-VO^{2+} and aspartic acid-VO^{2+} systems. One main problem in calculations with HYPERQUAD[26] for the glycine-VO^{2+} and L-alanine-VO^{2+} systems is the importance of hydrolysis products of VO^{2+} in the pH range 5-8.[11] The nature of such products and their formation constants are not accurately known and this is the main reason why there are so many models suggested for the same system.

Amino acid derivatives have provided encouraging *in vitro* and *in vivo* results from anti-diabetic studies with vanadium(V) and (IV) glutamic-γ-hydroxamic acid complexes[12] and vanadyl-cysteine methyl ester which showed activity equivalent to that of vanadyl sulfate[13]. A lot of work has been done on the interaction of oligopeptides with the vanadyl ion. For example, dipeptides such as glycyl-tyrosine coordinate to vanadate *via* the terminal amino and carboxylate functions plus the deprotonated amide takes place along with reduction of vanadate to vanadyl[14]. Direct coordination of the deprotonated OH functional group in amino acids such as L-tyrosine, L-serine, L-threonine and O-vanillin has not been observed in vanadium(IV) complexes. Although the isolation of solid complexes of the VO^{2+} cation and simple amino acids has often been claimed[15], pure compounds have apparently never been isolated from any aqueous oxovanadium(IV)-amino acid system until recently. The first isolated oxovanadium(IV) complex, $[VO(His)_4]SO_4.2H_2O$,[17] showed that the interaction of VO^{2+} and L-histidine forms a 1:4 species although solution speciation modeling studies suggest that a 1:2 complex is dominant at pH 7.[18] However, an oxovanadium(IV) histidine complex, $[V^{IV}O(hist)_2]ClO_4.H_2O$, has also been isolated and the structure determined by X-ray crystallography. [19] It adopts a distorted octahedral structure with one L-histidine ligand coordinated to the oxovanadium(IV) center in a tridentate fashion as a monoanion and the other in a bidentate fashion leaving a protonated imidazole group as a pendent group.

Since the ligand must dissociate from the vanadyl ion for the compound to be pharmaceutically active, use of well studied, non-toxic ligands becomes a priority. In this work we have chosen glycine and L-alanine as the amino acids which are bioligands. Glycine

is one of the non-essential amino acids and is used to help create muscle tissue and convert glucose into energy, hence its synergetic effects as a possible non-toxic anti-diabetic organo-vanadium pharmaceuticals is worth pursuing. We have, however, not been able to isolate a pure compound with glycine but we are certain of the purity of the alanine derivative that we have isolated.

3.2 Experimental

3.2.1 Reagents

Vanadyl sulfate trihydrate was obtained from BDH Limited (England). L-alanine (97%) (**1a**), glycine (98%) (**1b**), tetramethylammonium hydroxide (TMAOH) (10w%) and tetramethylammonium chloride (TMACl) (97%) were obtained from Sigma-Aldrich (USA). Hydrochloric acid (1 M) (analytical grade) and all solvents (reagent grade) were obtained from Merck Chemicals (SA) and used without further purification. Other reagent grade chemicals were also obtained from commercial sources and used as received.

3.2.2 Preparative work

(a) Synthesis of $[VO(ala)_4(H_2O)]SO_4.3H_2O$ (2a)

L-alanine (1.32 g, 14.9 mmol) and vanadyl sulfate trihydrate (0.32 g, 1.4 mmol) were refluxed for 3 hours in ethanol and a light blue precipitate started to form. The light blue mixture was left to cool to room temperature overnight. The light blue solid was filtered off, washed with cold water and ethanol and finally dried in an oven at 100 ^{o}C. Yield: 93.2%. Mp = 272-276 ^{o}C. IR ν (neat): 3352(m), 3119(m), 2937(m), 2825(m), 2739(m), 2617(m), 2532(m), 1745(s), 1698(vs), 1510(s), 1456(s), 1398(m), 1345(m), 1294(m), 1247(m), 1208(m), 1105(s), 1026(s), 956(vs), 857(s), 839(m), 532(s), 402(m) cm^{-1}. *Anal*. Calc (found). for $C_{12}H_{36}N_4O_{17}SV$ (591.44); C, 24.37 (24.15); H, 6.14 (6.21); N, 9.47 (8.06); S, 5.42 (6.23)%. UV/Vis (solid reflectance), λ_{max} (nm): 356, 587, 647, 810.

(b) Synthesis of $[VO(gly)_4(CH_3CH_2OH)]SO_4$ (2b)

This complex was prepared similarly to **2a**. Glycine (1.21 g, 16.1 mmol) and vanadyl sulfate trihdrate (0.35 g, 1.61 mmol) were refluxed for 3 hours in ethanol and a light blue precipitate started to form. The light blue mixture was left to cool to room temperature overnight. The

blue solid was filtered off, washed with cold water and methanol and finally dried in an oven at 100 ^{o}C. Yield: 89.3%. Mp = 198-200 ^{o}C. IR ν (neat): 3149(m), 3007(m), 2967(m), 2820(m), 2516(m), 1749(s), 1577(vs), 1494(s), 1441(s), 1405(s), 1330(s), 1191(m), 1107(s), 1031(s), 973(vs), 905(s), 890(s), 536(s), 464(m) cm^{-1}. *Anal*. Calc (found). for $C_{11}H_{28}N_4O_{14}SV$ (523.36); C, 25.24 (25.52); H, 5.39 (5.74); N, 10.71 (14.72); S, 6.13 (2.50)%. UV/Vis (solid reflectance), λ_{max} (nm): 344, 502, 612, 797.

3.2.3 ICP-OES analysis

Compounds **2a** (4.850 mg) and **2b** (5.291 mg) were separately dissolved in water and acidified with traceselect nitric acid and made up to 25 ml in a volumetric flask. Standard solutions containing 1 ppm, 2 ppm, 5 ppm, 10 ppm and 15 ppm of vanadium, were used to construct a calibration curve. Three wavelengths were used (290.8, 292.4 and 311.0 nm) for the detection of vanadium to ensure accuracy, and three repeats were performed at each wavelength. The best wavelength from the calibration curves was 292.4 nm. The vanadium content of compounds **2a** and **2b** at the most sensitive line, 292 nm, was 17.04(8) ppm and 22.60(9) ppm respectively. Vanadium content as a percentage for compound **2a** was found (calculated); 8.78 (8.61)% and for **2b**; found (calculated): 9.54 (10.0)%.

3.2.4 Potentiometric studies

The protonation and stability constants for the ligands and oxovanadium(IV) complexes were determined by potentiometric titration of approximately 25 ml samples. All solutions were prepared using freshly boiled and degassed deionized milli-Q water to ensure the removal of dissolved oxygen and carbon dioxide. The ligand concentration was 1 mM and metal-to-ligand ratios of 1:1, 1:2 and 1:10 were used. Titrations were performed over the pH range of 2-11 under a continuous flow of purified nitrogen using HCl and tetramethylammonium hydroxide (TMAOH). The vanadium stock solution containing 0.10 M HCl was standardized by titration with permanganate. The ionic strength of the titration solutions was kept constant at 0.10 M tetramethylammonium chloride (TMACl). The use of the bulky, non-coordinating cation, tetramethylammonium, was to eliminate the use of the non-innocent potassium and sodium ions in KCl and NaCl with respect to coordination in order to ensure that the model is fitted on accurately collected data. Titrations were controlled using the Tiamo software. The titration rate used was 0.01 ml/min and the pausing time was 60 s. The glass electrode was calibrated for a strong acid-base reaction by the Gran-method[20] using the program GLEE[21], to determine the standard potential, E^o. The ionic product of water (pK_w) of 13.83(1) at 25.0±0.1

^{o}C in 0.10 M TMACl was used in all calculations[22]. The following hydrolysis model of a vanadyl system was included in the model; $[(VO)_2(OH)_5]^-$ ($\log\beta_{20\text{-}5}$ = -22.0)[23] and $[VO(OH)_3]^-$ ($\log\beta_{10\text{-}3}$ = -18.0), while $[(VO)_2(OH)_2]^{2+}$ ($\log\beta_{20\text{-}2}$ = -6.95) and $[VO(OH)]^+$ ($\log\beta_{10\text{-}1}$ = -5.94) did not fit. The concentration stability constants $\beta_{pqr} = [M_pL_qH_r]/[M]^p[L]^q[H]^r$ were calculated by using the computer program HYPERQUAD[24]. The final values of the constants were obtained from an average of eight independent titrations using an average of around 400 data points in total for each refinement.

3.2.5 HPLC separations

A mixture of vanadyl sulfate trihydrate (213 mg) and glycine (147 mg) was dissolved in 25 ml of 0.001 M phosphate buffer pH 7.4. Another mixture of vanadyl sulfate trihydrate (205 mg) and L-alanine (168 mg) was dissolved in 25 ml of 0.01 M phosphate buffer pH 7.4. The mobile phase, 0.01 M phosphate buffer pH 7.4 was prepared by mixing KH_2PO_4 (1.370) and $NaHPO_4$ (1.099 g) and dissolved it in 1 L water. The mobile phase solution was filtered through a 0.45 µm membrane filter and degassed before use. The sample solutions were prepared immediately before analysis, and 20 µL were injected on to the column. The mobile phase flow rate was 0.5 ml/min and the eluted vanadium(IV)-amino acids species were detected at 254 nm.

3.3 Results and discussion

3.3.1 Synthesis of complexes

The synthetic goal of this work was to prepare neutral vanadium complexes containing bidentately coordinated low molecular mass amino acids, glycine and L-alanine (see scheme 3.1). Initial attempts to prepare the *bis*(amino acid) oxovanadium(IV) complexes employed a literature method with slight modifications.[25] To a stirred aqueous solution of amino acid, an equimolar amount from 10% tetramethylammonium hydroxide (TMAOH) solution was added. To this solution was added aqueous $VOCl_2$ (half mole equivalence to the amino acid ligand, prepared by the reaction of $VOSO_4$ with $BaCl_2$). The reaction yielded dark green precipitates of a mixture of the oxovanadium complex species with hydrolysis products as dominant species. In another attempt to synthesize **1c** and **1d**, vanadyl sulphate was stirred with the L-alanine or glycine in phosphate buffer of pH 7.4 and pH 7.9 respectively under inert conditions. However, vanadium hydrolysis products and vanadyl-phosphate precipitates

were observed (see figure 3.1). Elemental analysis revealed that there were no amino acids in the isolated precipitates from these phosphate buffered reactions. Stirring vanadyl sulfate alone in the phosphate-buffered solutions yielded the same precipitates and this confirmed that precipitates of vanadium phosphates were formed.

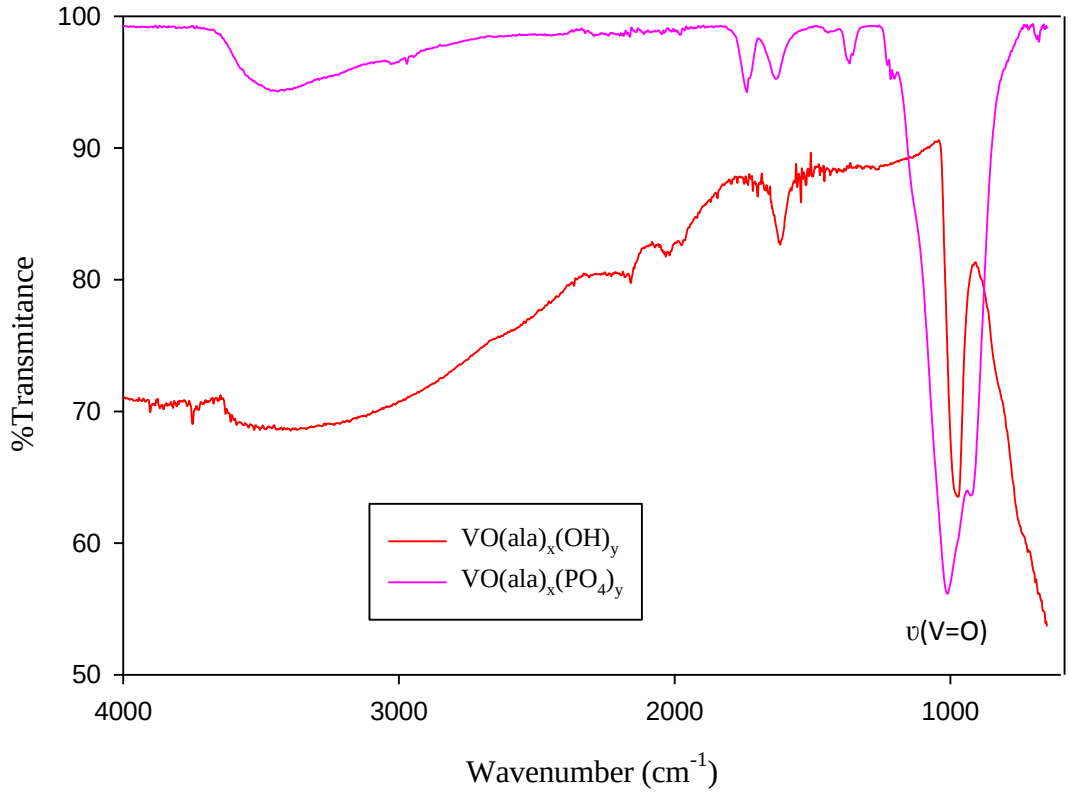

Figure 3.1: IR spectra of vanadium hydrolysis ($VO(ala)_x(OH)_y$) and vanadyl-phosphates ($VO(ala)_x(PO_4)_y$). x and y are hypothetical stoichiometric coefficients.

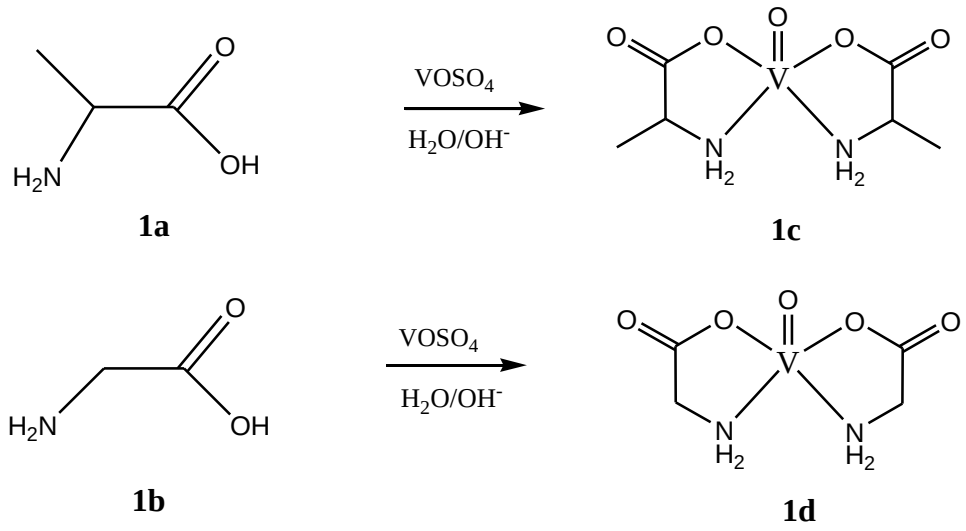

Scheme 3.1: Attempted synthesis of $[VO(gly)_2]$ (**1c)** and $[VO(ala)_2]$ (**1d)**

In an effort to circumvent hydrolysis, another synthetic route was adopted where the amino acid and vanadyl sulfate trihydrate were refluxed in ethanol. The elemental analysis data and spectral characterization suggested the chemical formulae, $[VO(ala)_4(H_2O)]SO_4.3H_2O$ (**2a**) and $[VO(gly)_4(CH_3CH_2OH)]SO_4$ (**2b**) (where ala is L-alanine and gly is glycine). $[VO(ala)_4(H_2O)]SO_4.3H_2O$ was very hygroscopic and readily dissolves in water. In **2b**, it is not certain if the ethanol is coordinating to the metal or it is ethanol of crystallization and these complexes need to be further characterized by single crystal X-ray diffraction. It was impossible, however, to recrystallize the two complexes because both of them underwent decomposition in most of the usual solvents. The composition of the complexes was further supported by the ICP-OES analysis results (see under section 3.2.3). The vanadium content was the same as the vanadium content from the suggested empirical formula in both complexes, $[VO(ala)_4(H_2O)]SO_4.3H_2O$ and $[VO(gly)_4(CH_3CH_2OH)]SO_4$. Thermal analysis techniques, such as DSC, TGA, and especially TG-FTIR analysis, could be employed for further characterization of these complexes.

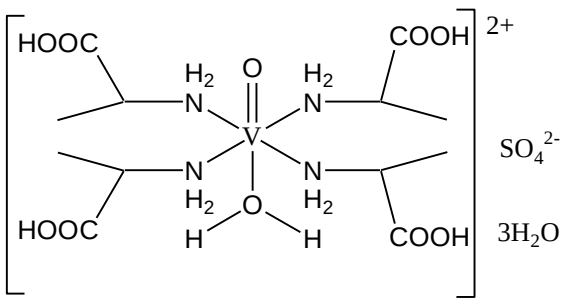

2a

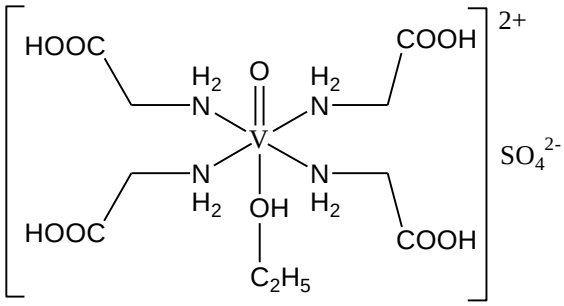

2b

Figure 3.2: Proposed structures of $[VO(ala)_4(H_2O)]SO_4.3H_2O$ (**2a)** and $[VO(gly)_4(CH_3CH_2OH)].SO_4$ (**2b)**

3.3.2 Spectroscopic characterization

A comparison of the most relevant IR bands of the amino acid ligands (glycine and L-alanine) and their corresponding oxovanadium complexes is shown in table 3.1. The assignments of the υ(V=O), υ(N-H), υ(C-H), υ(C=O), $\upsilon_{as}(COO^-)$, $\upsilon_s(COO^-)$, υ(V-N), δ(O-H), $\delta(COO^-)$, $\delta(NH_2)$, $\delta(NH_3^+)$ vibrations were made according to literature.[17,26] The presence of the $\upsilon_{as}(COO^-)$, $\delta(NH_3^+)$, $\upsilon_s(COO^-)$ and the absence of υ(C=O) bands around 1750 cm^{-1} in both glycine and L-alanine confirm that the amino acids exist as zwitterions. Complexes, **2a** and **2b**, exhibit the characteristic peak for VO^{2+} stretch vibration at 973 cm^{-1} and 953 cm^{-1} respectively (see figure 3.3). The V-N bands appear at 532 cm^{-1} and 536 cm^{-1} for complexes **2a** and **2b** respectively and are within reported ranges.[27,28]

In the comparison of the vibrations in the free amino acids ligands and complexes, there are major shifts associated to the $\delta(NH_2)$, υ(N-H), $\delta(NH_3^+)$, suggesting a coordination involving the amino group. There is not much change in the carboxylate stretches suggesting that carboxylate is not involved in the coordination. The position and non-splitting of the antisymmetric stretching vibration (around 1100 cm^{-1}) of the sulfate ion indicate that this anion is not coordinated to the metal centre.[29] The υ(V-O) bands in the complexes can be attributed to the water and ethanol molecules coordinating to the VO^{2+} (see figure 3.4). The proposed coordination in figure 3.2 was also seen in the first isolated oxovanadium of L-histidine.[17] The water molecules are responsible for the O-H stretch in the region 3400 cm^{-1}–3000 cm^{-1}.

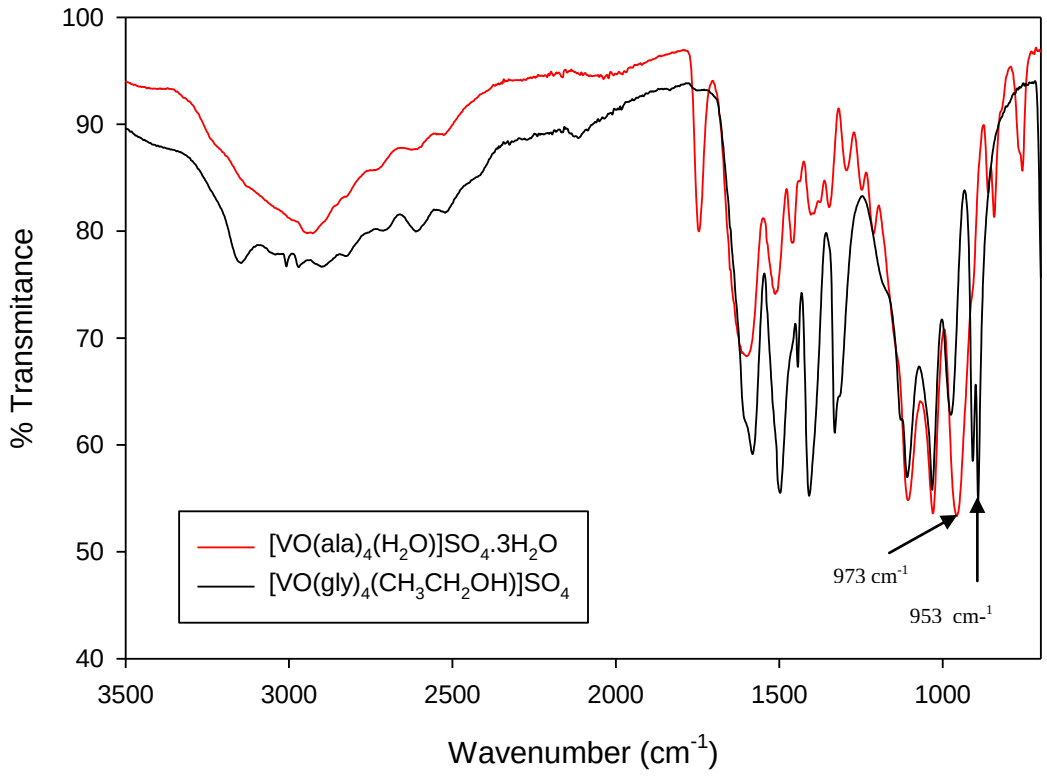

Figure 3.3: Mid-IR spectra of $[VO(ala)_4(H_2O)]SO_4.3H_2O$ and $[VO(gly)_4(CH_3CH_2OH)]SO_4$

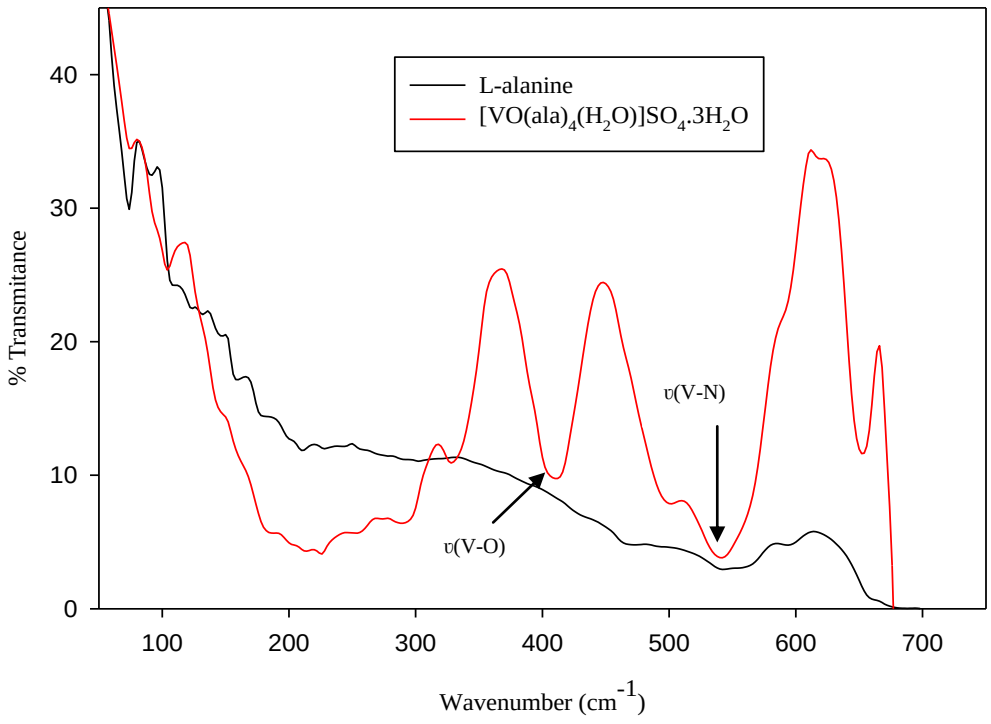

Figure 3.4: Far-infrared spectra of $[VO(ala)_4(H_2O)]SO_4.3H_2O$

Table 3.1: Characteristic IR bands of amino acid ligands and their corresponding vanadium(IV) complexes.

L-Alanine (cm^{-1})	**Glycine (cm^{-1})**	**2a (cm^{-1})**	**2b (cm^{-1})**	**Assignment**
3068(m)	3149(m)	3352(m)	3149(m)	υ(O-H)
3002(m)	3007(m)	3119(m)	3007(m)	υ(N-H)
2982(m) 2981(m)	2967(m), 2891(m)	2937(m) 2739(m)	2967(m), 2602(m)	υ(C-H)
-	-	1745(s)	1749(s)	υ(C=O)
1580(vs)	1577(vs)	1598(vs)	1577(vs)	$\upsilon_{as}(COO^-)$
1527(s)	1497(s)	-	-	$\delta(NH_3^+)$
1451(s)	1441(s)	1456(s)	1441(s)	$\upsilon_s(COO^-)$
1406(s)	1406(s)	1398(m)	1405(s)	δ(C-H)
1350(s)	1327(s)	1345(m)	1330(s)	δ(O-H)
1236(s)	1257(m)	1247(m)	1191(m)	υ(C-N)
-	-	1105(s), 1026(m)	1107(s), 1031(s)	$\upsilon(SO_4^{2-})$
-	-	973(vs)	953(vs)	υ(V=O)
890(s)	849(m)	857(s)	905(s)	$\delta(NH_2)$
766(s)	693(s)	-	-	$\delta(COO^-)$
-	-	532(s)	536(s)	υ(V-N)
-	-	402(m)	464(m)	υ(V-O)

(s = strong, vs = very strong, m = medium, υ_{as} = asymmetrical stretching mode, υ_s symmetrical stretching mode and δ = bending mode).

Theoretically, for a C_{4v} complex, three transitions should be observed in the region 1000 – 330 nm, corresponding to three d-d transitions (as discussed in chapter 2). Four bands may be observed when lowering the symmetry to C_{2v} since the degeneracy of the e_π level may be

removed.[26] The UV-vis solid reflectance spectra of the complexes $[VO(gly)_4(CH_3CH_2OH)]SO_4$ and $[VO(ala)_4(H_2O)]SO_4.3H_2O$ are shown in figures 3.5 and 3.6. The UV-vis solid reflectance spectrum of $[VO(gly)_4(CH_3CH_2OH)]SO_4$ exhibits peaks at 795, 612, 502 and 344 nm, which can be assigned to the ($d_{xy} \rightarrow d_{xz}$,), ($d_{xy} \rightarrow d_{yz}$), ($d_{xy} \rightarrow d_{x^2-y^2}$) and ($d_{xy} \rightarrow d_{z^2}$) transitions respectively. The UV-vis spectrum of $[VO(ala)_4(H_2O)]SO_4.3H_2O$ exhibits similar transitions at 810, 647, 587 and 356 nm. The four ligands are probably arranged equatorially around the VO^{2+} cation, generating a square-pyramidal complex. However, one of the four water molecules in **2a** and ethanol molecule in **2b,** may also be involved in coordination, occupying the position *trans* to the V=O bond. This arrangement is often found in oxovanadium(IV) complexes[30], generating a distorted octahedral complex. The four bands found in $[VO(ala)_4(H_2O)]SO_4.3H_2O$ and $[VO(gly)_4(CH_3CH_2OH)]SO_4$ are as a result of a large splitting of d_{xz} and d_{yz} orbitals. The relative movement of the z^2 level is far less predictable, since it is primarily involved in sigma bonding to the axial oxygen and only secondarily involved in the equatorial sigma bonding, e.g., as a hybrid ($4s\text{-}d_z^2$).[31]

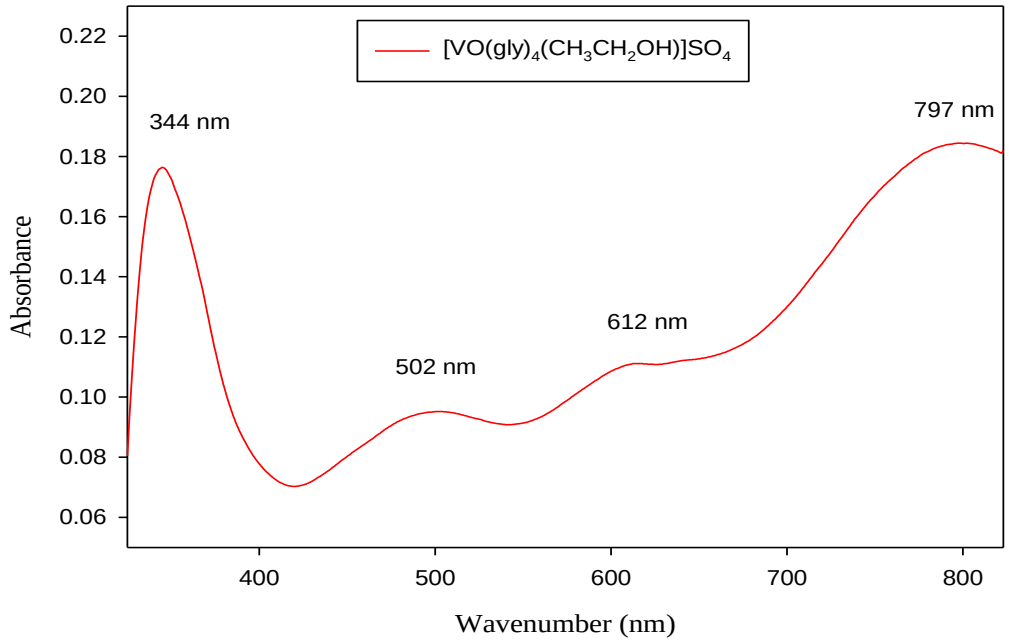

Figure 3.5: UV-vis solid reflectance spectra of $[VO(gly)_4(CH_3CH_2OH)]SO_4$

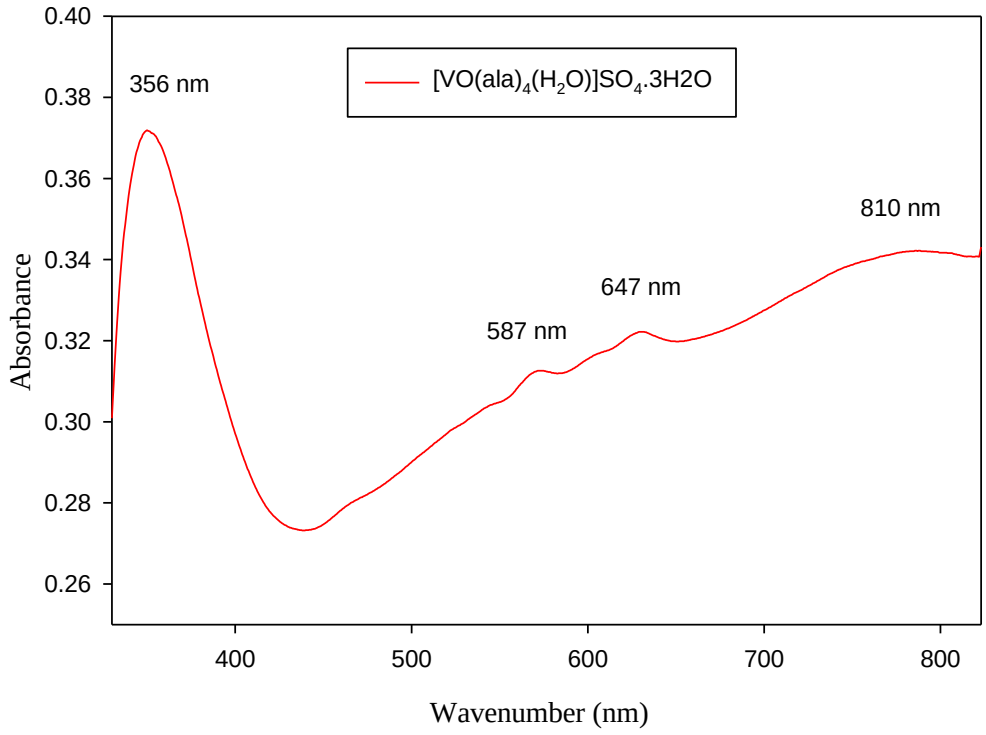

Figure 3.6: UV-vis solid reflectance spectra of $[VO(ala)_4(H_2O)]SO_4.3H_2O$

3.3.3 pH-metric solution speciation studies

The protonation constants of the ligands were calculated from an average of four independent titrations while an average of eight titrations were used for the stability constants calculations. The fitted curve (the one calculated by the HYPERQUAD program) tallied well with the titration curve for the proposed model (figure 3.7). The experimental data points with larger residuals were removed during the refinement. Data from the regions in which there was no complex formation and in a region in which complex formation was essentially complete were excluded (the red points in figure 3.7) from the calculations since they contributed no information regarding the formation constants. The statistical error (σ) was below 3 for all the refinements. The protonation (log*K*) and oxovanadium complex formation (log*β*) constants are listed in Table 3.2 together with standard deviations.

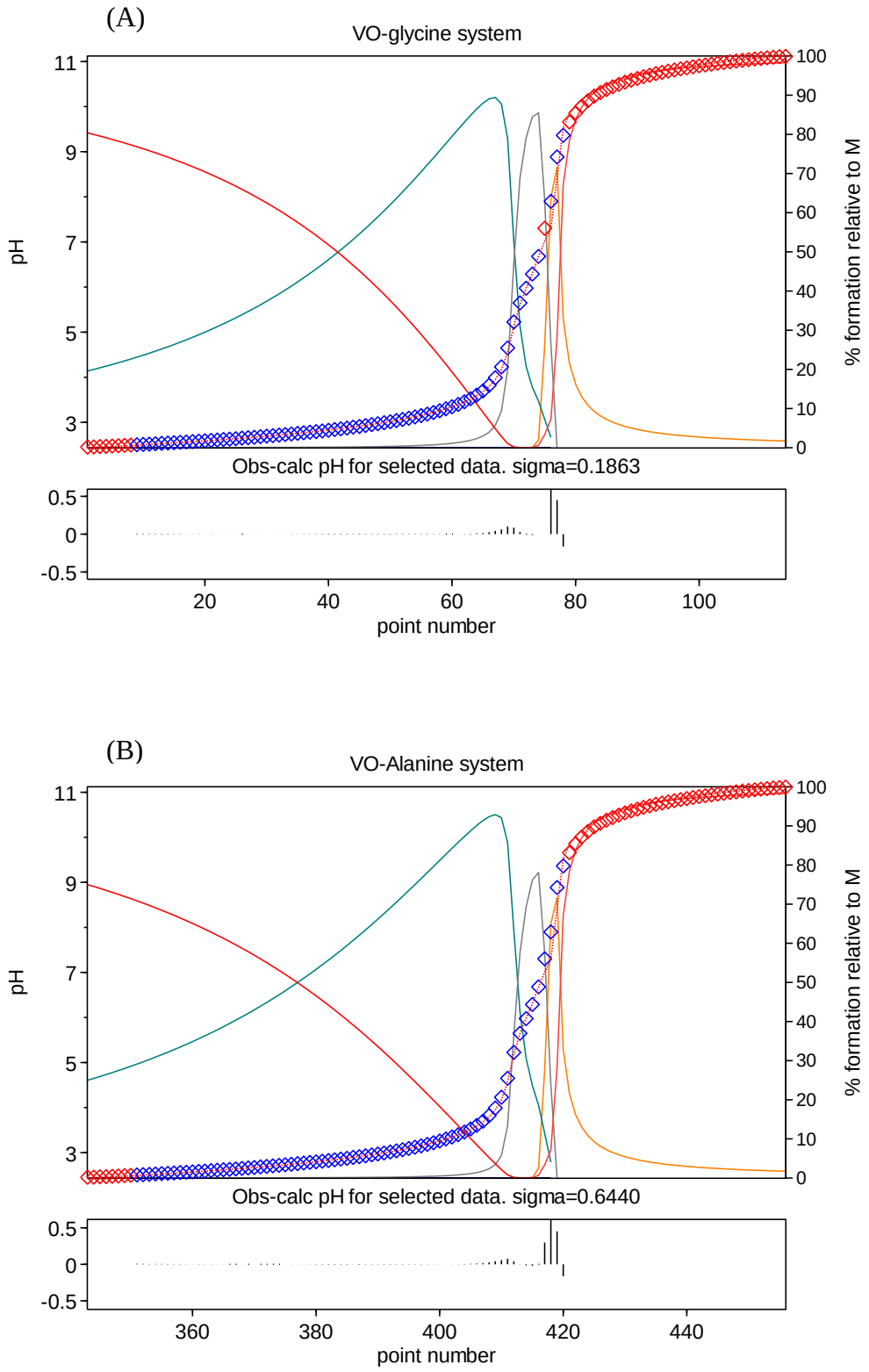

Figure 3.7: Titration and fitted curves of VO-glycine (A) and VO-alanine (B) systems. Experimental points (blue squares) and calculated (red continuous line). The other lines represent the species (not specified)

The ligands exhibit two protonation processes in the pH range 2-11 for the carboxylate and amine groups respectively. The logK_1 and logK_2 values depict the dissociation of the carboxylate and amine groups respectively. The protonation constants of glycine, pK_1=2.58(1) and pK_2=9.32(1), are in agreement with previous reports.[8,32] The difficulty in the pH-metric investigation of the VO^{2+}-N-donor ligands is that the deprotonation of the N-donors in general takes place in alkaline medium as shown in figures 3.7 and 3.8, and the amine group of both glycine and L-alanine is free from pH 8, hence relatively high pH is necessary to achieve an appropriate free ligand concentration for complex formation. This necessitated for large amounts of ligand (1:10 M:L) in order to prevent precipitation of the hydrolysis species.

Table 3.2: Protonation (log$K$) and stability (logβ) constants for the $V^{IV}O$-Glycine and $V^{IV}O$-L-alanine systems at I = 0.10 M TMACl and T = 25.0±0.1 ^{o}C. Standard deviations (errors in the last digit) are reported in parenthesis.

	Reaction	Ligand	
		Glycine	L-alanine
pK_1	$LH_2^+ \rightleftharpoons H^+ + LH$	2.58(1)	2.20(1)
pK_2	$LH \rightleftharpoons H^+ + L^-$	9.32(1)	9.62(1)
logβ_{110}	$VO^{2+} + L^- \rightleftharpoons [VO(L)]^+$	11.27(6)	9.89(5)
logβ_{111}	$VO^{2+} + H^+ + L^- \rightleftharpoons [VO(LH)]^{2+}$	-	11.16(3)
logβ_{120}	$VO^{2+} + 2L^- \rightleftharpoons [VO(L)_2]$	17.22(6)	18.27(6)

LH_2^+ = protonated L-alanine or glycine, LH= L-alanine or glycine

And L^-= deprotonated L-alanine or glycine.

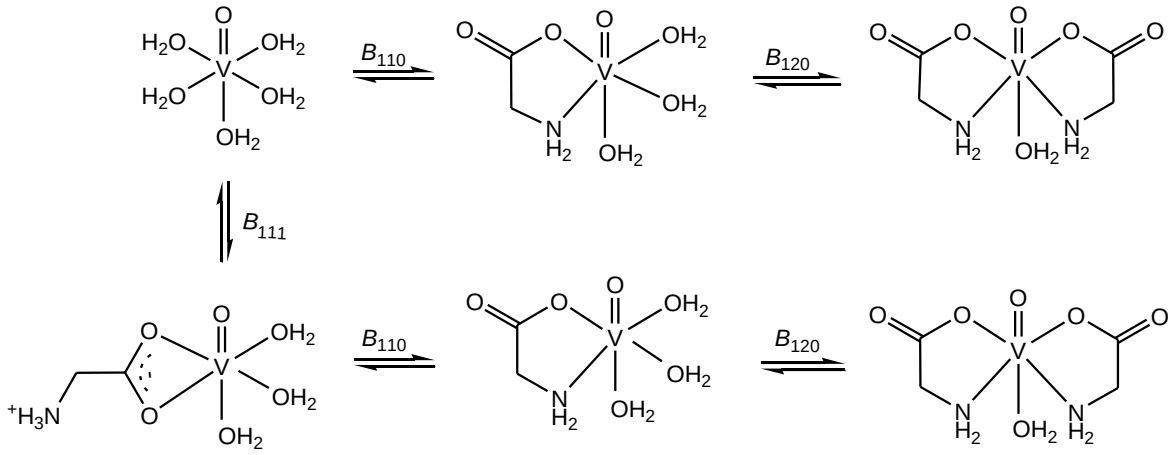

Scheme 3.2: The stepwise formation of oxovanadium(IV) complexes. L-alanine (LH) and and deprotonated L-alanine (L^-) are omitted in the complexation equilibria. The hydrolysis equilibria and the charges are also omitted.

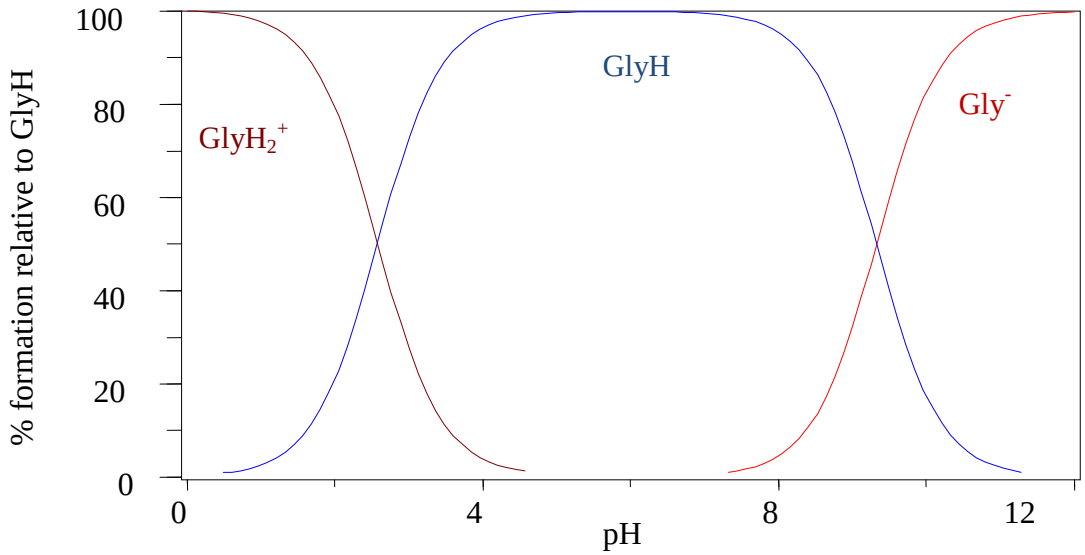

Figure 3.8: Species distribution as a function of pH for glycine. Gly^-=deprotonated glycine, GlyH=glycine and $GlyH_2^+$=protonated glycine

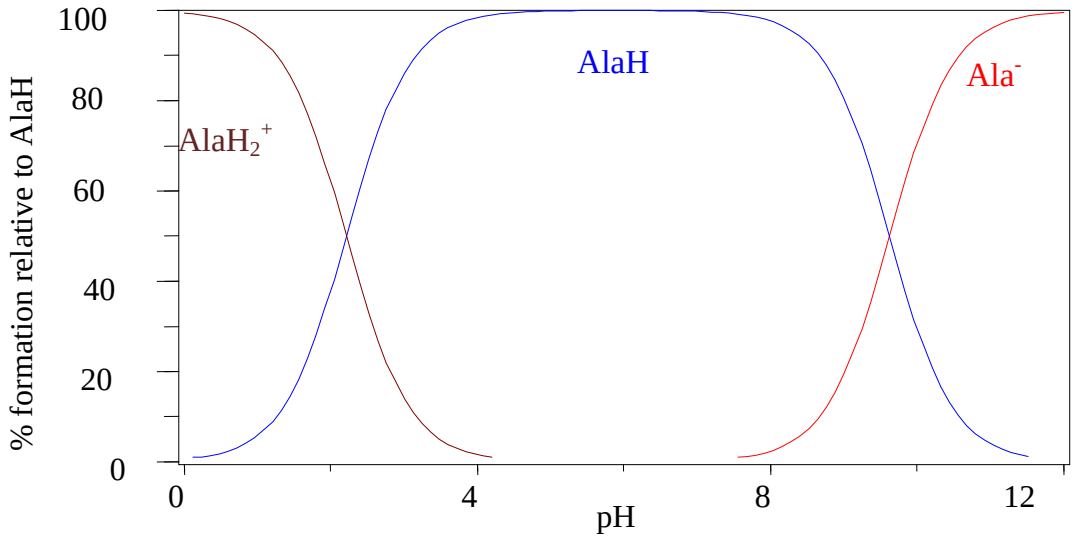

Figure 3.9: Species distribution as a function of pH for L-alanine. Ala^-= deprotonated L-alanine, AlaH= L-alanine, $AlaH_2^+$=protonated L-alanine

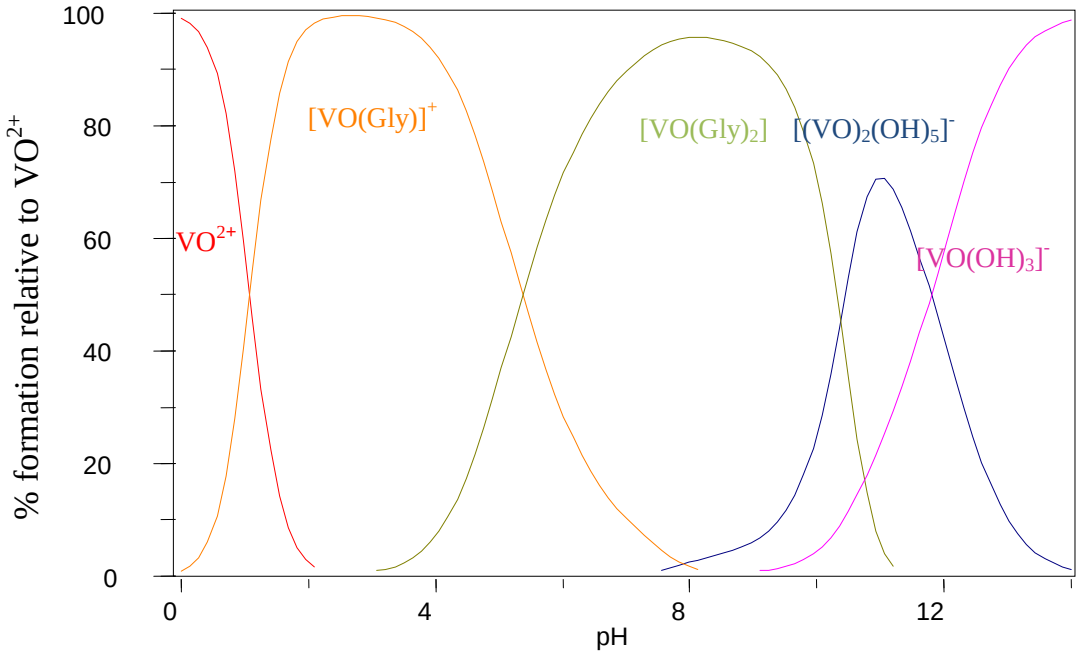

Figure 3.10: Speciation curves for complexes formed in the ($V^{IV}O$)-glycine system (VO^{2+}:GlyH is 1:4)

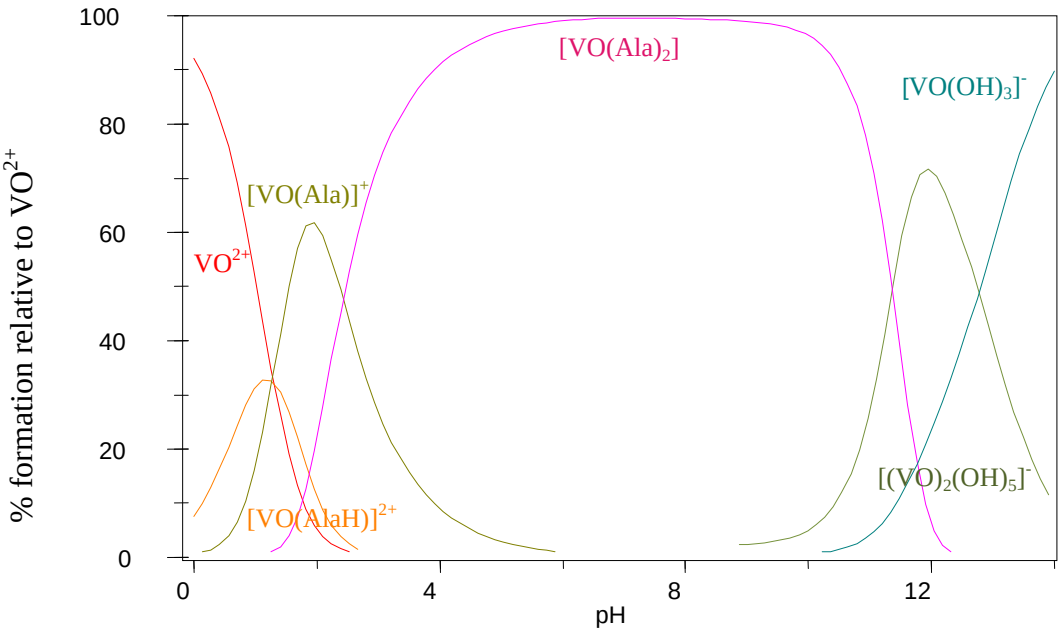

Figure 3.11: Speciation curves for complexes formed in the ($V^{IV}O$)-L-alanine (B) system (VO^{2+}:AlaH is 1:4)

Both the ($V^{IV}O$)-glycine and $V^{IV}O$-L-alanine systems revealed the presence of the species of interest, $[VO(gly)_2]$ and $[VO(Ala)_2]$, which formed at pH 3.5-11 and pH 1.5-12 respectively (see figures 3.10 and 3.11). Both systems cover the biological pH. At pH>3, however, the hydrolysis of the vanadyl ion takes place and this necessitated the use of 10:1 (glycine:VO^{2+}) molar ratio in order to suppress metal ion hydrolysis and possible concomitant precipitation of vanadium(IV) hydroxide species.[32]

HPLC speciation was done to confirm the presence of these species at pH 7.4 using a phosphate buffer system. To control the pH of the system, the phosphate buffer was used to prepare samples and the mobile phase. The elution of free uncoordinated vanadyl using the phosphate buffer as the mobile phase gave a signal at a retention time of 3.4 min. Two prominent peaks were observed in both systems at pH 7.4 and they suggest $[VO(Gly)_2]$ (retention time = 3.1 min) and VO^{2+}-phosphate (retention time = 3.4 min) in VO^{2+}-glycine system and VO^{2+}-phosphate (retention time = 3.4 min) and $[VO(Ala)_2]$ (retention time = 4.1 min) in VO-L-alanine system (see figures 3.12 and 3.13). The third smallest peak in VO^{2+}/glycine system is assigned to $[VO(Gly)]^+$ (retention time = 6.3 min). This agrees well with the species identified by potentiometric methods (see figures 3.10 and 3.11. However,

optimised separations of the fractions and further characterisation by LC-MS are needed to confirm these observed species. We can say that our pH-potentiometric solution model is reasonably well fitted despite the contradictions with literature[9] where several other species were identified in addition to our observations. But this will be qualified by a greater coverage of the pH ranges with these HPLC separations and confirmation by LC-MS.

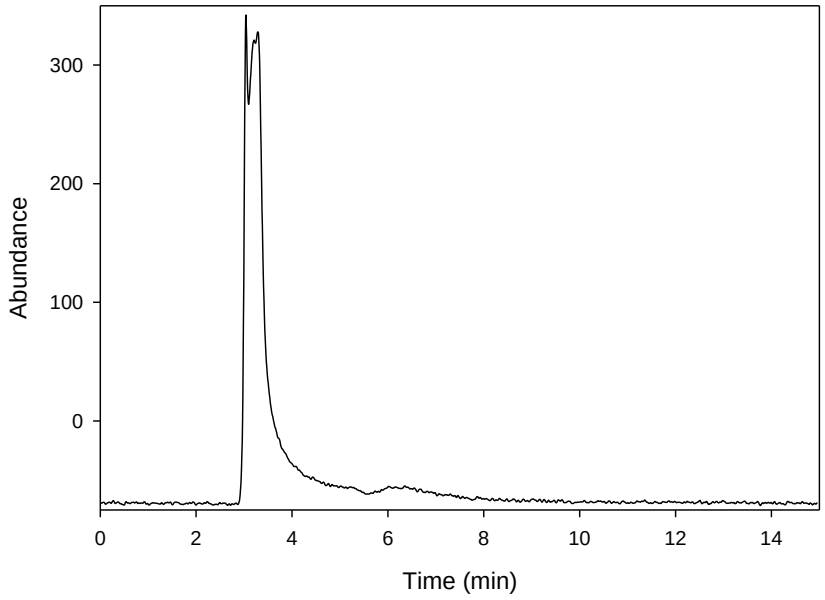

Figure 3.12: An HPLC chromatogram of VO^{2+}/glycine mixture at pH 7.4

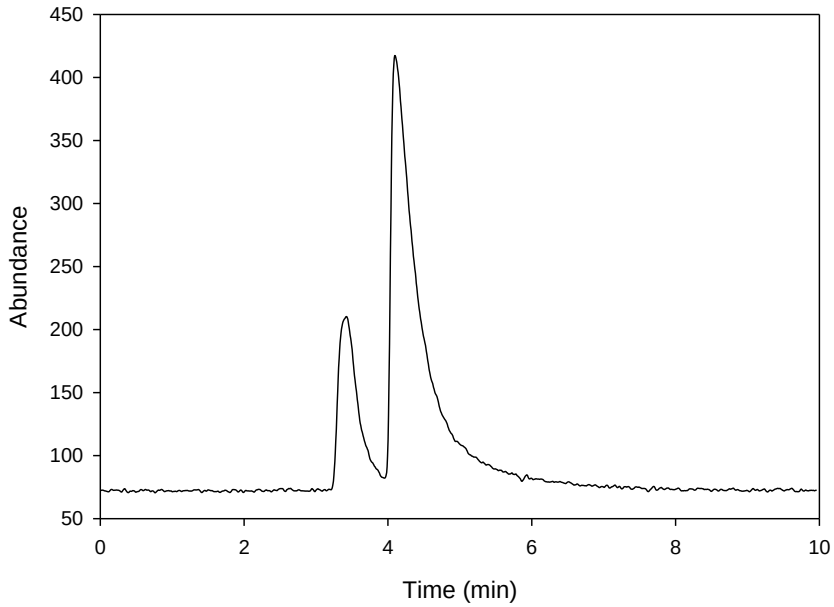

Figure 3.13: An HPLC chromatogram of VO^{2+}/L-alanine mixture at pH 7.4

The fitting of the titration data supports the formation of monomeric $[VOL]^+$ and $[VOL_2]$ species for both ligands as well as $[VOLH]^{2+}$ for L-alanine. The hydroxo binding ($[VOL_2(OH)]^-$ could not be fitted in both models while the assumption of the binary hydroxyl species $[(VO)_2(OH)_5]^-$ as well as $[VO(OH)_3]^-$ in highly basic solutions fitted well. It is possible, however, to confirm these hydrolysis species by EPR spectroscopy since they are both EPR-active. The overall stability constant for the ($V^{IV}O$)-L-alanine system (log β_{120} = 18.27(6)) is larger than for the glycine system (β_{120} = 17.22(6)). This can be explained by the fact that the amine nitrogen in L-alanine is more basic than that of glycine. The overall stability constants of both the $V^{IV}O$-glycine and $V^{IV}O$-L-alanine system are comparable to those given in literature[32] although the models and methods are different. For $V^{IV}O$-L-alanine system, however, the coordination of a protonated ligand is observed at low pH with logβ_{111} = 11.16(3). This suggests strong binding and the possibility of a symmetrically chelating carboxylate ion, with the amine nitrogen protonated. For the formation of monomeric $[VOL]^+$ and $[VOL_2]$ species (L=ligand), the very acidic carboxylic acid groups interact with VO^{2+} at very low pH and the mildly basic amine nitrogen able to interact with vanadyl at relatively higher pH. The result is the stabilization of these oxovanadium(IV) complex systems in the relavant biological pH. Although recent studies on VO^{2+}-amino acid systems show that at pH 6-8, the predominant species in solution is a 1:2 complex, solid state studies suggest that a 1:4 species can also be formed, such as the case with our isolated compounds.

3.3.4 Biological studies

The use of *in vitro* studies to evaluate the glucose uptake in cell lines following stimulation with insulin and other active compounds is a direct and sensitive method of determining the antidiatogenic effect of these compounds.[33,34] It allows for rapid screening of compounds in terms of their efficacy and toxicity in an ethically acceptable manner. Although the *in vitro* environment does not accurately mimic the *in vivo* situation, it offers unique opportunities and insights into the biochemical pathways which control the utilization of glucose by different cell types following exposure to various agents with potential diabetogenic effects.[34] Cytotoxicity and glucose uptake by vanadyl sulfate ($VOSO_4$) and oxovanadium(IV) complex of L-alanine (**2a**) on 3T3-L1 adipocytes, Chang liver and C2C12 muscle cells was done. The purity of oxovanadium(IV) complex of glycine as well as its characterization was not satisfactory and hence it was not included in the biological studies.

(a) Cytotoxicity

The results of the cytotoxicity of vanadyl salt and vanadium complex are presented in figure 3.13. The vanadium compounds ($VOSO_4$ and $[VO(ala)_4(H_2O)]SO_4.3H_2O$ (**2a**)) showed no cytotoxicity between 0.01-10 µM in the Chang liver cell lines tested but showed cytotoxicity in C2C12 muscle cell lines. In 3T3-L1 both $VOSO_4$ and $[VO(ala)_4(H_2O)]SO_4.3H_2O$ (**2a**) showed no cytotoxicity below 0.01 µM but exhibited cytotocixity between 0.1-10 µM. Therefore the concentrations which were used for glucose uptake depended on the MTT results. Ideally, based on the MTT, concentrations which can give an 80% or more viability of cells are usually used. A concentration of 10 µM, 0.1 µM and 0.01 µM of the oxovanadium(IV) compounds were chosen for the Chang cell lines whilst a concentration of 0.1 µM, 0.01 µM and 0.001 µM were used on C2C12 cell lines. Very low concentrations of 0.001 µM, 0.0001 µM and 0.00001 µM were used on 3T3-L1 since the compounds showed that they were very toxic above 0.01 µM.

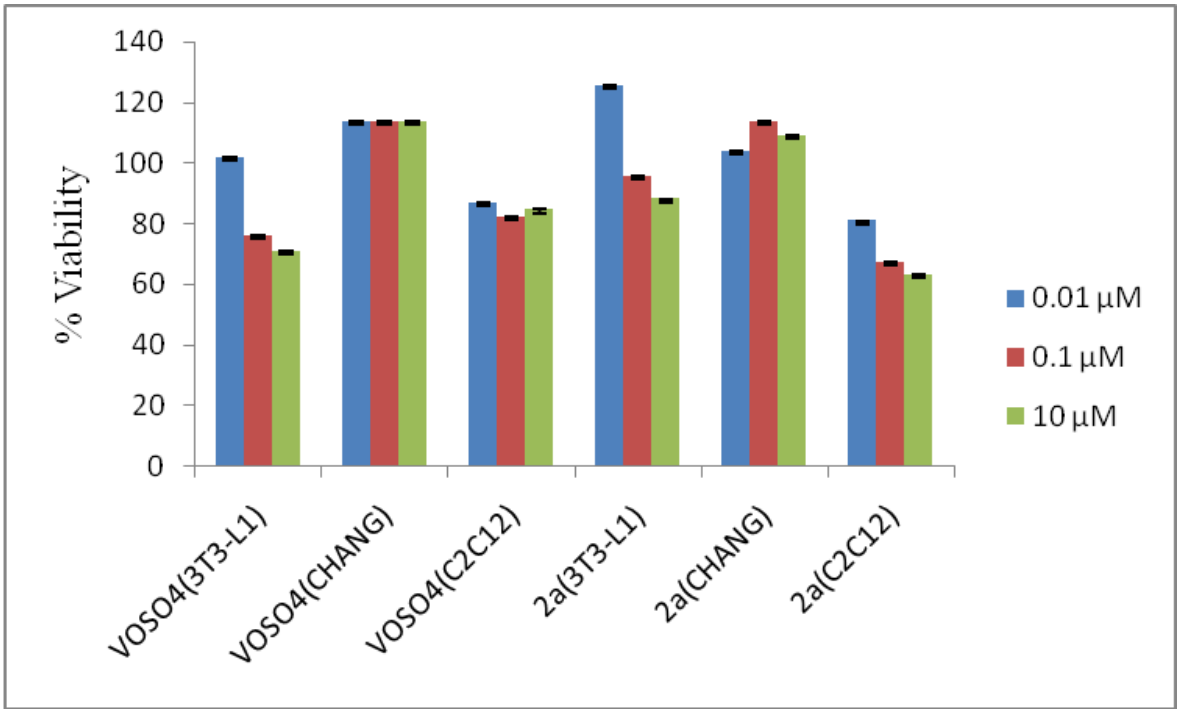

Figure 3.14: Cytotoxicity results of $VOSO_4$ and $[VO(ala)_4(H_2O)]SO_4.3H_2O$ (**2a**) at 0.01 µM, 0.1 µM and 10 µM on 3T3-L1, Chang liver and C2C12 muscle cells. The cell type is in parenthesis. Error bars indicate SEM (n = 3)

(b) Glucose uptake studies

The results for the glucose uptake for $VOSO_4$ and $[VO(ala)_4(H_2O)]SO_4.3H_2O$ (**2a**) are presented in figures 3.15, 3.16 and 3.17. In the Chang liver and C2C12 muscle cell lines, the oxovanadium(IV) compounds ($VOSO_4$, $[VO(ala)_4(H_2O)]SO_4.3H_2O$) (**2a**) enhanced glucose uptake relative to the control at concentrations of 10 µM and 0.1 µM respectively. However the compounds did not surpass the effects observed for metformin, a drug commonly used in the treatment of type 2 diabetes.[35] The uptake of glucose by the oxovanadium compounds in 3T3-L1 adipocytes cells was poor most probably due to the low concentrations used.

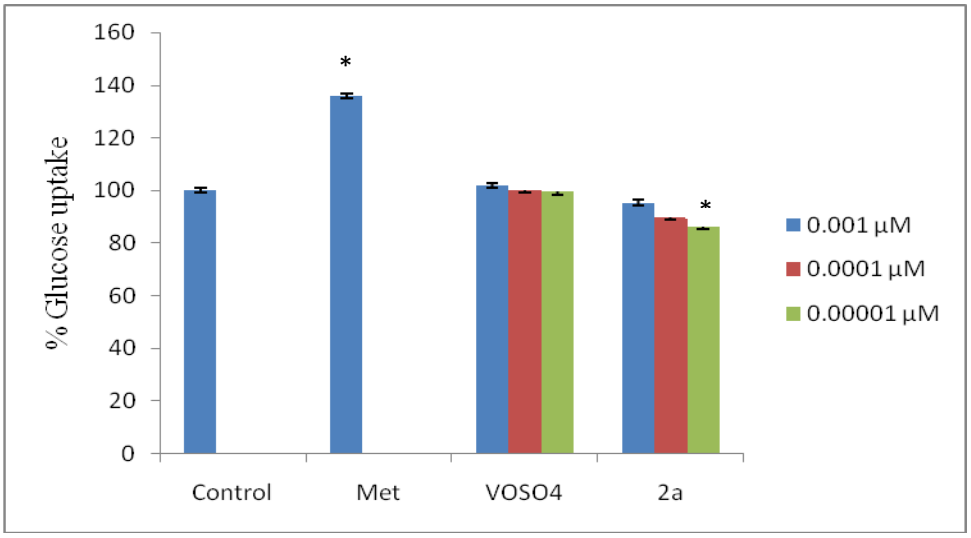

Figure 3.15: The effects of metformin (Met), vanadyl sulfate ($VOSO_4$), $[VO(ala)_4(H_2O)]SO_4.3H_2O$ (**2a**) at 0.001 µM, 0.0001 µM and 0.00001 µM on 3T3-L1 glucose uptake. The basal glucose uptake is represented as 100% (Control). Error bars indicate SEM (n = 3), *($p<0.05$) relative to the control

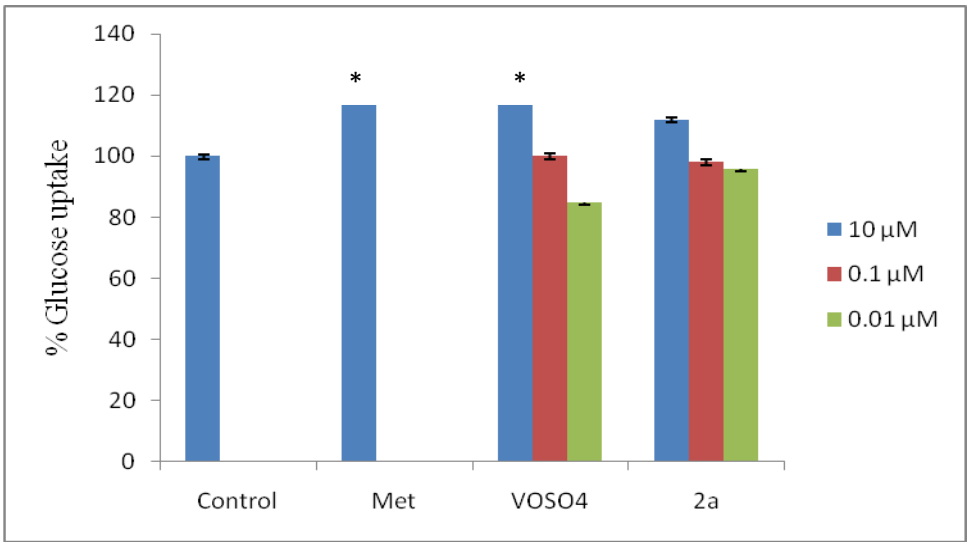

Figure 3.16: The effects of metformin (Met), vanadyl sulfate ($VOSO_4$), $[VO(ala)_4(H_2O)]SO_4.3H_2O$ (**2a**) at 10 µM, 0.1 µM and 0.01 µM on Chang glucose uptake. The basal glucose uptake is represented as 100% (Control). Error bars indicate SEM (n = 3), *($p<0.05$) relative to the control

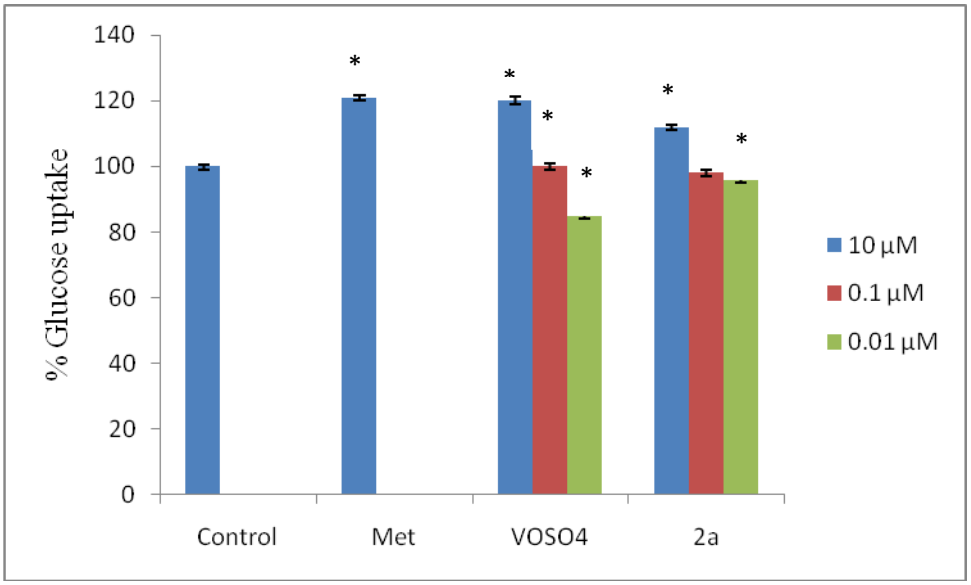

Figure 3.17: The effects of metformin (Met), vanadyl sulfate ($VOSO_4$), $[VO(ala)_4(H_2O)]SO_4.3H_2O$ (**2a**) at 0.1 µM, 0.01 µM and 0.001 µM on C2C12 glucose uptake. The basal glucose uptake is represented as 100% (Control). Error bars indicate SEM (n = 3), *($p<0.05$) relative to the control

The effect of the organic ligand in $[VO(ala)_4(H_2O)]SO_4.3H_2O$) makes little difference in this model compared with the inorganic salt, $VOSO_4$, but would perhaps become important in an *in vivo* model when considering the lipophilicity/hydrophilicity of the vanadium compounds[36]. It has been shown that the intestinal cell permeability of complexed vanadium compounds far exceeds that of the inorganic salt ($VOSO_4$),[37] and that would have an advantage when it was to absorption of the compounds into the bloodstream.

3.4 References

1. Rehder D, (1991), *Angew. Chem*., **103**, 152.
2. Ramakrishna R. S, Fernadopulle M. E, Nalliah B, (1971), *J. Inorg. Nucl. Chem*., **33**, 2071.
3. Chatt J, Davies N. R, Ahrland S, (1958), *Q. Rev. Chem. Scoc*., **12**, 265.
4. Pearson R. G, (1967), *Chem Br*., **3**, 107.
5. Reeder R. R, Rieger P. H, (1971), *Inorg. Chem*., **10**, 1258.
6. Napoli A, (1977), *J. Inorg. Nucl. Chem*., **39**, 463.
7. Pettit L. D, Swash J. C. M, (1976), *J. Chem. Soc. Dalton*, **7**, 588.
8. Fabian I, Nagypal I, (1982), *Inorg. Chim. Acta*, **62**, 193.
9. Costa Pessoa J, Vilas Boas L. F, Gillard R. D, Lancashire R. J, (1988), *Polyhedron*, **14**, 2145.
10. Costa Pessoa J, Vilas Boas L. F, Gillard R. D, (1990), *Polyhedron*, **17**, 2101.
11. Costa Pessoa J, Vilas Boas L. F, Gillard R. D, (1989), *Polyhedron*, **8**, 1173
12. Goldwaser J, Li J, Gefel D, Gershonov E, Fridkin M, Shechter Y, (2000), *J. Inorg. Biochem*., **80**, 21.
13. Sakurai H, Tsuchiya K, Nukatsuka M, Kawada J, Ishikawa S, Yoshida H, Komatsu M, (1990), *J. Clin. Nutr. Biochem*., **8**, 193.
14. Crans D. C, Holsts H, Keramidas A, Rehder D, (1995), *Inorg. Chem*., **34**, 2524.
15. Pessoa C. J, Boas V. L. F, Gillard R. D, Lancashire R. J, (1988), *Polyhedron*, **7**, 1245.
16. Rehder D, Ebel M, (2006), *Inorg. Chem*., **45**, 7083.
17. Williams P. A. M, Baran E. J, (1997), *Transition Met. Chem*., **22**, 589.
18. Sundberg R. J, Martin R. B, (1974), *Chem. Rev*., **74**, 471.
19. Islam K. M, Tsuboya C, Miyashita Y, Okamoto K, Kanamori K, (2007), *Acta Cryst*., **E63**, 1052.
20. Gran G, (1952), *Analyst*, **77**, 661.
21. Gans P, O'Sullivan B, (2000), *Talanta*, **51**, 33.
22. Bazzicalupi C, Bencini A, Bianchi A, Danesi A, Giorgi C, Valtancoli B, (2009), *Inorg. Chem*., **48**, 2391.
23. Henry P, Mitchell P. C. H, Prue E. J, (1973), *J. Am. Chem. Soc., Dalton Trans*., 1156.
24. Gans P, Sabatini A, Vacca A, (1996), *Talanta*, **43**, 1739.
25. McLauchlan C. C, Hooker J. D, Jones M. A, Dymon Z, Backhus E. A, Greiner B. A, Dorner N. A, Youkhana M. A, Manus L. M, (2010), *J. Inorg. Biochem*., **104**, 274.

26. Selbin J, (1965), *Chem Rev*., **65**, 153.
27. Ghosh T, Bhattacharya S, Das A, Mukherjee G, Drew G. B, (2005), *Inorg. Chim. Acta*, **358**, 989.
28. Ballhausen C. J, Gray H. B, (1962), *Inorg. Chem*., **1**, 111.
29. Nakamoto K, (1978), *Infrared and Raman Spectra of Inorganic and Coordination Compounds*, *Wiley*, **3**, 1134.
30. Vilas Boas L, Costa Pessoa J, Wilkinson G, Gillard R. D, McCleverty J. A, (1987), *Comprehensive Coordination Chemistry*, *Pergamon Press*, **3**, 109.
31. Tomiyasu H, Gordon G, (1973), *J. Coord. Chem*., **3**, 47.
32. Pessoa C. J, Boas L. F, Gillard R. D, Lancashire R. J, (1988), *Polyhedron*, **14**, 1245.
33. Galante P, Mosthaf L, Kellerer M, Berti L, Tippmer S, Bossenmaier B, Fujiwara T, Okuno A, Horikoshi H, Haring H. U, (1995), *Diabetes*, **44**, 646.
34. Nedachi T, Kanzaki M, (2006), *Am. J. Physiol. Endocrinol*., **291**, E817.
35. Davidson M. B, Peters A. L, (1997), *Am. J. Med*., **102**, 99.
36. Walmsley R. S, Tshentu Z. R, Fernandes M. A, Frost C. L, (2010), *Inorg. Chim. Acta*, **363,** 2215.
37. Westland A.D, Tarafder M. T. H, (1981), *Inorg. Chem*., **20**, 3992.

CHAPTER 4

IMIDAZOLYL-CARBOXYLIC ACID COMPLEXES OF OXOVANADIUM(IV)

4.1 Introduction

The use of imidazole compounds is well established in the field of medicinal chemistry, finding applications as anti-cancer,[1] anti-bacterial,[2] anti-fungal[3] and anti-diabetic[4] drugs, to name a few. The imidazole residue is one of the most versatile binding sites in proteins.[5] Imidazoles are extremely versatile ligands in that they are able to interact with many metal ions in not only synthetic environments, but also in natural systems.[6] This study explores the use of imidazole derivatives as binding moiety to oxovanadium(IV) since imidazoles are known to play a significant role in a large variety of biological processes.[7,8] It is therefore envisaged that these ligands should not pose a threat to the body once cleaved from the vanadium ion *in vivo* since these are prodrugs and the necessary metabolite is vanadium in a form of vanadyl or vanadate.

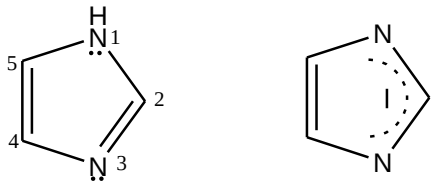

(a) (b)

Figure 4.1: Basic structure of imidazole (a), and the anionic form (b)

Imidazole is a planar, 5-membered, aromatic molecule, consisting of a trigonal nitrogen with two electrons in the p-orbital of the N-1 "pyrrole" nitrogen. At position 3 (N-3), a heterocyclic, "imino" nitrogen contains a lone pair of electrons in a hybrid orbital and a single electron in the p-orbital. The electrons in the unhybridised p-orbital of N-1 form part of the aromatic sextet.[9] The N-1 electrons are not available for bond formation since the aromaticity of the imidazole would be compromised. However, if deprotonation were to occur, a lone pair of electrons would be available for bonding and it would potentially be a bridging ligand in this form (see figure 4.1). Alkylation of the 1-position should increase the basicity of the imidazole nitrogen and therefore result in a stable coordination mode of

(N,COO^-)-donor moiety. The presence of an alkyl group may also help to increase the lipophilicity of the overall complex, which is one of the requirements for a candidate oral drug. It is envisaged that the less basic nature of imidazoles, unlike the amine function in amino acids, would results in the coordination of the imidazolyl-carboxylate moiety in the requisite pH range thus preventing the early hydrolysis experienced with amino acids.

The syntheses and characterization of the oxovanadium(IV) complexes with imidazole-4-carboxylic acid, imidazole-2-carboxylic acid and 1-methylimidazole-2-carboxylic acid as coordinating ligands is presented. The stability constants for the complexation of oxovanadium(IV) to these ligands were determined. The vanadium species distribution plots as a function of pH are also presented. The anti-diabetic potential of these complexes has also been investigated *via* the *in vitro* glucose assay using 3T3-L1 adipocytes, C2C12 muscle cells and Chang liver cells.

4.2 Experimental

4.2.1 Reagents

Vanadyl sulfate hydrate was obtained from BDH Limited (England). Methylimidazole (99%) and imidazole-4-carboxylic acid (98%) were obtained from Sigma-Aldrich (USA). Imidazole-2-carboxaldehyde (97%) was obtained from Fluka (USA). All solvents were obtained from Merck Chemicals (SA) and were of reagent grade and used without further purification. Other reagent grade chemicals were also obtained from commercial sources and used as received.

4.2.2 Preparative work

(a) 1-Methylimidazole-2-carboxaldehyde

1-Methylimidazole-2-carboxaldehyde was prepared according to a literature method.[10-12] To a suspension of 1-methylimidazole (2.20 g, 0.020 mol) in dry diethylether (50 mL) was added 2.5 M butyllithium (8.40 ml, 0.021 mol) at -78 °C. After stirring for an hour, DMF (2.33 ml, 0.030 mol) was added and this solution stirred overnight. After completion of the reaction, 2 mL of water was added followed by 15 mL of 4 N HCl. The aqueous layer was made basic by addition of potassium carbonate following which; the product was extracted into chloroform. This organic layer was concentrated and the product was distilled at $3.0x10^{-1}$

mBar and 80 ^{o}C to yield a brownish crystalline solid after cooling. Yield: 76.1%. δ_H (NMR 400MHz, $CDCl_3$): 4.03 (3H, NCH_3), 7.16-7.27 (2H, Im-H), 9.81 (1H, CHO); δ_C NMR (400 MHz, $CDCl_3$): 35.20, 127.69, 131.74, 144.00, 182.37. IR ν(KBr): 3108(m), 2956(m), 2835(m), 1671(s), 1532(w), 1509(m), 1479(m), 1380(s), 1330(s), 1289(s), 1218(m), 1150(m), 1077(m), 920(s), 766(s), 682(s) cm^{-1} *Anal.* Calc. (found) for $C_5H_6N_2O$ (110.11): C, 54.54 (54.25); H, 5.49 (5.65); N, 25.44 (25.19)%.

(b) Imidazole-2-carboxylic acid.H_2O (Im2COOH)

An aqueous 30% H_2O_2 (10 g) was added dropwise to a stirred solution of imidazole-2-carboxaldehyde (2.88 g, 0.030 mol) in water (10 ml). The reaction was allowed to proceed at room temperature for 72 hours, following which the water was removed *in vacuo* at room temperature to afford a white crystalline solid. This solid was washed with a stirred mixture of diethylether/water (4:1) to remove the excess peroxide. Note: heating causes decarboxylation. Yield: 97.5%. Mp = 156-158 ^{o}C. δ_H (400 MHz, D_2O): 7.56 (2H, s, Im-H); δ_C (400 MHz, D_2O): 158.86, 141.02, 120.49. IR ν(KBr): 3392(m), 3124(m), 2861(m), 1618(s), 1502(m), 1462(m), 1421(s), 1388(s), 1322(m), 1108(s), 925(s), 910(s), 819(m), 797(s), 774(m) cm^{-1}. *Anal*. Calc. (found) for $C_4H_6N_2O_3$ (130.11); C, 36.92 (37.18); H, 4.65 (4.94); N, 21.53 (21.47)%.

(c) 1-Methylimidazole-2-carboxylic acid.H_2O (MeIm2COOH)

The procedure followed that of Im2COOH above except that 1-methylimidazole-2-carboxyaldehyde was used and the yield was quantitative after the removal of water under high vacuum (no washing with diethylether/water was necessary). Note: heating causes decarboxylation. Yield: 100%. Mp = 99-101 ^{o}C. δ_H (400 MHz, D_2O): 7.42, 7.39 (2H, s, Im-H) and 4.08 ppm (3H, s, NCH_3); δ_C (400 MHz, D_2O): 158.67, 139.68, 125.83, 118.46, 36.73. IR ν (KBr): 3347(m) 3119(m), 2663(w), 1641(s), 1683(m), 1507(s), 1449(m), 1388(s), 1338(s), 1285(s), 1173(m), 1123(s), 961(m) 910(m), 776(s), 685(s) cm^{-1}. *Anal*. Calc. (found) for $C_5H_8N_2O_3$ (144.12); C, 41.67 (41.28); H, 5.59 (5.23); N, 19.44 (19.12)%.

(d) $VO(im4COO)_2.H_2O$ (2a)

This complex was prepared according to a literature method but with slight modifications.[13] To a stirred aqueous solution of Im4COOH (0.254 g, 2.26 mmol), was added 10% TMAOH (1.04 ml, 1.13 mmol). To this solution was added aqueous $VOCl_2$ (1.13 mmol), prepared by the reaction of $VOSO_4$ with $BaCl_2$. The reaction was allowed to stir overnight, following

which the light blue precipitate was collected, washed with methanol and ether and dried in an oven at 100 ^{o}C. Yield: 64.6%. Mp > 300 ºC. IR ν (neat): 3129(m), 2992(m), 2856(m), 1606(s), 1573(s), 1499(m), 1439(m), 1356(s), 1209(m), 1080(m), 1012(m), 981(s), 878(m), 819(s), 780(s) cm^{-1}. *Anal*. Calc. (found) for $C_8H_8N_4O_6V$ (307.11); C, 31.29 (31.20); H, 2.63 (2.67); N, 18.24 (18.14)%. UV/Vis (solid reflectance), λ_{max} (nm): 339 , 570 , 712.

(e) VO(im2COO)$_2$.H$_2$O (2b)

This complex was prepared in the same manner as **2a,** except that an aqueous solution of $VOSO_4$ was added to the ligand solution instead of aqueous $VOCl_2$. Yield: 69.9%. Mp > 300 ºC. IR ν (neat): 3448(m), 3129(w), 3008(m), 2906(m), 1625(s), 1558(m), 1487(m), 1398(s), 1338(m), 1277(m), 1171(m), 1112(s), 984(s), 908(m), 829(m), 769(s), 658(s) cm^{-1}. *Anal*. Calc. (found) for $C_8H_8N_4O_6V$ (307.11); C, 31.29 (31.21); H, 2.63 (2.53); N, 18.24 (18.07)%. UV/Vis (solid reflectance), λ_{max} (nm): 333, 559, 715.

(f) VO(MeIm2COO)$_2$.H$_2$O (2c)

This complex was prepared similarly to **2a**. However, upon stirring overnight a blue precipitate did not form. The blue solution was then allowed to stand for 24 hours and a light blue precipitate formed, which was filtered and washed with methanol and then ether and dried in an oven at 100 ^{o}C. Yield: 62.3%. Mp = 218-220 ºC. IR ν (neat): 3134 (m), 1628(s), 1487(s), 1426(s), 1327(s), 1286(m), 1180(s), 1166(s), 963(s), 837(m), 797(s), 769(s), 698(s) cm^{-1}. *Anal*. Calc. (found) for $C_{10}H_{12}N_4O_6V$ (335.17); C, 35.83 (36.01); H, 3.61 (3.47); N, 16.72 (16.67)%. UV/Vis (solid reflectance), λ_{max} (nm): 352, 578, 718.

4.2.3 Potentiometric studies

The protonation and stability constants for the ligands and oxovanadium(IV) complexes were determined by potentiometric acid/base titrations as explained in chapter 3. The following hydrolysis model of a vanadyl system was included in the model; $[VO(OH)_3]^-$ ($\log\beta_{10-3}$ = -18.0) and $[(VO)_2(OH)_5]^-$ ($\log\beta_{20-5}$ = -22.0) while $[VO(OH)]^+$ ($\log\beta_{10-1}$ = -5.94) and $[(VO)_2(OH)_2]^{2+}$ ($\log\beta_{20-2}$ = -6.95) were not used.[14] The concentration stability constants $\beta_{pqr} = [M_pL_qH_r]/[M]^p[L]^q[H]^r$ were calculated by using the computer program HYPERQUAD.[15] The final values of the constants were obtained from an average of eight independent titrations using an average of around 500 data points in total for each refinement.

4.3 Results and discussion

4.3.1 Synthesis and general considerations

The synthesis of 1-methylimidazole-2-carboxaldehyde was carried out under argon and in dry diethylether. The presence of oxygen and water reduce the yield of 1-methylimidazole-2-carboxaldehyde since butylithium is deactivated. Care must be taken to maintain the temperature at not more than -50 ^{o}C as higher temperatures also deactivate the butylithium. The 1-methylimidazole-2-carboxaldehyde decomposes *via* decarboxylation if it stays for more than one week at room temperature before it is converted to 1-methylimidazole-2-carboxylic acid. The 1-methylimidazole-2-carboxylic acid and imidazole-2-carboxylic acid were prepared from the corresponding imidazole-2-carboxaldehydes by the hydrogen peroxide facilitated oxidation in water. This reaction requires no heating and water was the only by-product of oxidation, making it an environmentally friendly option. The only purification necessary was the removal of residual water *in vacuo*, at room temperature for 1-methylimidazole-2-carboxylic acid yielding a quantitative product but imidazole-2-carboxylic acid crystallized out with a mole equivalent of hydrogen peroxide. This was removed by washing with diethylether to prevent the oxidation of vanadium(IV) to vanadium(V) by the peroxide during the synthesis of the complexes. The purity of the ligands was ascertained by elemental analysis and NMR characterization.

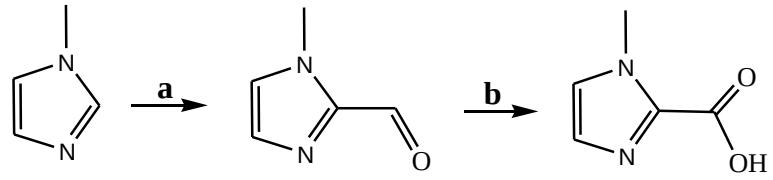

Scheme 4.1: Synthesis of 1-methylimidazole-2-carboxylic acid. **a.** Butyllithium, DMF, diethylether. **b.** H_2O_2, water

The complexes were synthesized by addition of an aqueous vanadyl chloride or vanadyl sulfate solution to an aqueous solution of the corresponding ligand in a 1:2 molar ratio in the presence of a base. There was no hydrolysis products observed. Attempts to synthesize **2a** and **2c** using $VOSO_4$ instead of $VOCl_2$ yielded impurities of sulfates which could not be washed away with water. The complexes which precipitated out of solution were easily collected by filtration. The compounds (**2a**-**c**) are slightly soluble in water and tend to decompose in organic solvents, such as acetonitrile, alcohols and DMF, upon dissolution at elevated temperatures and hence cryatal growth has been a challenge.

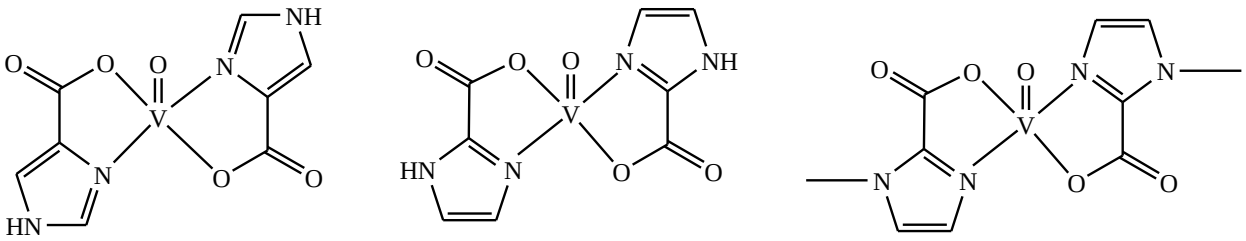

Figure 4.2: Chemical structures of $[VO(im4COO)_2]$ (**2a**), $[VO(im2COO)_2]$ (**2b**) and $[VO(MeIm2COO)_2]$ (**2c**)

4.3.2 Spectroscopic characterization

The formation of the aldehyde in 1-methylimidazole-2-carboxaldehyde was confirmed by the appearance of the peak at 9.65 ppm in the MNR spectrum of this compound (see figure 4.4(A)). The confirmation of the oxidation of imidazole-2-carboxaldehydes to imidazole-2-carboxylic acids was exhibited by the disappearance of the aldehyde peak at 9.7-9.8 ppm in the NMR spectra as depicted by figures 4.3(A) and 4.3(B).

(A)

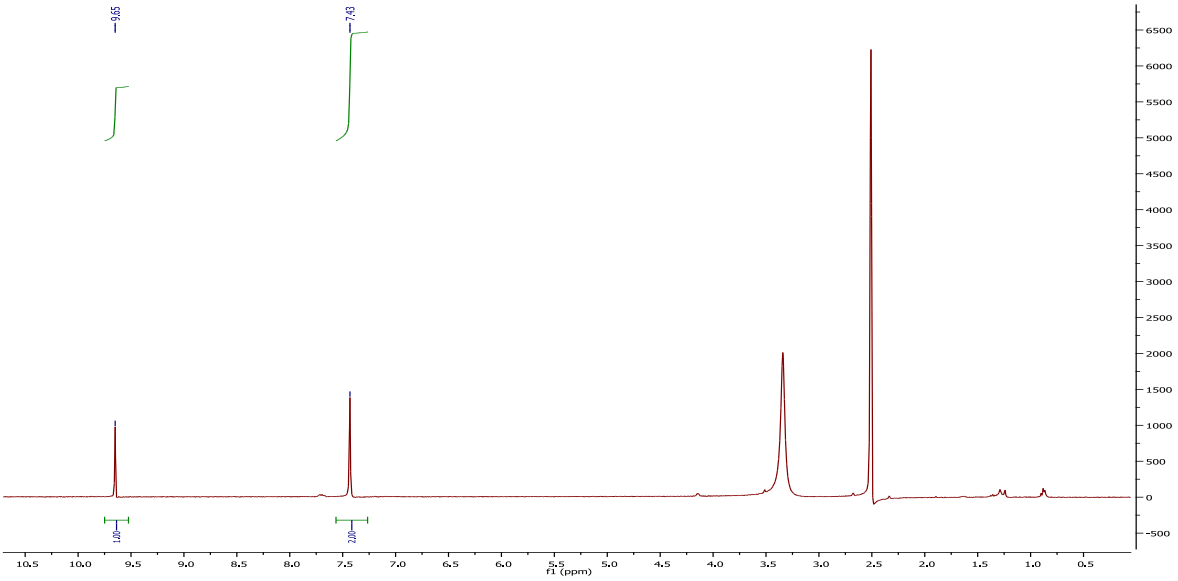

(B)

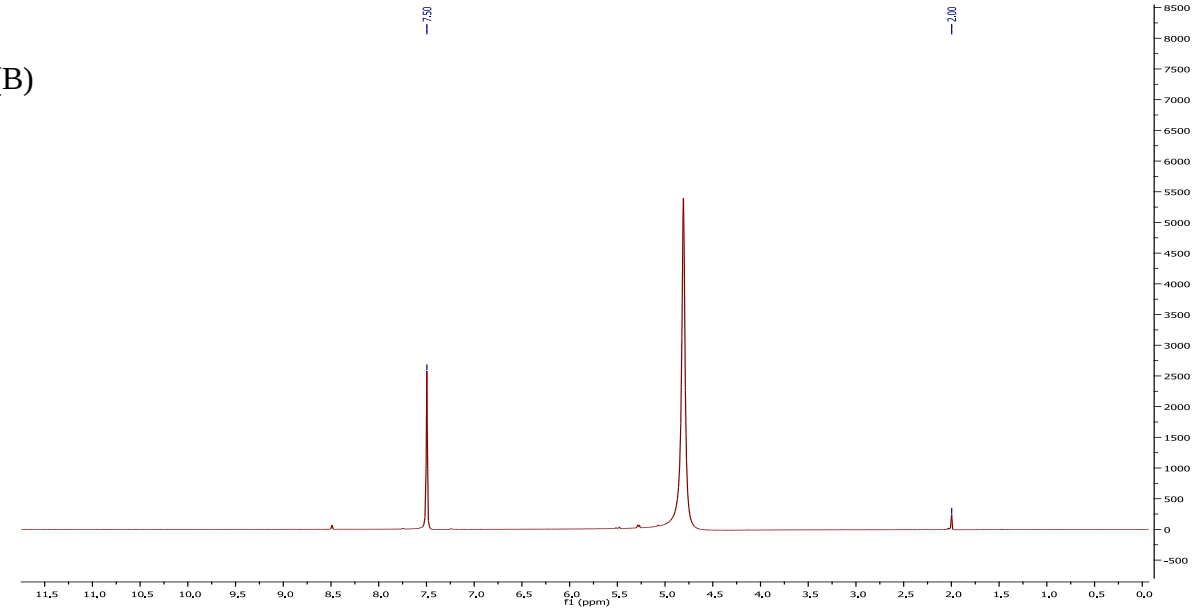

Figure 4.3: ^{1}H NMR spectra of imidazole-2-carboxaldehyde (A) and imidazole-2-carboxylic acid (B)

(A)

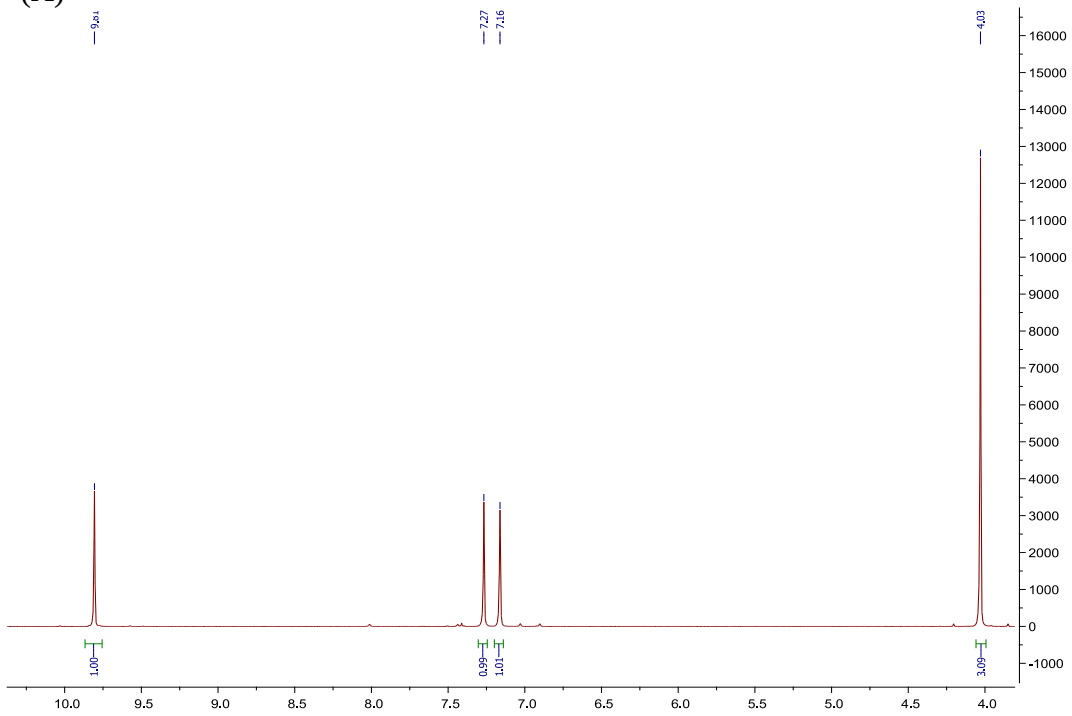

(B)

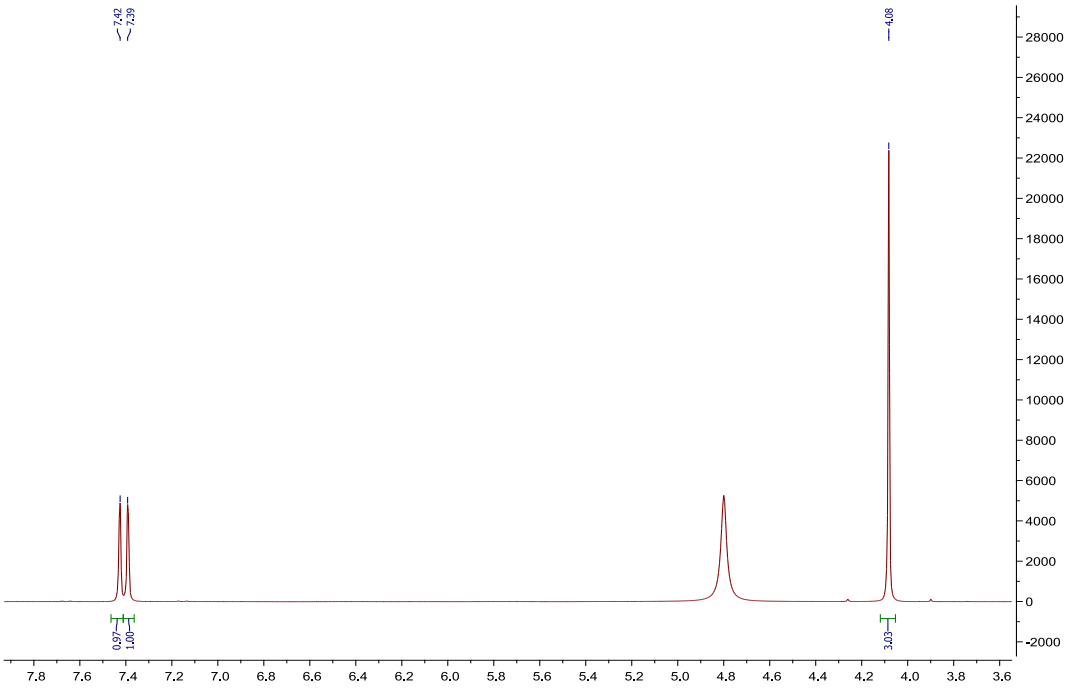

Figure 4.4: ^{1}H NMR spectra of 1-methylimidazole-2-carboxaldehyde (A) and 1-methylimidazole-2-carboxylic acid (B)

In the IR spectra of the complexes (**2a-c**) there are strong absorption bands at 981, 984 and 963 cm^{-1} respectively, which are assigned to the V=O stretch and are within the range 930-1030 cm^{-1} reported in the literature[16]. The IR spectra for the ligands were also compared with those of their corresponding complexes and major shifts were observed as shown in figures 4.5, 4.6 and 4.7. In imidazole ring systems, the ν(C=N) is usually observed at about 1650 cm^{-1}. [17] The coordination-induced shift of this stretching frequency from 1618-1641 cm^{-1} in the free ligands to 1606-1628 cm^{-1} in the complexes was observed, signifying that coordination occurred through the imidazolyl nitrogen.[18]

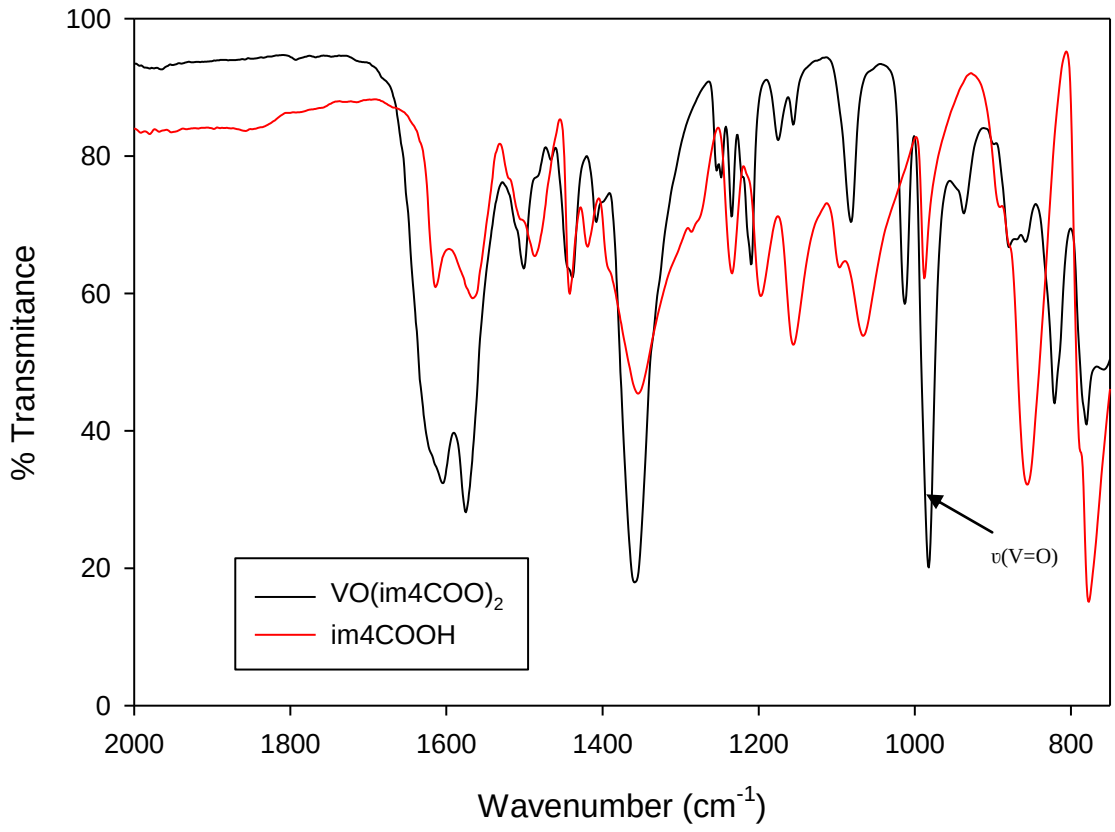

Figure 4.5: The IR spectra of im4COOH and $VO(im4COO)_2$

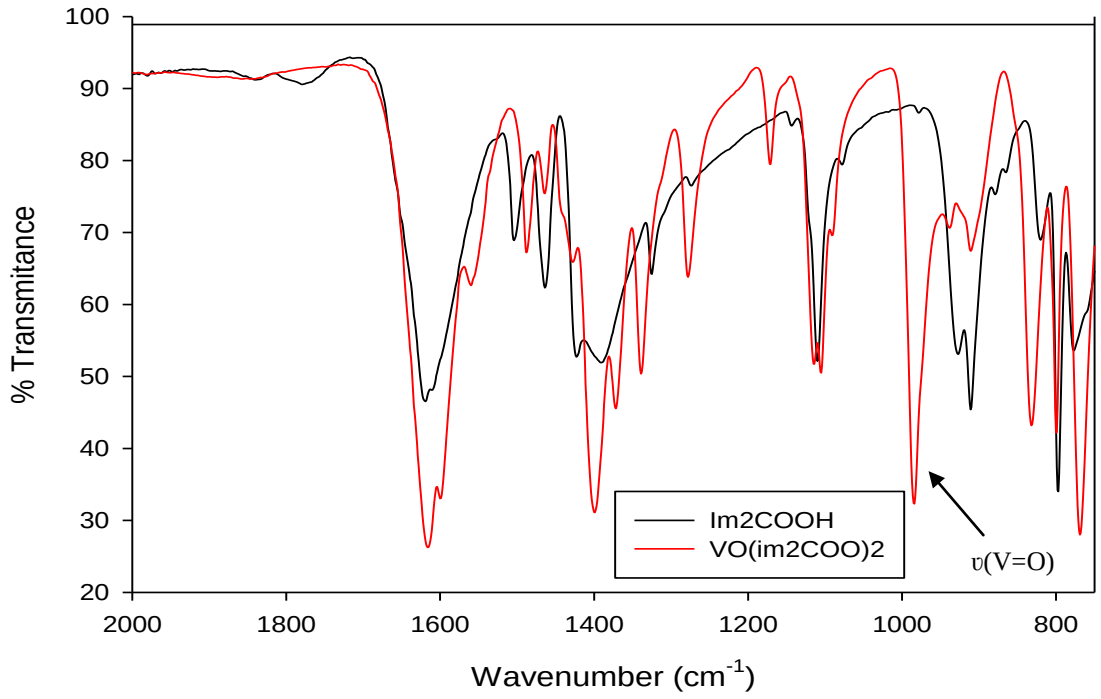

Figure 4.6: The IR spectra of im2COOH and $VO(im2COO)_2$

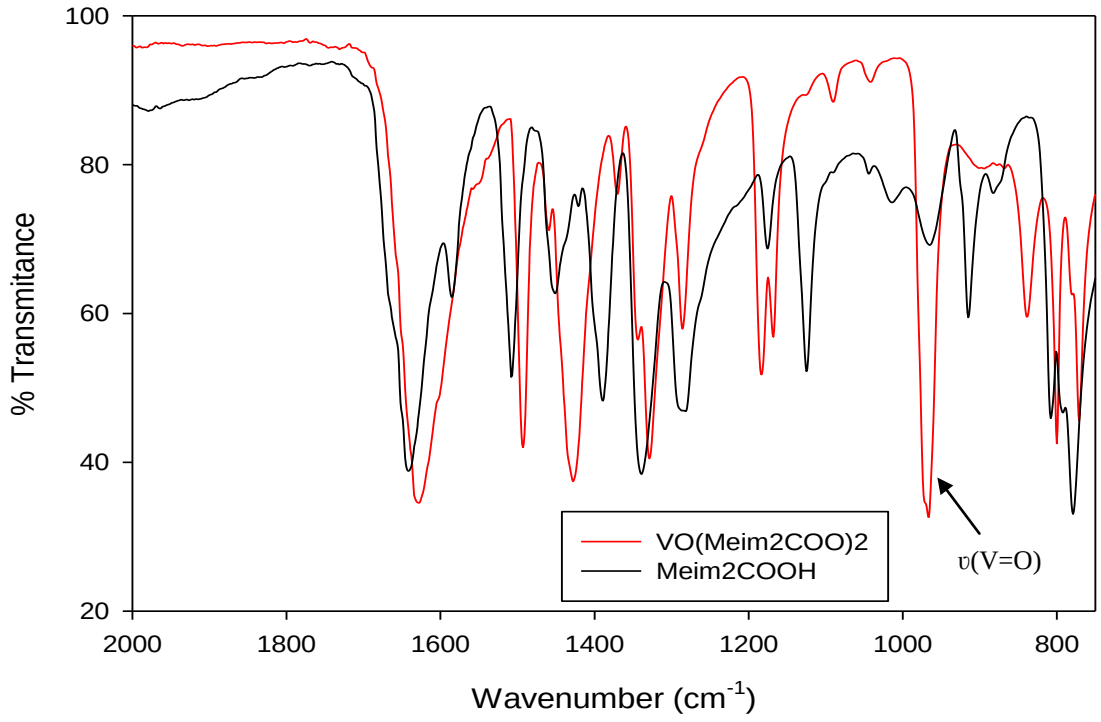

Figure 4.7: The IR spectra of Meim2COOH and $VO(Meim2COO)_2$

The square-pyramidal oxovanadium(IV) complexes typically display three low intensity d-d transitions in the range of 330-1000 nm[19]. The $b_2 \rightarrow a_1$, $b_2 \rightarrow b_1$ and $b_2 \rightarrow e$ transitions fall in the ranges 332-362 nm, 555-593 nm and 700-720 nm respectively (see figure 4.8).

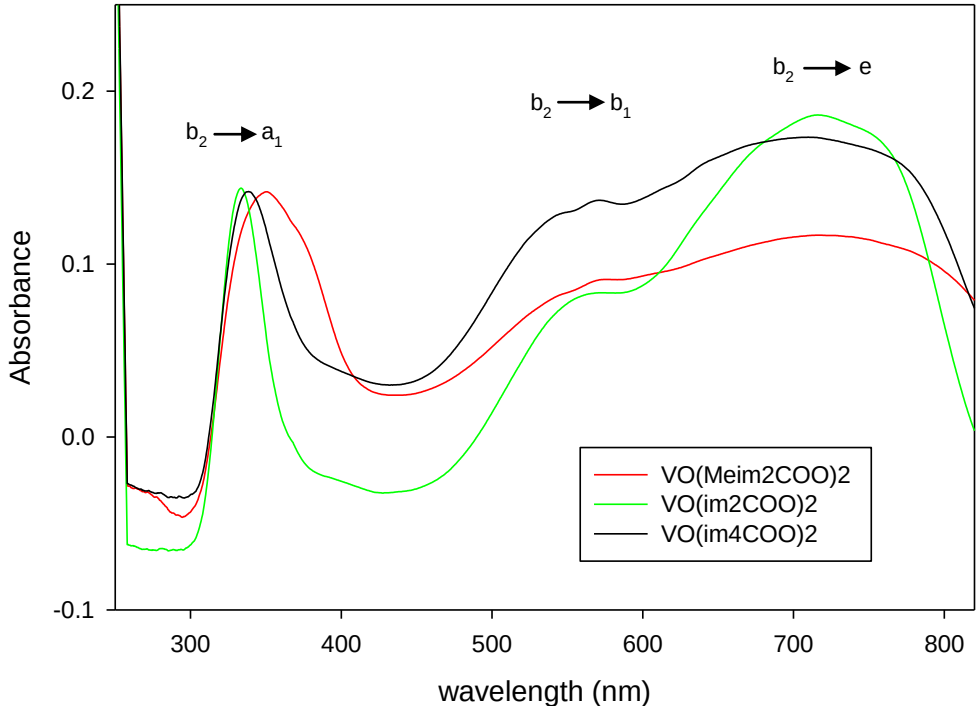

Figure 4.8: UV-vis spectra of $VO(im4COO)_2$, $VO(im2COO)_2$ and $VO(Meim2COO)_2$

4.3.3 pH-metric solution speciation studies

The equilibrium constants were derived by best-fitting of the experimental data with a chemical model of the equilibrium system (see figure 4.9). The experimental data points with larger residuals were removed during the refinement. Data from the regions in which there was no complex formation and in a region in which complex formation was essentially complete were excluded from the calculations since they contributed no information regarding the formation constants. They only represented the effects of dilution and their inclusion adversely affected the quality of the fit.

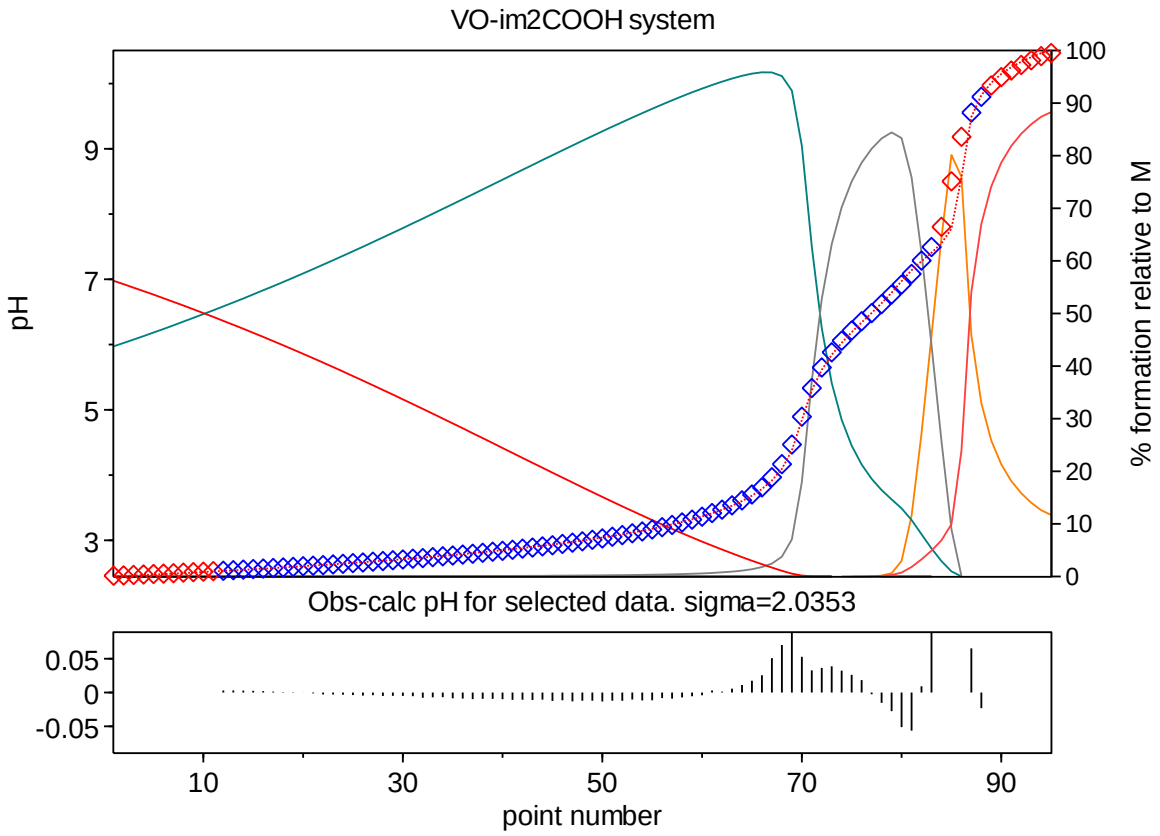

Figure 4.9: Titration and fitted curves of VO-imidazole-2-carboxylic acid. Experimental points are represented by blue squares and the calculated least-squares fit by the red dotted line. The other lines represent the species (not specified)

The protonation (log$K$) and oxovanadium complex formation (logβ) constants are listed in Table 4.1 together with standard deviations. The ligands exhibit two protonation processes in the pH range 2-11 for the carboxylate and imidazole groups respectively. The logK_2 values for the protonation of imidazole in all cases, imidazole-4-carboxylic acid (6.13), imidazole-2-carboxylic acid (6.44) and 1-methylimidazole-2-carboxylic acid (6.75), are lower than those of free imidazole (6.95)[21] and free 1-methylimidazole (7.20)[22] respectively. The latter is slightly more basic probably due to the presence of the electron releasing methyl substituent. The low logK_1 values (2.70, 2.72 and 1.29) for imidazole-4-carboxylic acid, imidazole-2-carboxylic acid and 1-methylimidazole-2-carboxylic acid respectively suggest internal hydrogen bonding between the protonated imidazole and a carboxylate. This suggests that these ligands exist in a zwitterion form such as that observed for simple amino acids in water. The pyrole sites in imidazole-4-carboxylic acid and imidazole-2-carboxylic acid do not dissociate in the pH range measured. The proposed interactions of these ligands with the acid

in aqueous solutions are represented by Scheme 4.2. The ligand imidazole-2-carboxylic acid shows similar interactions and stability with vanadyl as imidazole-4-carboxylic acid.

Table 4.1: Protonation (log*K*) and stability (log*β*) constants for the $V^{IV}O$-(imidazole,COO) systems at *I* = 0.10 M TMACl and T = 25.0±0.1°C. Comparison with other $V^{IV}O$-(imidazole/pyridine,COO) systems is also presented. Standard deviations (errors in the last digit) are reported in parenthesis

	Reaction	Ligand				
		Im-4-COOH	Im-2-COOH	Meim-2-COOH	Im-4-acetic acid*[21]	Picolinic acid*[22]
pK_1	$LH_2^+ \rightleftharpoons H^+ + LH$	2.70(3)	2.72(3)	1.29(12)	3.19(1)	~1
pK_2	$LH \rightleftharpoons H^+ + L^-$	6.13(1)	6.44(2)	6.75(3)	7.34(1)	5.19(2)
$\log\beta_{110}$	$VO^{2+} + L^- \rightleftharpoons [VO(L)]^+$	7.11(2)	7.53(3)	9.84(6)	6.10(1)	6.66(2)
$\log\beta_{111}$	$VO^{2+} + H^+ + L^- \rightleftharpoons [VO(LH)]^{2+}$	-	-	14.85(7)	11.04(4)	-
$\log\beta_{120}$	$VO^{2+} + 2L^- \rightleftharpoons [VO(L)_2]$	11.38(8)	11.62(6)	15.49(9)	10.70(1)	12.11(2)

LH_2^+=imH4COOH$^+$, imH2COOH$^+$ or MeimH2COOH$^+$; LH=im4COOH, im2COOH or Meim2COOH; L^-=im4COO$^-$, im2COO$^-$ or Meim2COO$^-$. *T = 25.0±0.1 °C and *I* = 0.20 M KCl using *ca* 0.2 M KOH as titrant

(A)

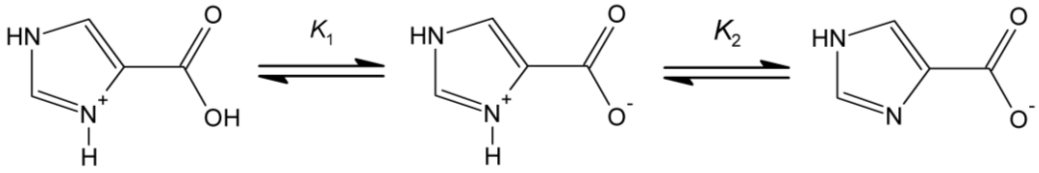

(B)

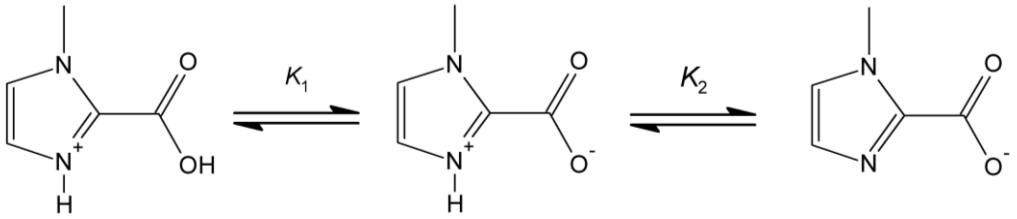

Scheme 4.2: The protonation steps for im4COOH (A) and Meim2COOH (B)

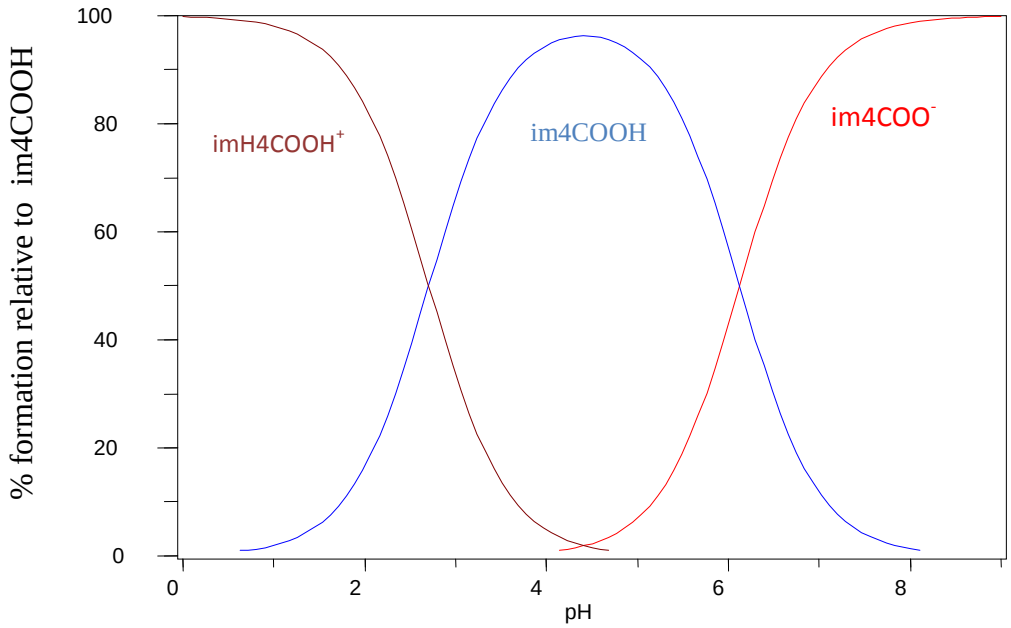

Figure 4.10: Species distribution as a function of pH for imidazole-4-carboxylic acid

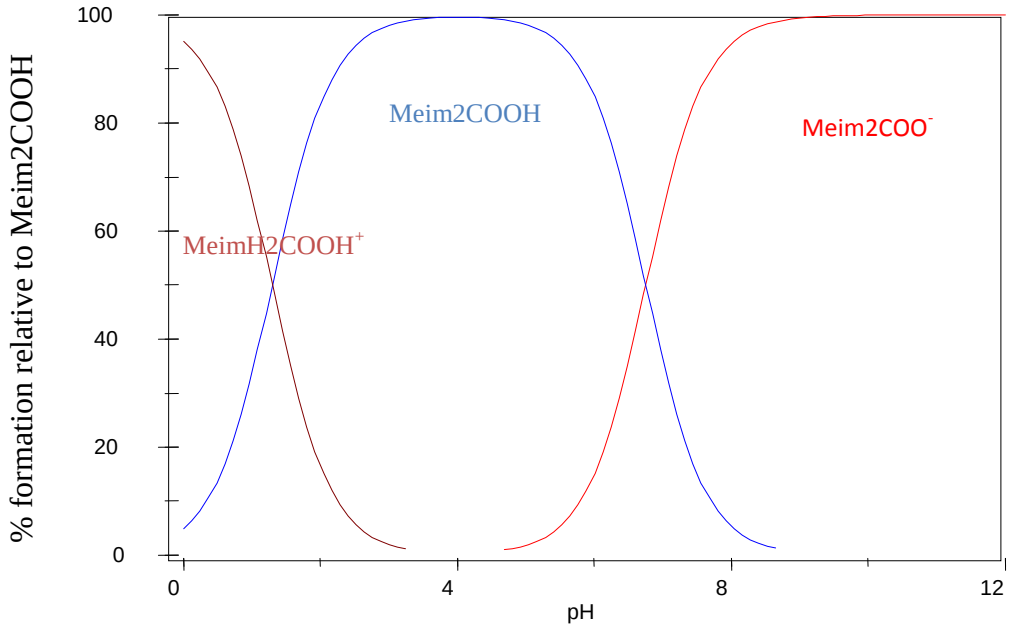

Figure 4.11: Species distribution as a function of pH for 1-methylimidazole-2-carboxylic acid

The species distribution as a function of pH for imidazole-4-carboxylic acid and 1-methylimidazole-2-carboxylic acid are shown in figures 4.10 and 4.11. The imidazole-4-

carboxylic acid speciation shows that at pH 2.70 imidazole-4-carboxylic acid is 50% protonated (i.e. the carboxyl oxygen is protonated) and at pH 6.13 the mildly basic imidazole nitrogen is 50% protonated. The pK_a for these weak acids corresponds to the pH at half neutralization, i.e. where the concentration of the undissociated acid mirrors the concentration of the acid.

The proposed interactions of these ligands in aqueous solutions with oxovanadium(IV) are represented by Scheme 4.3. The ligand imidazole-2-carboxylic acid shows similar interactions and stability with vanadyl as imidazole-4-carboxylic acid. The species distribution diagrams are represented by Figures 4.12, 4.13 and 4.14 for the ($V^{IV}O$)-imidazole-4-carboxylic acid, ($V^{IV}O$)-imidazole-2-carboxylic acid and ($V^{IV}O$)-1-methylimidazole-2-carboxylic acid systems, respectively.

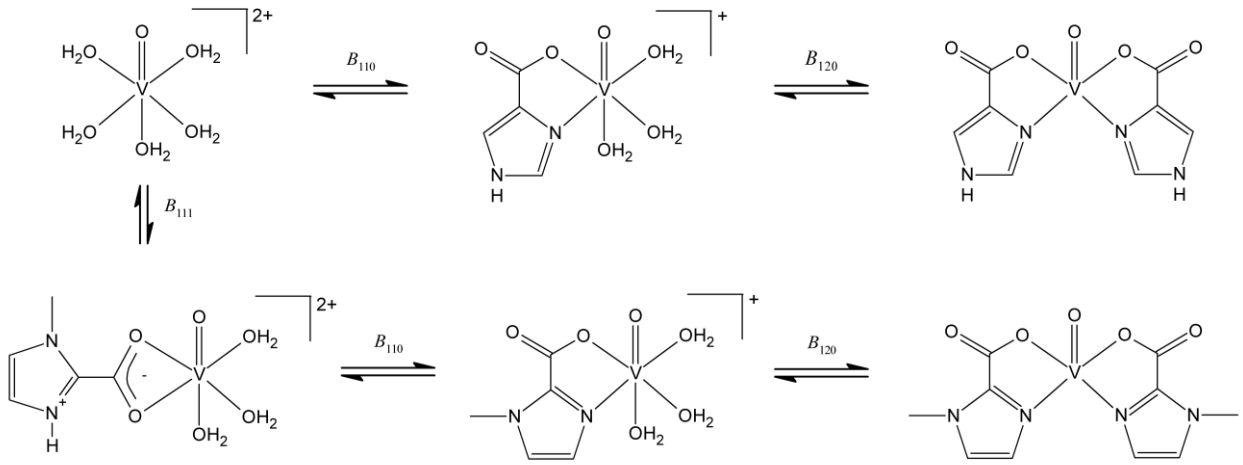

Scheme 4.3: The stepwise formation of oxovanadium(IV) complexes formed with imidazole-4-carboxylic acid and 1-methylimidazole-2-carboxylic acid

The ligands adopt bidentate chelation. The first binding constants could be calculated with a 1:1 metal-to-ligand ratio and precipitation due to the formation of hydrolysis products was observed for titrations with a 1:2 metal-to-ligand ratio. Extensive $V^{IV}O$ complexation was obtained with a high ligand excess (10-fold), allowing for the determination of the second binding constant. The fitting of the titration data supports the formation of monomeric $[VOL]^+$ and $[VOL_2]$ species as well as $[VOLH]^{2+}$ for 1-methylimidazole-2-carboxylic acid. Similarly to the VO^{2+}-glycine and VO^{2+}-L-alanine systems, the hydroxo binding ($[VOL_2(OH)]^-$) could not be fitted in both models while the assumption of the binary hydroxyl species $[(VO)_2(OH)_5]^-$ as well as $[VO(OH)_3]$- in highly basic solutions fitted well.

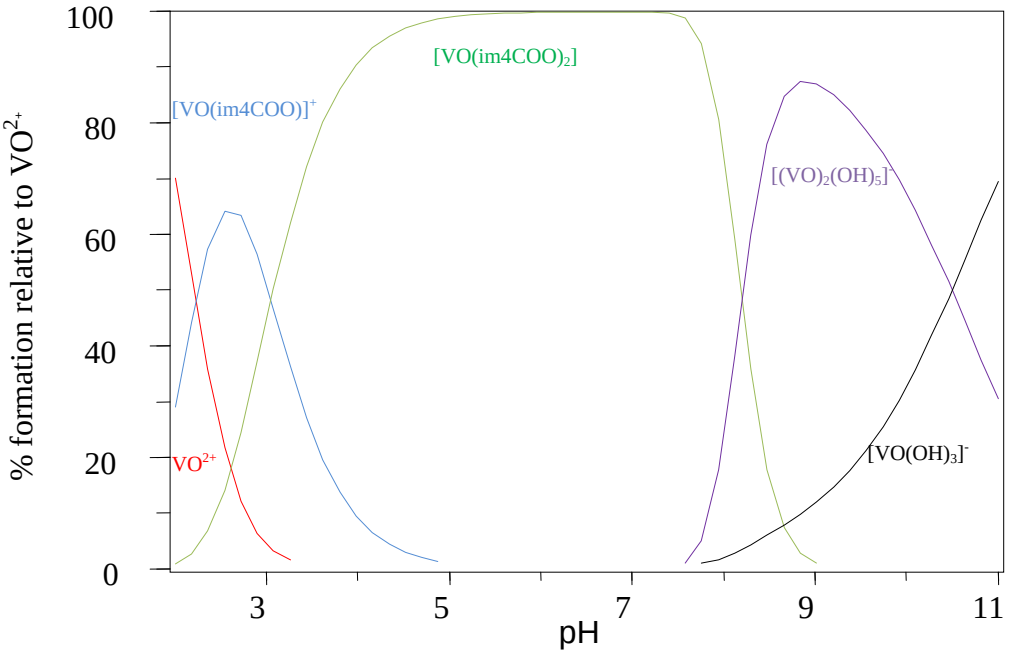

Figure 4.12: Speciation curves for complexes formed in the ($V^{IV}O$)-imidazole-4-carboxylic acid system (M:L ratio is 1:4)

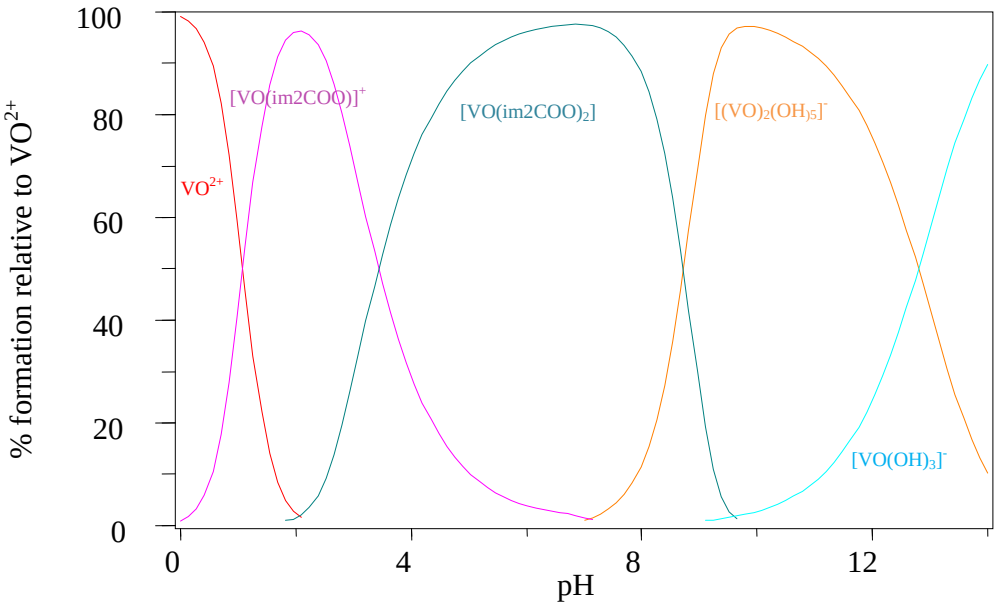

Figure 4.13: Speciation curves for complexes formed in the ($V^{IV}O$)-imidazole-2-carboxylic acid system (M:L ratio is 1:4)

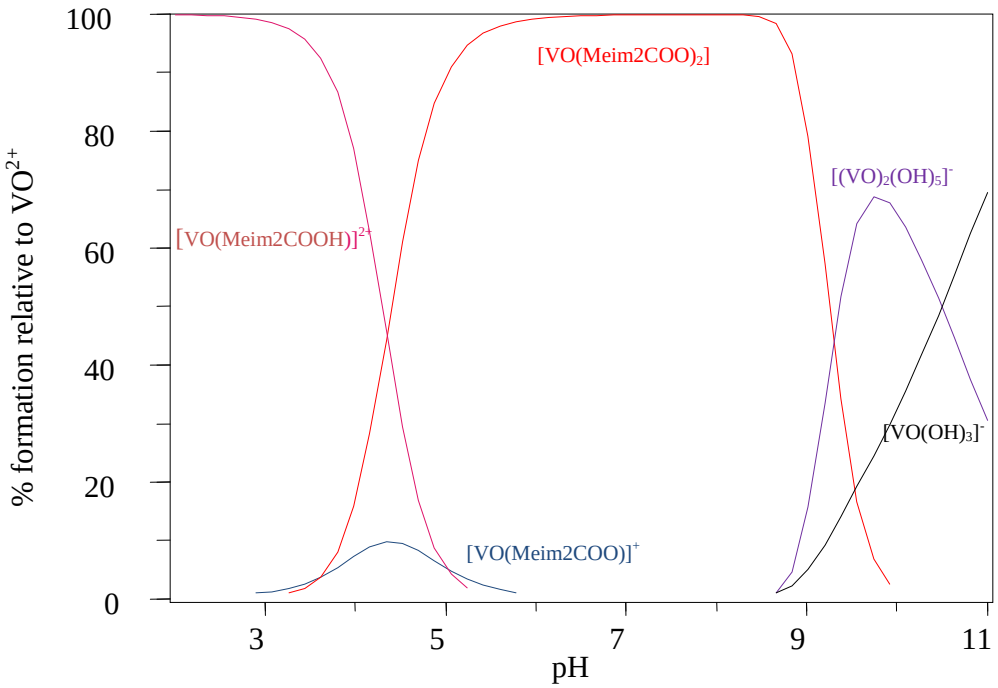

Figure 4.14: Speciation curves for complexes formed in the ($V^{IV}O$)-1-methylimidazole-2-carboxylic acid system (M:L ratio is 1:4)

The overall stability constant for the ($V^{IV}O$)-*N*-methylimidazole-2-carboxylic acid system (log β_{120} =15.49(9)) is far larger than that for imidazole-4-carboxylic acid system (log β_{12} =11.38(8)) and imidazole-2-carboxylic acid system (log β_{12} =11.62(6)). This can be explained by the fact that the imidazole nitrogen in 1-methylimidazole-2-carboxylic acid is more basic. However, the overall stability constant of the ($V^{IV}O$)-imidazole-4-carboxylic acid and ($V^{IV}O$)-imidazole-2-carboxylic acid systems are comparable to that of ($V^{IV}O$)-imidazole-4-acetic acid (im-4-acetic acid) (log β_{120} =10.70(1))[22] and that with mildly basic pyridine nitrogen of picolinic acid (log β_{120} =12.11(2))[23] (see table 4.1) intimating that inclusion of an electron donating group in the 1 position of imidazole is important to effect stability. In addition, six-membered ring chelate formation in the ($V^{IV}O$)-imidazole-4-acetic acid system results in weaker binding compared with five-membered ring systems studied here.

For the 1-methylimidazole-2-carboxylic acid system, however, the coordination of a protonated ligand is observed at low pH with log β_{111}=14.84(7). This suggests strong binding and the possibility of a symmetrically chelating carboxylate ion, with the imidazole nitrogen protonated (see Schemes 4.2 and 4.3). For the formation of monomeric $[VOL]^+$ and $[VOL_2]$

species, the very acidic carboxylic acid groups interact with VO^{2+} at very low pH and the mildly basic imidazole is able to interact with vanadyl at relatively higher pH. The result is the stabilization of these oxovanadium(IV) complex systems in the relevant biological pH range.

4.3.4 Biological studies

(a) Cytotoxicity

To ascertain if any of the vanadium compounds ($VO(MeIm2COO)_2$, $VO(im2COO)_2$, $VO(im4COO)_2$) were toxic, MTT assays were performed on each of the cell lines to determine cell viability. Figure 4.15 shows the results of the cytotoxicity test. Most of the compounds are toxic at concentrations above 0.1 µM on 3T3-L1 cell lines and only the vanadyl sulfate is non toxic on Chang cells at concentrations 0.01-10 µM. Even at a low concentration of 0.01 M , $VO(im4COO)_2$ and $VO(Meim2COO)_2$ are still toxic on 3T3-L1 adipocytes. However, the greatest cell viability is achieved on 3T3-L1 adipocytes by $VO(im2COO)_2$ at a concentration of 0.001 M.

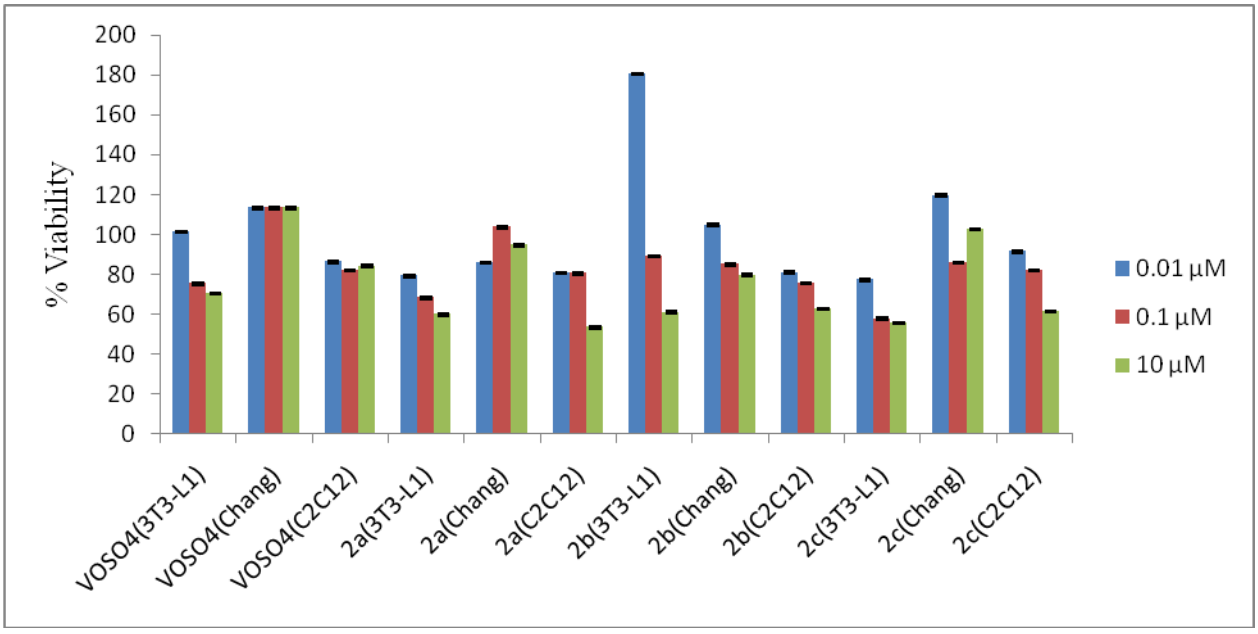

Figure 4.15: Cell viability of $VOSO_4$, $VO(im4COO)_2$ (**2a**), $VO(im2COO)_2$ (**2b**) and, $VO(MeIm2COO)_2$ (**2c**) at 0.01 µM, 0.1 µM and 10 µM on 3T3-L1, Chang and C2C12 cells. The cell type is in parenthesis. Error bars indicate SEM (n = 3)

The concentrations which were used for glucose uptake depended on the MTT results. At concentrations 10 µM, 0.1 µM and 0.01 µM the compounds were not cytotoxic on Chang cell lines but on C2C12 only a concentration of 10 µM was cytotoxic, therefore concentrations of 0.1 µM, 0.01 µM and 0.001 µM were used for the glucose uptake studies. Very low concentrations of 0.001, 0.0001 and 0.00001 µM were used on 3T3-L1 for glucose uptake since the compounds showed that they were very toxic at 0.01 µM.

(b) Glucose uptake studies

The results of glucose uptake are presented in figures 4.16, 4.17 and 4.18. As depicted in figure 4.17, the oxovandium(IV) compounds ($VOSO_4$, $VO(Meim2COO)_2$, $VO(im4COO)_2$) enhanced glucose uptake at a concentration of 10 µM on the Chang liver cells, either equaling or surpassing the effects observed for metformin, a first-line drug commonly used in the treatment of type 2 diabetes particularly in overweight and obese people.[24] The uptake of glucose by the oxovanadium compounds in 3T3-L1 muscle cells was poor most probably due to the low concentrations used. Out of the three oxovanadium(IV) complexes, $VO(im4COO)_2$ (**2a)** showed the best glucose uptake at concentrations 0.001 µM on 3T3-L1 adipocytes, 10 µM on Chang liver cells and 0.1 µM on C2C12 muscle cells. At present there is no known special explanation attributed to the unique properties of $VO(im4COO)_2$ on glucose uptake since the three compounds are very similar. The glucose uptake of all the three complexes are well comparable to the effect of oxovanadium(IV) complexes of Schiff base ligands and hydroxyphenyimidazolines on Chang liver cells, but they also showed enhanced glucose uptake on 3T3-L1 adipocytes and C2C12 muscle cells in contrast to the compounds studied here.[25,26]

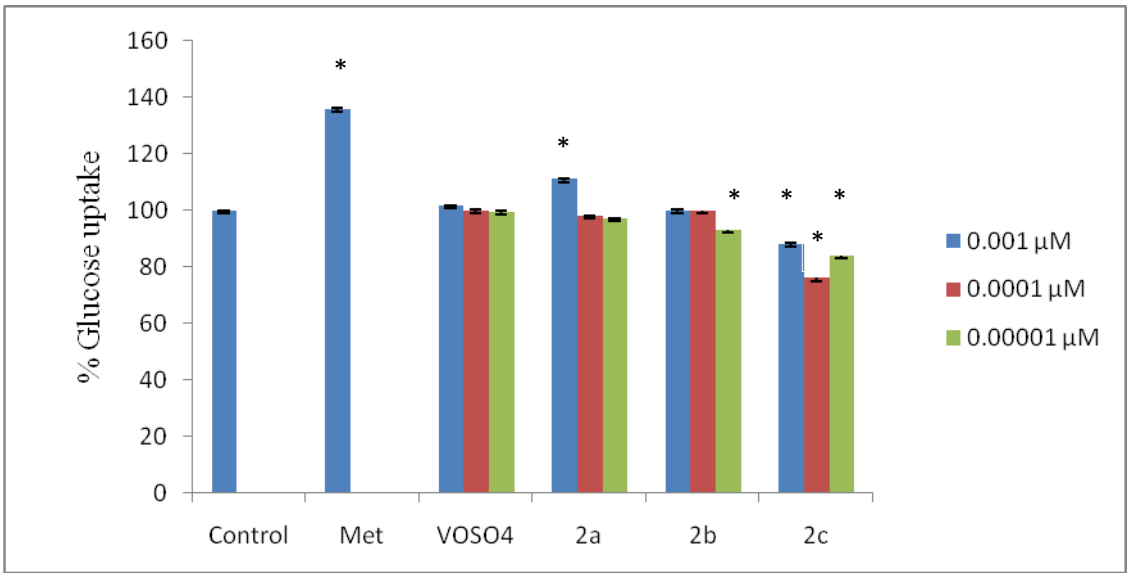

Figure 4.16: The effects of metformin (Met), $VOSO_4$, $VO(im4COO)_2$ (**2a**), $VO(im2COO)_2$ (**2b**) and $VO(MeIm2COO)_2$ (**2c**) at 0.001 µM, 0.0001 µM and 0.00001 µM on 3T3-L1 glucose uptake. The basal glucose uptake is represented as 100% (Control). Error bars indicate SEM (n = 3). *p < 0.05 relative to the control

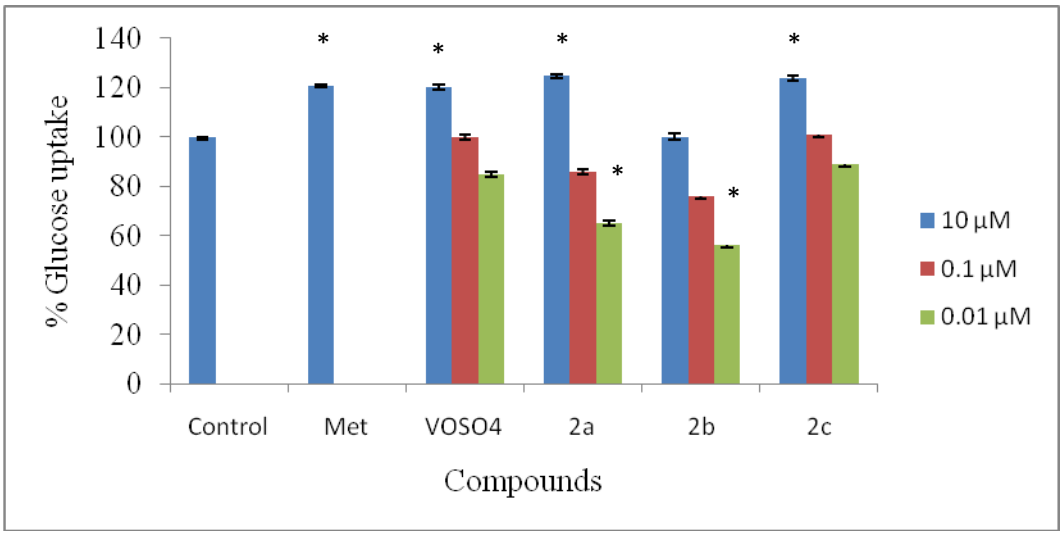

Figure 4.17: The effects of metformin (Met), $VOSO_4$, $VO(im4COO)_2$ (**2a**), $VO(im2COO)_2$ (**2b**), and $VO(MeIm2COO)_2$ (**2c**) at 10 µM, 0.1 µM and 0.01 µM on Chang glucose uptake. The basal glucose uptake, is represented as 100% (Control). Error bars indicate SEM (n = 3). *p < 0.05 relative to the control

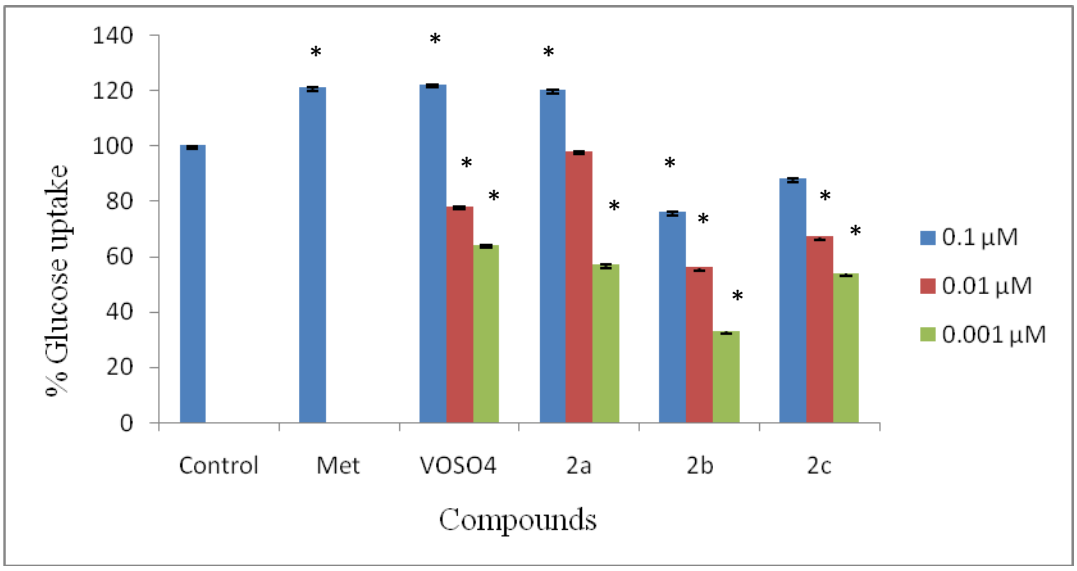

Figure 4.18: The effects of metformin (Met), $VOSO_4$, $VO(im4COO)_2$ (**2a**) $VO(im2COO)_2$ (**2b**), and $VO(Meim2COO)_2$ (**2c**), at 0.1 µM, 0.01 µM and 0.001 µM on C2C12 glucose uptake. The basal glucose uptake is represented as 100% (Control). Error bars indicate SEM (n = 3). *p < 0.05 relative to the control

Although the *in vitro* model used may have certain shortcomings, in that it does not exactly replicate *in vivo* conditions[25], it does provide a simple and ethical platform for the rapid assessment of new complexes. It can be seen that the vanadium salt ($VOSO_4$) almost always performs better than the complexes presented in chapters 3 and 4 and this is in agreement with the fact that these are prodrugs. Under physiological condition, the ligands would dissociate and make vanadium available in a form of vanadyl or vanadate which is the active species, hence the lower activity under *in vitro* conditions compared with $VOSO_4$ which is readily convertible to vanadate under the conditions employed. Therefore, it can be concluded that the glucose assay may not necessarily be the best platform for screening the candidate vanadium anti-diabetic drugs despite the ethical nature of their practice.

4.4 References

1. Congiu C, Cocco M. T, Onnis V, (2008), *Bioorg. Med. Chem. Lett*., **18**, 989.
2. Khabnadideh S, Rezaei Z, Khalafi-Nezhad A, Bahrinajafi R, Mohamadi R, Farrokhroz A. A, (2003), *Bioorg. Med. Chem. Lett*., **13**, 2863.
3. Göker H, Ertan R, Akgün H, Yulug N, (1991), *Arch. Pharm*., **324**, 283.
4. Crane L, Anastassiadou M, Hage S. E, Stigliani J. L, Baziard-Mouysset G, Payard M, Leger J. M, Bizot-Espiard J. G, Ktorza A, Caignard D. H, Renard P, (2006), *Bioorg. Med. Chem*., **14**, 7419.
5. Sigel H, Tribolet R, Yamauchi O, (1990), *Inorg. Chem*., **9**, 330.
6. Bouwman E, Douziech B, Gutierrez-Soto L, Beretta M, Driessen W. L, Reedijk J, Mendoza-Diaz G, (2000), *Inorg. Chim. Acta*, **304**, 250.
7. Place C, Zimmermann J, Mulliez E, Guillot G, Bois C, Chottard J, (1998), *Inorg. Chem*., **37**, 4030.
8. Kesicki E. A, DeRoschn M. A, Freeman L. H, Walton C. L, Harvey D. F, Trogler W. C, (1993), *Inorg. Chem*., **32**, 5851.
9. Tshentu Z. R, (2006), *PhD Thesis, Rhenium complexes with multidentate imidazole ligands, Nelson Mandela Metropolitan University, Port Elizabeth.*
10. Roe A. M, (1963), *J. Chem. Soc*., 2189.
11. Oberhausen K. J, Richardson J. F, Buchanan R. M, Pierce W, (1989), *Polyhedron*, **8**, 659.
12. Kruse L. I, Kaiser C, DeWolf W. E, Finkelstein J. A, Frazee J. S, Hilbert E. L, Ross S. T, Flaim K. E, Sawyer J. L, (1990), *J. Med. Chem*., **33**, 781.
13. McLauchlan C. C, Hooker J. D, Jones M. A, Dymon Z, Backhus E. A, Greiner B. A, Dorner N. A, Youkhana M. A, Manus L. M, (2010), *J. Inorg. Biochem*., **104**, 274.
14. Henry R. P, Mitchell P. C. H, Prue J. E. J, (1973), *J. Am. Chem. Soc*., *Dalton Trans*., 1156
15. Gans P, Sabatini A, Vacca A, (1996), *Talanta*, **43**, 1739.
16. Ligtenbarg A. G. J, Spek A. L , Hage R, Feringa B. L, (1999), *J. Am. Chem. Soc*., *Dalton Trans*., 659.
17. Lane T. J, Nakagawa I, Walker J. L, Kandathil A. J, (1962), *Inorg. Chem*., **1**, 267.
18. Westland A. D, Tarafder M. T. H, (1981), *Inorg. Chem*., **20**, 3992.
19. Selbin J, (1965), *Chem. Rev*., ***6*5**, 153.
20. Varnagy K, Sovago I, Agoston K, Liko Z, Süeli-Vargha H, Sanna D, Micera G, (1994), *J. Chem. Soc. Dalton Trans*., **20**, 2939.

21. Pettit L. D, Powell K. J, (2007), *Stability Constants Database-IUPAC and Academic Software*.
22. Sanna D, Micera G, Buglyo P, Kiss T, Gajda T, Surdy P, (1998), *Inorg. Chim. Acta*, **268(2**), 297.
23. Alderighi L, Gans P, Ienco A, Peters D, Sabatini A, Vacca A, (1999), *Coord. Chem. Rev*., **184**, 311.
24. Davidson M. B, Peters A. L, (1997), *Am. J. Med*., **102**, 9.
25. Nejo A. A, Kolawole G. A, Opuka A. R, Wolowska J, O'Brien P, (2009), *Inorg. Chim. Acta*., **362**, 3993.
26. Walmsley R. S, Tshentu Z. R, Fernandes M. A, Frost C. L, (2010), *Inorg. Chim. Acta*, **363,** 2215.

CHAPTER 5

CONCLUSIONS AND FUTURE WORK

5.1 Conclusions

Two novel oxovanadium(IV) complexes of glycine and L-alanine were successfully synthesized and partially characterised. The spectroscopic studies suggested that the amino acids coordinate to the oxovanadium through the amine-nitrogen and the geometry suggested by the electronic spectra is distorted octahedral. The oxovanadium(IV) complex of glycine, $[VO(gly)_4(CH_3CH_2OH)]SO_4$, was isolated but was not very pure and structural characterization was tentative, and as a result biological studies were not done. The oxovanadium(IV) complex of L-alanine, $[VO(ala)_4(H_2O)]SO_4.3H_2O$, was isolated and the glucose uptake effect was investigated using 3T3-L1, Chang liver and C2C12 muscle cells at various concentrations. The compound had significant glucose uptake on Chang liver cells only at a concentration of 0.1-10 µM whilst in the C2C12 muscle and 3T3-L1 cells the compound showed little anti-hyperglycemic activities due to the low concentrations used as a result of cytotoxicity. The acidity constants of glycine and L-alanine, and the stability constants of their corresponding oxovanadium(IV) complexes were determined by potentiometric acid-base titrations, but there is contradiction in the of coordination of these simple amino acids to $V^{IV}O$ from evidence of solid state and solution studies.

Three imidazole derivatives and their corresponding oxovanadium(IV) complexes were successfully synthesized and characterized. However, the isolated solid state complexes lack water-solubility which is one of the desired properties of these glucose-lowering compounds. The electronic spectroscopic studies of the oxovanadium(IV) complexes of 1-methylimidazole-2-carboxylic acid ($[VO(Meim2COO)_2]$), imidazole-2-carboxylic acid ($[VO(im2COO)_2]$) and imidazole-4-carboxylic acid ($[VO(im4COO)_2]$) suggest that a square pyramidal geometry can be tentatively assigned and confirmation of the structures by X-ray crystallography was not done as crystals could not be developed during the course of the study. The (imidazole,COO^-) donor set has been shown to stabilize $V^{IV}O$ through bidentate coordination. The binding constants for the 2-substituted imidazole indicate a stronger binding mode for this donor set. The calculations for the species distribution in the experimental pH range showed that the neutral *bis*-coordinated complexes are dominant over

the biological pH range. In this system the solid state compounds isolated agreed well with the solution model with respect to coordination.

All complexes increased glucose utilization in Chang liver and to some extent in C2C12 muscle cells over basal values. Glucose uptake was not significant in 3T3-L1 adipocytes due to the low concentrations used. However, the *in vitro* results cannot give reliable observations because it has got so many limitations and therefore *in vivo* studies on these compounds are recommended.

5.2 Suggestions for future work

Since the oxovanadium(IV)-imidazole derivatives complexes are not soluble in water, modification of the 1-position of the imidazole by introducing an alcohol group, e.g. ethanol, that can improve the physicochemical properties of this (imidazole,COO) moiety. These complexes could be investigated further *via* an *in vivo* model using the Zucker fatty rats since the *in vitro* glucose uptake assay does not provide adequate information. The Zucker fatty rat is a model for type II diabetes.[1] The investigation would include, determination of plasma glucose levels at certain times after administration of vanadium compounds, as well as the determination of plasma and tissue vanadium concentrations, as well as toxicity studies.

The study of the vanadium distribution in tissue is important since the biological action of the complexes on target organs may be controlled by varying physicochemical properties of the organic ligand.[2] This analysis can be done by sacrificing the mice after administration of the complexes and then removing the selected organs for washing and digestion and then finally analysing for vanadium concentrations using atomic absorption spectrometry or inductively coupled plasma mass spectrometer (ICP-MS).

After the biological administration of the vanadium complexes, the complexes may dissociate due to vanadium complexation reactions with the vast number of biological ligands present. To illustrate that the synthesized vanadium complexes convert to the active metabolites for glucose level lowering it is necessary to investigate the species that are present in the blood system. Due to the complex matrix of blood and the relatively low concentration of the vanadium in blood, a hyphenated reversed phase chromatographic system (HPLC) coupled to the highly sensitive inductively coupled plasma mass spectrometer (ICP-MS) as detector could be used. In this manner speciation of vanadium complexes in blood can be achieved.

The glucose stimulated insulin secretion (GSIS) studies can also be carried out using these vanadium complexes**.** This would render the vanadium-based anti-diabetic drugs useful in cases where type 2 diabetics cease to produce sufficient insulin. Initial studies by our group revealed that vanadium may possibly stimulate the secretion of insulin (i.e. an alternate pathway to the accepted pathway). The amount of insulin secretion would be quantified using the ^{125}I radioimmunoassay (Rat Insulin RIA kit).[3] Pancreatic cells (INS-1) would be seeded and incubated in RPMI+glutamax media containing glucose concentrations of 11.1 mM and 33.3 mM. This media would then replaced with media containing low (3.33 mM) and high (16.3 mM) glucose concentrations as well as the oxovanadium compounds. The insulin secreted under basal (3.3 mM) and stimulated (16.3 mM) conditions can then be quantified using the radioimmunoassay,[3] and the stimulatory index can be calculated.

5.3 References

1. Kurtz K. W, Morris R. C, Pershadsingh H. A, (1989), *Hypertension*, **13**, 896.
2. Sanna D, Buglyo P, Micera G, (2010), *J. Biol. Chem*., **15**, 825.
3. Liske R, Reber K, (1976), *Horm. Res*., **7**, 214.